PERFORMANCE OF ROTARY ENTHALPY EXCHANGERS

by

GUNNAR STIESCH

A thesis submitted in partial fulfillment of

the requirements for the degree of

MASTER OF SCIENCE

(Mechanical Engineering)

at the

UNIVERSITY OF WISCONSIN-MADISON

1994

ABSTRACT

Rotary regenerative heat and mass exchangers allow energy savings in the heating and cooling of ventilated buildings by recovering energy from the exhaust air and transferring it to the supply air stream. In this study the adsorption isotherms and the specific heat capacity of a desiccant used in a commercially available enthalpy exchanger are investigated experimentally, and the measured property data are used to simulate the regenerator performance and to analyze the device in terms of both energy recovery and economic profitability.

Based on numerical solutions for the mechanism of combined heat and mass transfer obtained with the computer program MOSHMX for various operating conditions, a computationally simple model is developed that estimates the performance of the particular enthalpy exchanger and also of a comparable sensible heat exchanger as a function of the air inlet conditions and the matrix rotation speed. The model is built into the transient simulation program TRNSYS, and annual regenerator performance simulations are executed. The integrated energy savings over this period are determined for the case of a ventilation system for a 200 people office building (approx. 2 m^3/s) for three different locations in the United States, each representing a different climate.

Life cycle savings that take into account the initial cost of the space-conditioning system as well as the operating savings achieved by the regenerator are evaluated for both the enthalpy exchanger and the sensible heat exchanger over a system life time of 15 years. The present worth of the accumulated savings ranges from $ 28,000 to $ 38,000 for the enthalpy exchanger and from $ 7,000 to $ 24,000 for the sensible heat exchanger. The enthalpy exchanger results in greater payoffs in all locations, but its advantage is most significant in a warm and humid climate where the sensible heat exchanger performs poorly.

ACKNOWLEDGMENTS

Many thanks are owed for the completion of this work and I would like to express my gratitude towards those who contributed to making it possible.

Professor Sanford Klein invited me to the Solar Lab, and during the past 16 months he was not only my major - and a great - academic advisor who constantly helped me find the answers to any kind of engineering problem, but he was also an exceptional teacher who made his students actually have fun in the two thermodynamics classes he taught. Professor John Mitchell also contributed substantially to the progress of this project, especially towards the end, when his knowledge of all kinds of HVAC-systems was of great value. Thanks to Professor William Beckman, the director of the Solar Lab, for his efforts in finding a sponsor for the second part of this project and for cultivating such an extraordinary environment as the Solar Lab, where it is a pleasure to work in.

The German Academic Exchange Service provided me with the opportunity of attending graduate school in the United States by funding the one-year exchange program between the universities of Hannover and Madison which was initiated by Dipl.-Ing. Frank-Detlef Drake. The third semester of my studies were funded by the University of Wisconsin-Madison Graduate School. I would also like to thank Tom James and Randy Dahmen from the Carnes Company for providing samples of their products as well as information about it.

Special thanks go to all my friends in the Lab and in the UW-Sailing Team. Meeting with you at places other than the university helped making my stay in America an exceptional fun and rewarding experience. Finally, I would like to thank my family and my friends back home in Germany. Your visits, letters and phone calls were always greatly appreciated.

TABLE OF CONTENTS

LIST OF FIGURES

LIST OF TABLES

Nomenclature

a	partial derivative of a thermodynamic state property function
A	adsorption potential,
	matrix surface area for heat and mass transfer,
	annual cash flow,
	empirical constant
B	empirical constant
c_p	specific heat
C	contaminant concentration
D	matrix diameter
D_h	hydraulic diameter
E_o	characteristic energy of adsorption
F_1	first combined potential of heat and mass transfer
F_2	second combined potential of heat and mass transfer
g	geometric gradient of cash flow series (inflation rate)
G	integration constant
h	heat transfer coefficient
h_w	mass transfer coefficient
i	interest or discount rate
i_f	specific enthalpy of humid air
i_{fg}	specific heat of vaporization
i_s	specific differential heat of adsorption
i_w	specific enthalpy of water vapor
I_m	specific enthalpy of the matrix
k	thermal conductivity

L	matrix length in flow direction
LCS	life cycle savings
Le	Lewis number, ratio of mass transfer to heat transfer resistance
m_{ads}	mass of adsorbed contaminant
$\dot{m}_{exh}$	mass flow rate of the exhaust stream
$\dot{m}_{sup}$	mass flow rate of the supply stream
M_f	mass of fluid within the matrix
M_m	matrix mass
n	exponent
N	period of economic analysis
NTU_T	number of transfer units for heat transfer
NTU_w	number of transfer units for mass transfer
Nu	Nusselt number, dimensionless surf. temperature gradient
p	total pressure
p_s	saturation pressure
p_v	vapor pressure
P	present worth of cash flow series
q	dimensionless adsorption capacity for volatile organic compounds
Q_{sens}	sensible heat recovery
Q_{tot}	total heat recovery (sensible plus latent)
R	gas constant
t	time
T	temperature
U_B	bias error
U_P	precision error
U_f	total uncertainty of function f

v	face velocity of air stream in the matrix
V	voltage
$\dot{V}$	volumetric flow rate
w_f	humidity ratio of humid air
w_m	humidity ratio of air in equilibrium with matrix
W_m	adsorption capacity of the matrix
W_o	adsorption capacity of the matrix at saturated conditions
x	matrix coordinate in flow direction
z	dimensionless length in flow direction

Greek Symbols

b_j	time fraction of period j, T_j / T
e_i	regenerator effectiveness for enthalpy transfer
e_T	regenerator effectiveness for sensible heat transfer
e_w	regenerator effectiveness for humidity transfer
F	dimensionless time coordinate, Q / T
j	relative humidity air
g_i	combined capacitance ratio of the F_i -potential
G	dimensionless rotation speed (ratio of "matrix flow rate" to air flow rate)
l_i	dimensionless wave speed of the F_i -wave
Q	time coordinate
t	dimensionless time coordinate, Q / TG
T	period of one matrix rotation
w	rotation speed

Subscripts

amb	ambient state
ei	exhaust inlet state
eo	exhaust outlet state
f	fluid or air state
i	1 or 2, index for the two combined heat and mass transfer potentials, enthalpy
j	1 or 2, index for stream or period
m	matrix state
sat	saturated state
si	supply inlet
so	supply outlet
T	temperature
w	water

1 INTRODUCTION

A significant fraction of today's energy consumption is due to air-conditioning of buildings, which involves both heating and cooling. For example, more than one fifth of the total energy needs in the United States is used for this purpose (Corradini and Mitchell [11]). Recent requirements for clean air in offices, hospitals, restaurants and other public buildings have resulted in recommendations given by the American Society of Heating, Refrigerating and Air-Conditioning Engineers (ASHRAE [2]) to increase outdoor air ventilation. Since energy costs and environmental concerns are also increasing, the task of designing efficient air-conditioning systems is of growing importance.

Thermal comfort is determined by both the temperature and the humidity of the air (ASHRAE [1]), and for this reason air-conditioning operations involve both heat and mass transfer mechanisms. These operations are either cooling and dehumidification or heating and humidification. It is possible to decrease the amount of energy required to condition an air stream that is ventilated into a building by using rotary regenerators that allow to recover energy from the exhaust air stream which is then disposed into the environment (Hausen [18]). If these regenerators are made out of a material that is able to transfer mass (water) as well as heat between the air streams, the two air-conditioning mechanisms can be executed in one device. Typically rotary regenerators are used in commercial buildings, where high ventilation rates are required, rather than in residential buildings, because the relatively high first cost of this equipment has to be recaptured by significant energy savings.

The performance of such regenerators and the energy that can be recovered by operating them in air-conditioning systems is a function of both the design and the material of these devices. The purpose of this thesis is to investigate the impact of the material on the system performance and to examine one particular desiccant material in detail.

In the first part of this study, the thermo-physical properties of one relatively new desiccant material that is used in a commercially available energy recovery regenerator is experimentally investigated and analyzed. Existing theories for rotary heat and mass exchangers are applied to the experimental data in order to estimate the performance of this material and compare it to other materials that are commonly used in this type of regenerators.

However, the existing models can describe the regenerator performance only within a very limited range of operating parameters, and therefore a new model is developed that allows regenerator performance estimates for all operating conditions that typically occur when the regenerators are operated in air-conditioning systems. A computer program based on the newly developed model is written, and the effect of various operating parameters, such as air inlet conditions and regenerator rotation speed, on the air outlet properties and on the energy recovery is investigated with this program.

Simulations over longer periods of time are run for both summer and winter conditions and the resulting benefits of rotary regenerators in air-conditioning systems are discussed with respect to their relatively high first cost.

Finally, an experimental examination of the possible transfer of hazardous compounds from the exhaust to the supply side of the rotary regenerator is made. This topic is of interest since even a small exchange of these contaminants can diminish the purpose of an air conditioning system - to supply a room or building with clean air at comfortable conditions - tremendously.

1.1 Rotary Regenerators

In rotary heat exchangers, heat is transferred from the hot fluid to a solid energy carrier (the matrix) during the first period, and, during the second period, from the solid to the cold stream. Continuous operation is permitted by rotating the matrix cyclically from one air stream to the other (Figure 1.1). Rotary heat exchangers also allow mass (water) transfer between the two air streams if the matrix contains a water adsorbing desiccant. In this case the heat exchangers exchange both sensible and latent energy, and at operating conditions where the total amount of transferred energy is at its maximum, they are referred to as enthalpy exchangers.

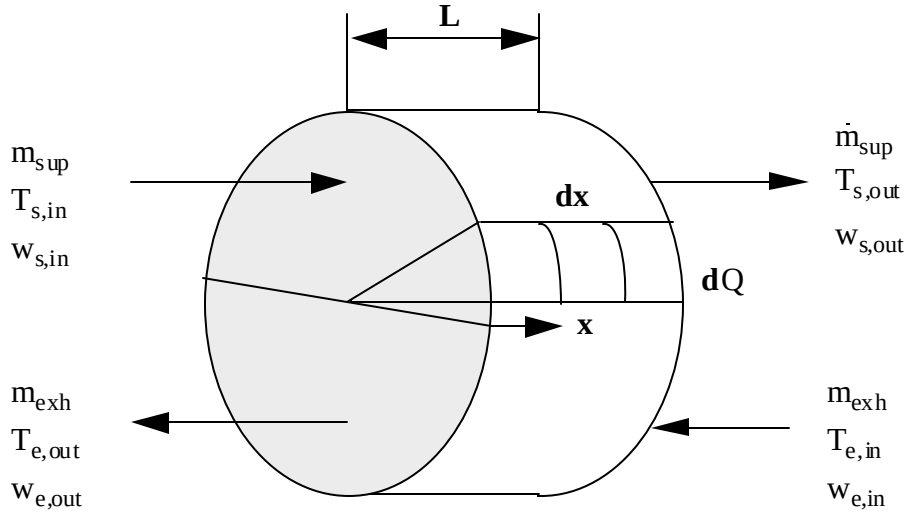

Figure 1.1: Matrix of a Rotary Regenerator

The matrices of the rotary regenerators investigated in this study consist of an aluminum foil that is coated with a desiccant material in the case of an enthalpy exchanger. As shown in Figure 1.2, one layer of folded aluminum foil is positioned between two layers of flat foil in order to form small triangular passes through which the air flows during operation. Spokes provide stability for the structure and assure that the aluminum foil does not vibrate when air is blown through the matrix.

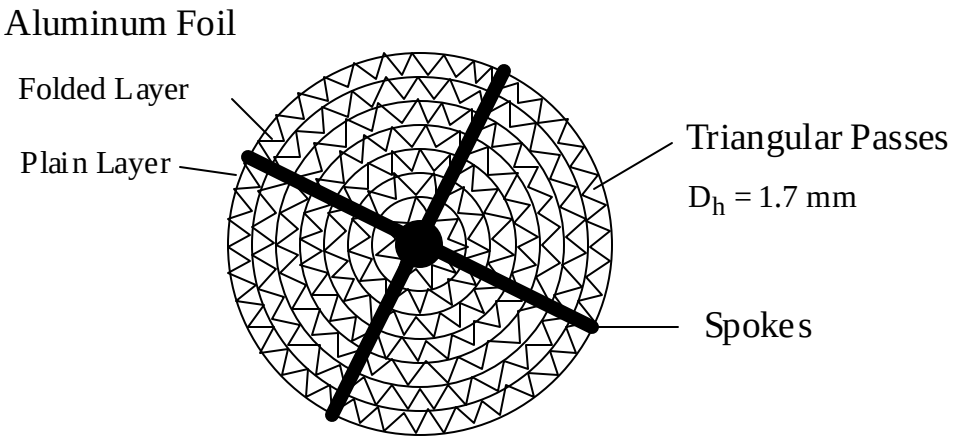

Figure 1.2: Matrix Structure

1.2 Performance Characteristics

Compared to rotary heat exchangers that transfer sensible heat only, enthalpy exchangers have several advantages. The most important advantage of an enthalpy exchanger is that the total amount of energy that can be recovered from the exhaust air stream is significantly higher due to the contribution of latent heat. Bowlen [5] states that the energy recovery in the cooling/dehumidifying mode can be up to 2.5 times greater than for an equally sized sensible heat exchanger, and approximately 40% greater in the heating/humidifying mode. These figures will be quantified in the annual performance simulations presented in Chapter 6.

Furthermore, enthalpy exchangers can be run at lower outdoor temperatures in the winter without ice blocking the matrix channels, because water is transferred in the adsorbed phase rather than the condensed phase as it is done in sensible heat exchanger matrices. This phenomena has also been observed and described by numerous other authors (i.e., Fisk [16], Holmberg [19], Klein [21], Bowlen [5]).

Figure 1.3 shows a typical application of a sensible heat exchanger or an enthalpy exchanger in a space-conditioning system, which will be used to briefly discuss the basic performance differences between these two exchangers. In both cases, the hot outdoor air (state 1) is precooled by the colder exhaust air (state 5) through the regenerator during the summer, while it is preheated by the exhaust air in a winter application. The remaining part of the cooling/heating load has to be made up by conventional cooling or heating equipment for either regenerator type.

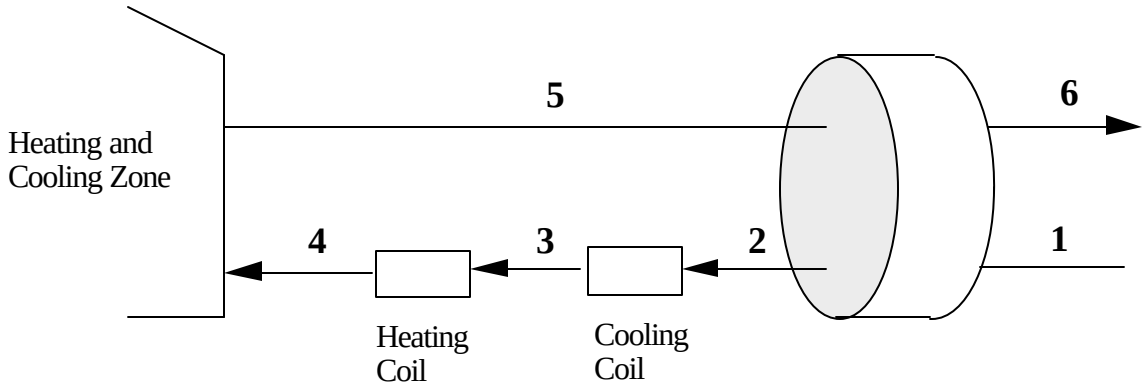

Figure 1.3: Air-Conditioning System with Regenerative Recovery Unit

The performance difference between heat- and enthalpy exchangers can best be seen if the air inlet and outlet states are plotted on a psychrometric chart. Figure 1.4 and Figure 1.5 show these charts for a sensible heat- and an enthalpy heat exchanger, respectively, in a summer application. The heat exchanger transfers sensible heat only and therefore the humidity ratios of the two air streams remain constant throughout the process (states 1 and 2 and states 5 and 6 are on horizontal lines). The enthalpy exchanger can transfer both sensible and latent heat, so that the humidity ratios change during the combined heat and mass transfer process, and the outlet states (states 2 and 6) are now on a straight line between the two inlet states (states 1 and 5). If lines of constant enthalpy are added to the chart, it becomes apparent that the amount of energy that can be recovered by the enthalpy exchanger is substantially greater than the amount of energy recovered by a sensible heat exchanger. Therefore the additional load, that has to be met with the cooling coil,

can be decreased.

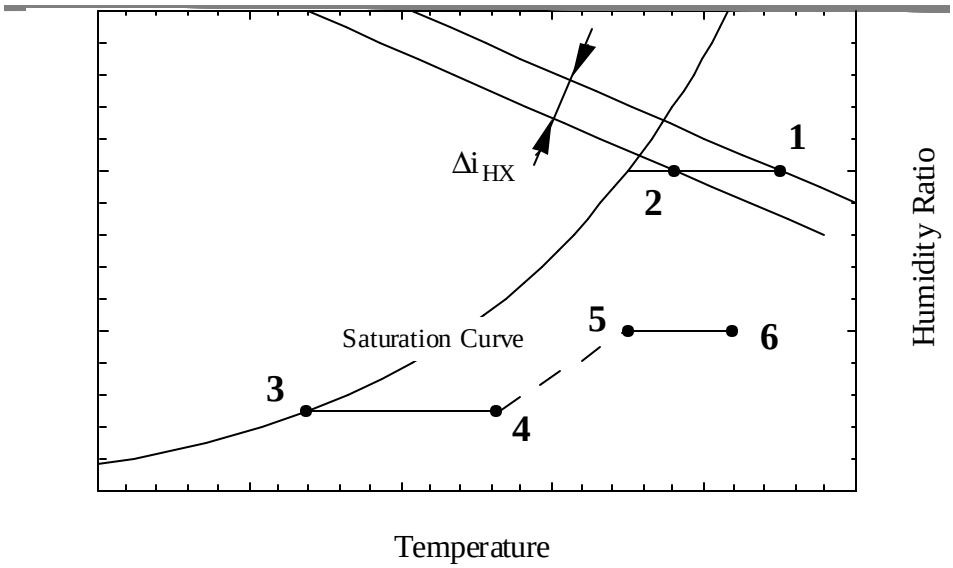

Figure 1.4: Air Cooling Using a Sensible Heat Exchanger

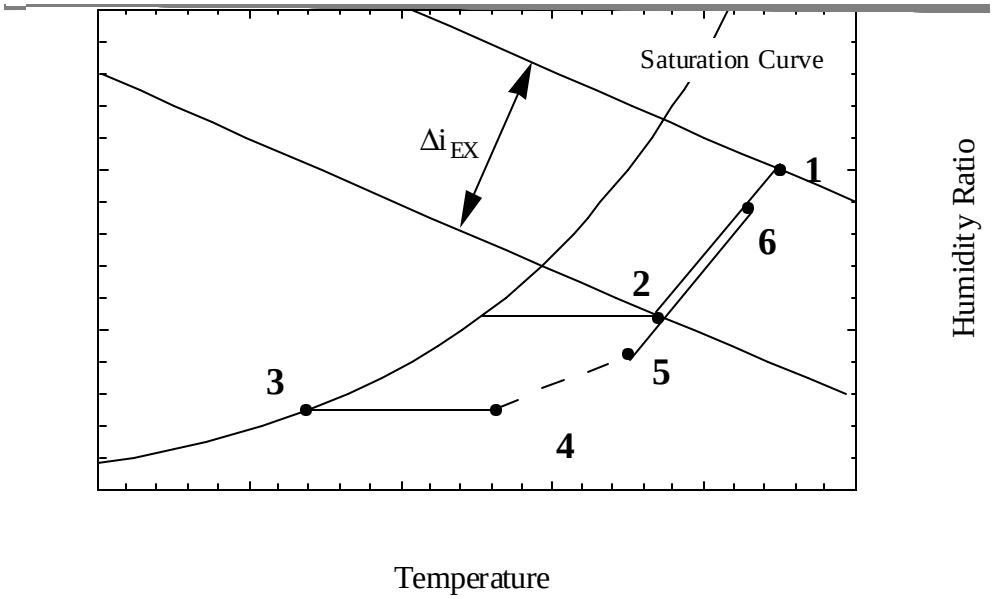

Figure 1.5: Air Cooling Using an Enthalpy Exchanger

The operating characteristics in the heating/humidifying mode are shown in Figure 1.6 and

Figure 1.7 for a heat exchanger and an enthalpy exchanger, respectively. In this case the enthalpy exchanger raises the supply air stream humidity to a more comfortable level (state 2) without the need of an additional, energy consuming humidification equipment.

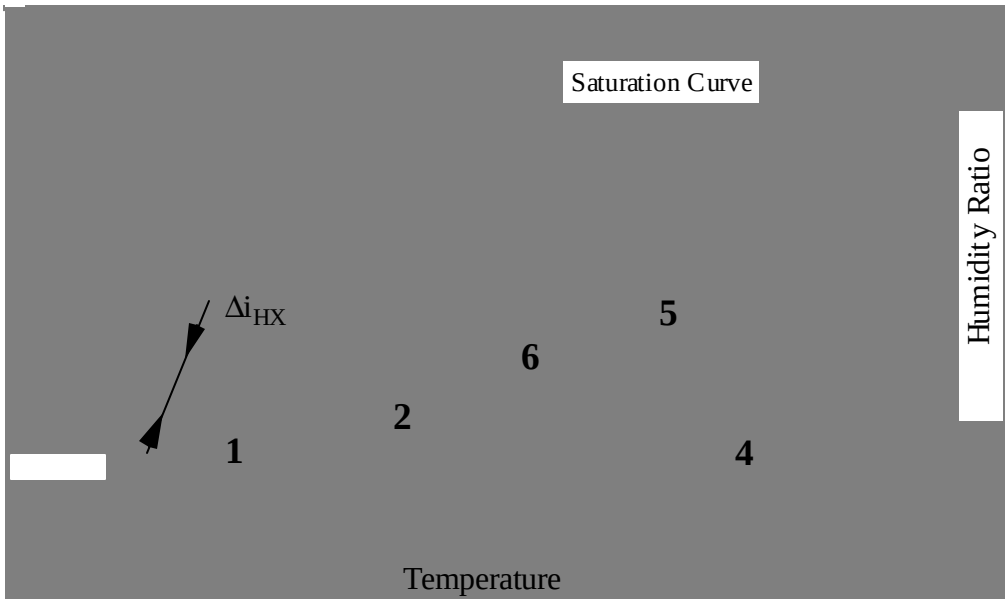

Figure 1.6: Air Heating Using a Sensible Heat Exchanger

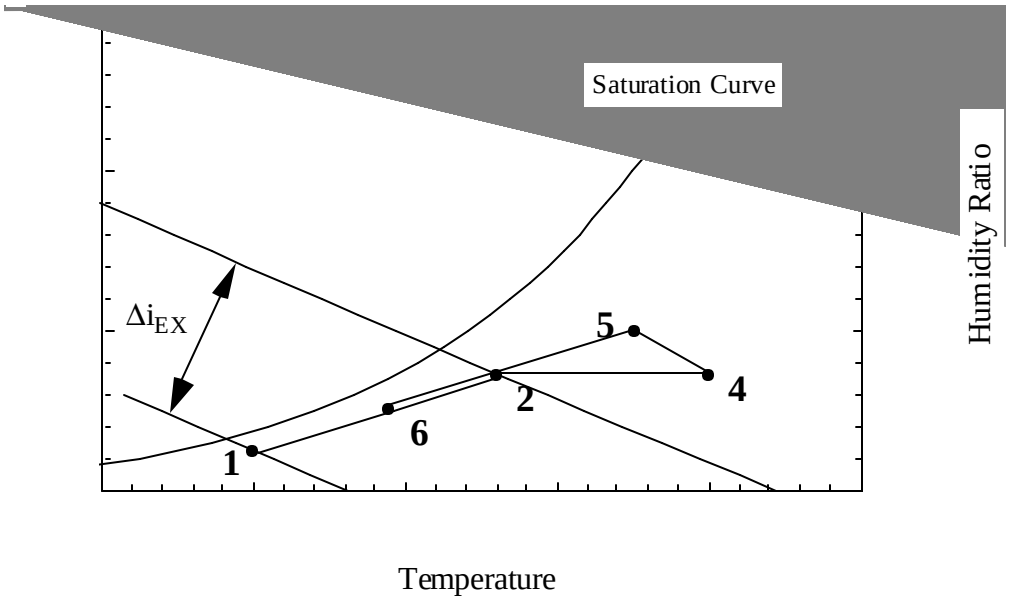

Figure 1.7: Air Heating Using an Enthalpy Exchanger

The fact that the outlet states (states 2 and 6) are on a straight line between the inlet states

(states 1 and 5) for an enthalpy exchanger, results also in the advantage that this regenerator can be operated at its maximum possible effectiveness at lower ambient temperatures without condensation in the exhaust stream that can freeze and block the matrix if temperatures are below 0°C. For the particular inlet conditions shown in Figures 1.6 and 1.7, the sensible heat exchanger can only be operated at a temperature effectiveness of 40% without condensate accumulating on the matrix, whereas the enthalpy exchanger can still run at its optimum effectiveness, which is typically between 70% and 80% for rotary regenerators. This advantage especially pays off in cold winter climates, such as in Madison, WI, where enthalpy exchangers can run at high efficiencies for many more hours than heat exchangers, and therefore allow energy savings that exceed those of heat exchangers by even more than the fraction of the transferred latent energy.

It should be noted at this point, that the outlet states of enthalpy exchangers will only be on a straight line between the inlet states if the Lewis number of the matrix material is equal to unity. This dimensionless parameter is defined as the ratio of the number of transfer units for heat transfer to the number of transfer units for mass (humidity) transfer:

$$Le = \frac{NTU_T}{NTU_w} \tag{1.1}$$

It depends on the type of desiccant used and the mass transfer resistance within the desiccant which is related to the thickness of the desiccant coating. The effect of Lewis numbers greater than one, which is a decrease in the humidity transfer effectiveness, on the enthalpy exchanger outlet states for a fixed pair of inlet states is shown in Figure 1.8.

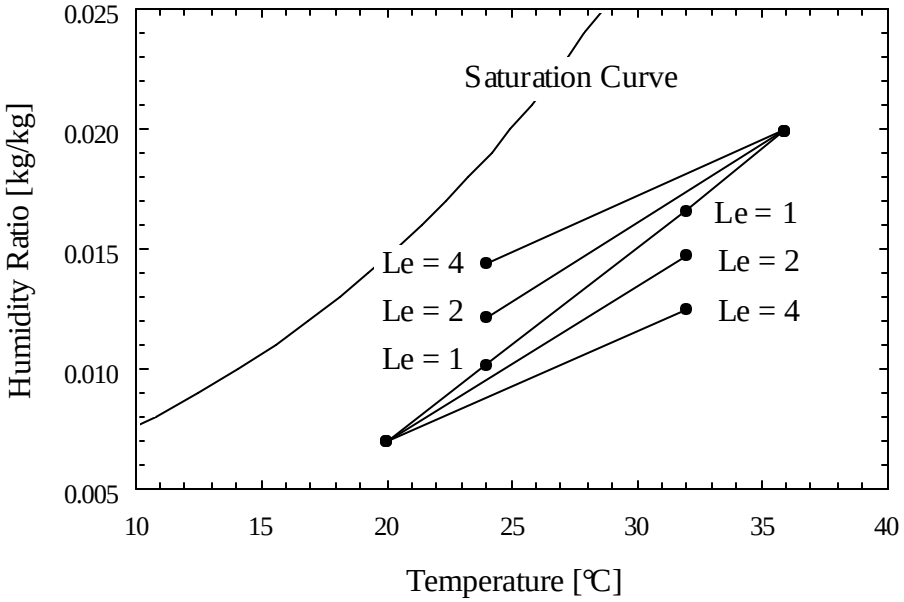

Figure 1.8: Enthalpy Exchanger Outlet States for Various Lewis Numbers

There is no easy way of measuring Lewis numbers and values for this parameter suggested by various authors in the literature differ considerably (Holmberg [19] and Schultz [31] suggest a Lewis number of unity whereas Van den Bulck [36] suggests numbers between two and four).

A constant Lewis number of one was assumed in this study. This assumption might over predict the energy recovery, but it was chosen because it represents the best possible case as opposed to the worst possible case represented by the sensible heat exchanger which has an effective Lewis number of infinity.

2 ADSORPTION FUNDAMENTALS

The performance of a solid desiccant regenerative enthalpy exchanger as it is shown in Figure 1.1 is not only a function of the geometric matrix design but also of the thermo-physical equilibrium properties of the desiccant (Van den Bulck [36]). These properties include the adsorption isotherms for water vapor, the isosteric heat of adsorption and the thermal capacity of the dry solid desiccant.

Two kinds of adsorption exist, one is physical adsorption, the other is chemisorption. Physical adsorption is a reversible process and occurs when relatively weak intermolecular forces cause the adsorption. Chemisorption involves a chemical reaction between the adsorbing and the adsorbed molecules, and the process is generally irreversible. However, the effect of chemisorption on the enthalpy exchanger performance is negligible (Van den Bulck [36]), and therefore it is not dealt with in this study.

2.1 Physical Adsorption

The process of physical adsorption of gases on solid surfaces has been examined for a long time, and there are numerous technical papers and several reference handbooks which cover the subject in detail (i.e., Barrer [3], Gregg and Sing [17], Ruthven [29]). The International Union of Pure and Applied Chemistry (Sing [32]) has published a monogram that provides the exact definitions and nomenclature to use in the discussion of physical adsorption. The adsorbable gas is the adsorptive, the adsorbing solid is the adsorbent and the adsorbed phase is the adsorbate. The following description is based on the cited literature references.

Physical adsorption is a phenomena that occurs when a gas or a liquid gets into contact with a solid surface. In contrast to the process of absorption where the molecules of the absorbate

penetrate into the volume of the absorbent, adsorption is a phenomena in which the adsorbed molecules do not diffuse into the lattice of the solid. Molecules of the adsorptive attach to or detach from the surface of the solid in a dynamic transfer process, and the molecules that accumulate on the surface form an interfacial layer that has properties similar to the liquid phase of the adsorptive. The attraction to the surface is caused by weak, intermolecular Van der Waals forces, which, in case of a pure substance, produce the phase change from gas to liquid. The process of adsorption is reversible for many adsorbate-adsorbent systems.

2.2 Adsorbent Classification

In order to adsorb a large amount of adsorptive, the adsorbing solid needs to have a large surface area per unit of mass or volume. Therefore typical adsorbents are either porous solids or porous compacts of powders. Their specific internal surface area, expressed as area per mass [m^2/kg], is often many orders of magnitude greater than their outer surface area. The adsorbents are conventionally classified according to the average diameter of their inner pores which vary from less than 20 A° for micro-porous adsorbents to more than 500 A° for macro-porous adsorbents. In general three different ranges of diameters are distinguished and these adsorbent types have different adsorption characteristics and are studied and modeled separately. These groups are referred to as micro-porous, meso-porous and macro-porous adsorbents.

Another characteristic property of adsorbents is their adsorption isotherm which is defined as the adsorption capacity in [kg of adsorbed gas / kg of adsorbent] as a function of

temperature and vapor pressure. The International Union of Pure and Applied Chemistry (Sing [32]) has accepted a classification of 6 different adsorption isotherms. Representative shapes for these types are shown in Figure 2.1.

The isotherm types No. 1 and No. 3 are the most common ones and they are also relevant for this study.

Type I isotherms are characteristic for micro-porous adsorbents. The adsorption-desorption loop is reversible and the water uptake governed by the filling of the internal pore volume rather than the coverage of the internal surface area. The vapor molecules within the pores are subjected to a continuous force field generated by the surrounding surfaces. Examples of this important class of adsorbents are various types of charcoal and silica gel (Van den Bulck [36]).

Adsorbents that are characterized by type III isotherms are non-porous or macro-porous solids like polymers, graphitized carbon or silica aerogels. The intermolecular forces between the adsorptive molecules are much greater than the forces between the adsorbent and the adsorptive. As it will be shown in the following sections, the polymer desiccant investigated in this study is characterized by such a type III isotherm.

The type II isotherm is characteristic for non-porous surfaces, macro-porous adsorbents and some compacted powders. The B.E.T. theory, named after its developers Brunauer, Emmett and Teller, is accepted as the standard to predict the adsorption/desorption process for this kind of isotherms. Examples for materials with type II isotherms are graphitized carbon, and compact powders of silica.

Hysteresis is characteristic for type IV and type V isotherms. This phenomena is traditionally explained by the occurrence of capillary condensation within ink-bottle type pores and it is most often observed for meso-porous adsorbents. The intermolecular forces for the type IV isotherm are similar to those for type I and II isotherms. The adsorption of water vapor on low-density silica gel is an example for type IV. The type V isotherms are similar in nature to type III, except that the average pore size is smaller. Examples are the adsorptions of organic vapors on

meso-porous adsorbents.

Type VI isotherms illustrate the stepwise adsorption in multilayers on a non-porous surface or a macro-porous adsorbent, and is similar to the type II isotherm. Each step represents the coverage of a subsequent monolayer. This type of adsorption is fairly rare, i.e., the adsorption of argon or krypton on graphitized carbon at cryogenic temperatures.

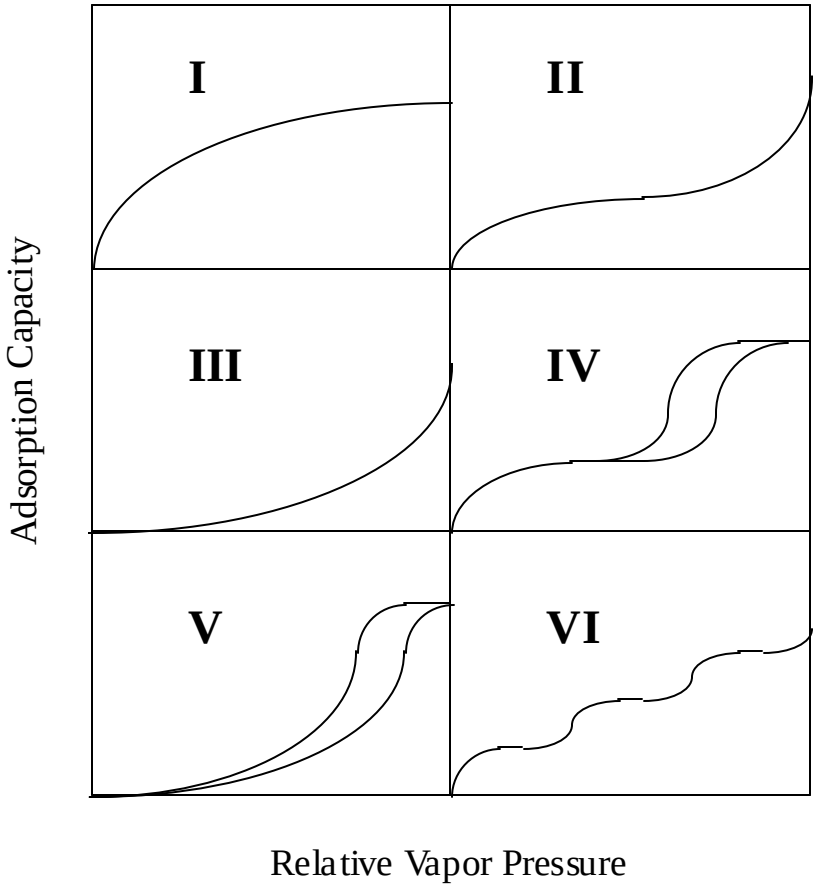

Figure 2.1: Classification of Adsorption Isotherms Accepted by the International Union of Pure and Applied Chemistry

2.3 Potential Theory of Adsorption

The adsorption capacity of a desiccant material is not only dependent on the relative humidity of the surrounding air but also on its temperature. Thus, the relation of capacity to both temperature and relative humidity must be known in order to determine the performance of a rotary enthalpy exchanger. It is convenient to find a function that involves both of these parameters and allows prediction of the desiccant adsorption capacity at any given temperature-humidity combination. Such a function is given by the Polanyi theory which was first introduced by Polanyi [28] and further developed by Dubinin [14].

Polanyi introduced the so-called adsorption potential, A, and assumed that the adsorption capacity W_m of an adsorbent is a function of A only:

$$A = RT \ln\left(\frac{p_s}{p_v}\right) \tag{2.1}$$

$$W_m = f(A) \tag{2.2}$$

p_v represents the actual vapor pressure and p_s the saturation pressure at the corresponding temperature. Using the definition of A (Equation 2.1), the Polanyi assumption (Equation 2.2) and the Clausius-Clapeyron equation for the differential heat of adsorption, it can be shown that the adsorption potential A is the difference in Gibbs free energy between the adsorbed phase and the saturated liquid phase of the adsorptive at the same temperature (Van den Bulck [36]).

The advantage of this theory is that the adsorption capacity W_m is reduced to a function of only one variable and therefore the entire temperature and humidity ranges can be shown in one characteristic curve. Dubinin [14] examined experimental adsorption equilibrium data for many systems and showed that this characteristic curve can often be approximated by the equation:

$$W_m = W_o \exp\left[-\left(\frac{A}{E_o}\right)^n\right] \tag{2.3}$$

where W_o is the total micro-pore volume, and E_o is the characteristic energy of adsorption. Since this equation has been shown to apply only to homogeneous systems of pores, a more complex equation, referred to as the Dubinin-Polstyanov equation [14], is often used to calculate the adsorption capacity of an adsorbent:

$$W_m = W_{o,1} \exp\left[-\left(\frac{A}{E_{o,1}}\right)^{n_1}\right] + W_{o,2} \exp\left[-\left(\frac{A}{E_{o,1}}\right)^{n_2}\right] \tag{2.4}$$

This expression will be used in later sections to describe the adsorption behavior of both the water-based polymer desiccant and regular density silica gel.

3 ADSORPTION ISOTHERM MEASUREMENT - WATER VAPOR

The purpose of the measurements reported in this thesis is to determine adsorption isotherms of the examined desiccant matrix material at equilibrium conditions. In order to be able to fit a Polanyi-function, that has to be valid over a range of temperatures and humidities, to the measured data, the desiccant adsorption capacity needs to be measured at several different temperatures and relative humidities.

3.1 Experimental Apparatus and Procedures

3.1.1 Desiccant Samples

In the beginning the adsorption capacity of four different matrix materials was investigated. The samples were in form of the desiccant coated aluminum foil, used as a matrix in rotary enthalpy exchangers as shown schematically in Figure 1.2. The solid material stores energy and transfers it by rotation between the two air streams that are passed in counterflow configuration through the triangular flow channels.

The 6.35×10^{-5} m thick foil was cut to sizes of approximately 10 cm by 20 cm, resulting in a dry sample weight of round about 4 g. One sample was an uncoated 1145 H19- aluminum foil as used in matrices of heat exchangers that transfer sensible heat only. This material was also the base for the other three samples where the same aluminum foil was coated with a desiccant.

The second sample was coated with acrylate monomers / polymers applied in a solvent solution and has been used in many enthalpy exchanger applications. The third sample was coated with aluminum boehmite ($Al_2O_3 \cdot H_2O$) and has also been used for some time. Due to environmental

concerns relating to the solvent, these two materials are being phased out of use.

The desiccant material that is intended to replace these two was represented by the fourth sample. In this material, the desiccant is applied with water as the solvent and it is said to contain less than 1% hazardous ingredients per overall coating weight. This desiccant is basically made of two polymers dissolved in water and several inert coating conditioners in lower concentrations.

Since the water-based polymer desiccant is supposed to replace the older materials, this study concentrates on the properties of this material and on the performance of enthalpy exchangers using it as their matrix.

3.1.2 Experimental Setup

In order to measure the weight of the dry or humid samples, they were placed in a closed jar containing air of the desired relative humidity (Figure 3.1). The temperature was controlled by placing the jar into an oven or refrigerator and after an equilibrium state was reached the samples were taken out of the jar and were weighed on a digital scale whose last significant digit is 0.0001 g.

The dry weight was determined by hanging the sample above a very strong hygroscopic material which adsorbs the water vapor in the air within the jar. Therefore the relative humidity of the air around the sample becomes essentially zero and the water initially adsorbed by the sample is desorbed into the air and adsorbed by the hygroscopic material at the bottom of the jar. In this study phosphorus pentoxide was used to dry the sample, and at a temperature of 22°C it took approximately 12 hours until an equilibrium state was reached. The dry weight of each sample was measured 4 times in order to determine an estimate of the experimental error. It turned out that the deviation in the results of the four independent measurements is very small (0.05% to 0.15%), which suggests that the uncertainty involved in this measurement is negligible.

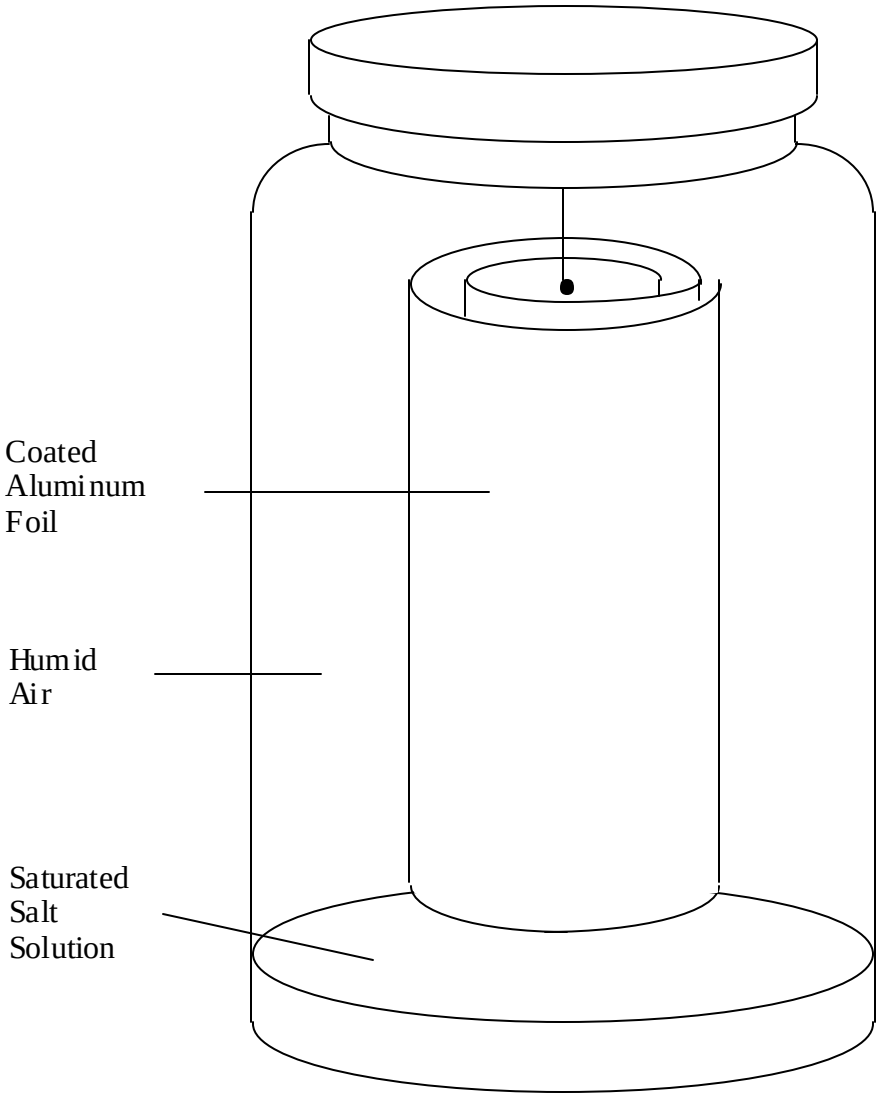

Figure 3.1: Experimental Setup

Relative humidities between 1% and 100% can be achieved by placing a suitable salt-water-solution below the sample in the jar. Pure water will result in a relative humidity of 100% in the air. This value can be lowered by dissolving certain amounts of salt in the water. Values for the reduction of the vapor pressure in the air are given for various salts, as a function of the salt concentration, in the CRC Handbook of Tables for Applied Engineering Science [13].

However, because of the small amount of solution it is rather difficult to tailor a very exact concentration, and therefore only saturated solutions of three different salts were used in this experiment. Saturated solutions can be obtained fairly easy by putting such an amount of salt into distilled water that the salt cannot be further dissolved and a visible sediment remains. If the water temperature during the mixing process is maintained higher than the temperature required for the adsorption capacity measurement, the salt dissolves quickly and the risk of having a solution that is not quite saturated can be eliminated.

A correlation for the relative humidity above saturated solutions of many salts in terms of temperature is provided in the CRC Handbook of Chemistry and Physics [12]:

$$j = A \cdot \exp\left[\frac{B}{T}\right] \cdot 100\% \tag{3.1}$$

where T is the thermodynamic temperature in degrees Kelvin and A and B are constants which are valid in a specified temperature range. For the three chosen salts these constants are given in Table 3.1, and within the given temperature range the equation is generally accurate to ±2%.

Salt	**Formula**	**Temperature Range**	***A***	***B***
Magnesium Chloride	$MgCl_2 \cdot 6H_2O$	5 - 45°C	29.26	34 K
Sodium Chloride	NaCl	10 - 40°C	69.20	25 K
Potassium Nitrate	KNO_3	0 - 50°C	43.22	225 K

Table 3.1: Constants for Calculation of Humidity Above Saturated Salt Solutions

Saturated solutions of the mentioned salts lead to relative humidities of approximately 33%, 75% and 92% and combined with the values for 0% and 100% relative humidity, five data points are provided to characterize the humidity spectrum.

The adsorption capacity of the desiccant at each of these humidities was measured at temperatures of 5°C, 22°C and 40°C. Each temperature-humidity combination was measured at least ten times in order to determine the uncertainty involved in these measurements. The time that was required to reach the equilibrium was different for each salt and temperature, but in general an

equilibrium was established within 12 hours.

Since the desiccant sample had to be taken out of its equilibrium surroundings in order to measure its weight, and since the weight change was very rapid in the first seconds after the sample came into contact with non-equilibrium air, the weight was determined 10 s, 20 s, 30 s, 45 s and 60 s after opening the jar. Thereafter the equilibrium weight at time zero was extrapolated from the measured weight-time function.

3.2 Experimental Data and Analysis

3.2.1 Maximum Adsorption Capacity

A major reason for measuring the maximum adsorption capacity of the various materials was to get a first idea of how the new water-based desiccant behaves compared to the two older materials and to learn something about the equilibrium time, thus the speed of adsorption and desorption. After the samples were taken out of the jars that contained a small amount of pure water at 22°C below the samples, resulting in a relative humidity of 100%, they were placed in a surrounding of T = 22°C and j = 25% to 30%. The change in weight and therefore the change in water content was determined as a function of time. Weight versus time curves for the three different desiccant materials are shown in Figure 3.2.

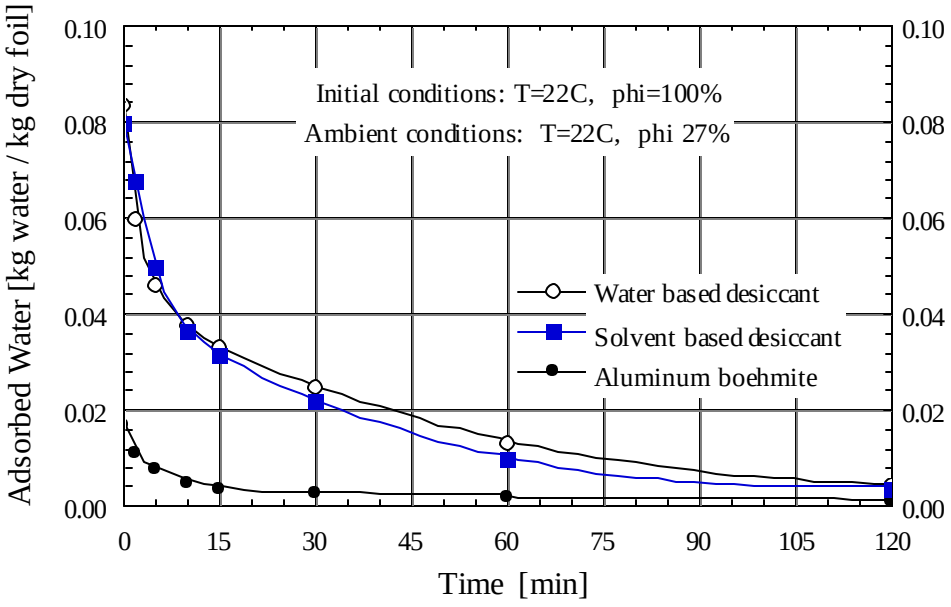

Figure 3.2: Maximum Adsorption Capacity and Desorption Velocity

The plot shows that the aluminum boehmite sample adsorbs much less water than the solvent- and the water-based samples which adsorb approximately equal amounts of water at these conditions. The rate at which water is desorbed after the samples are exposed to ambient conditions is also very similar for both the solvent- and the water-based desiccants. These results suggest that there will probably be little difference in the performances of enthalpy exchangers using these two materials as their matrix.

The fact that the adsorption-time functions are almost horizontal after the relatively short time of two hours shows that the rate of adsorption and desorption is rather high. For this reason, a time of 12 to 15 hours within surroundings of constant temperature and relative humidity should be well in excess for the samples to reach an equilibrium when the adsorption capacity is measured.

3.2.2 Equilibrium Adsorption Isotherms

The equilibrium adsorption isotherms of a desiccant matrix material have to be known in order to estimate the performance of enthalpy exchangers. These isotherms were determined for the new water-based polymer desiccant. Four similar samples of the same material were examined in the way described in Section 3.1. The average values for the adsorption capacity as a function of temperature and relative humidity are shown in Table 3.2, and the three determined equilibrium adsorption isotherms for 5°C, 22°C and 40°C are plotted in Figure 3.3.

	T = 5 °C	**T = 22 °C**	**T = 40 °C**
j **= 0**	0	0	0
j **= 33%**	0.00840	0.00350	0.00204
j **= 75%**	0.02246	0.01429	0.01090
j **= 92%**	0.05786 (φ = 97%)	0.03900 (φ = 92.4%)	0.02532 (φ = 88.7%)
j **= 100%**	0.08527	0.08527	0.08527

Table 3.2: Adsorption Capacity as a Function of Temperature and Relative Humidity

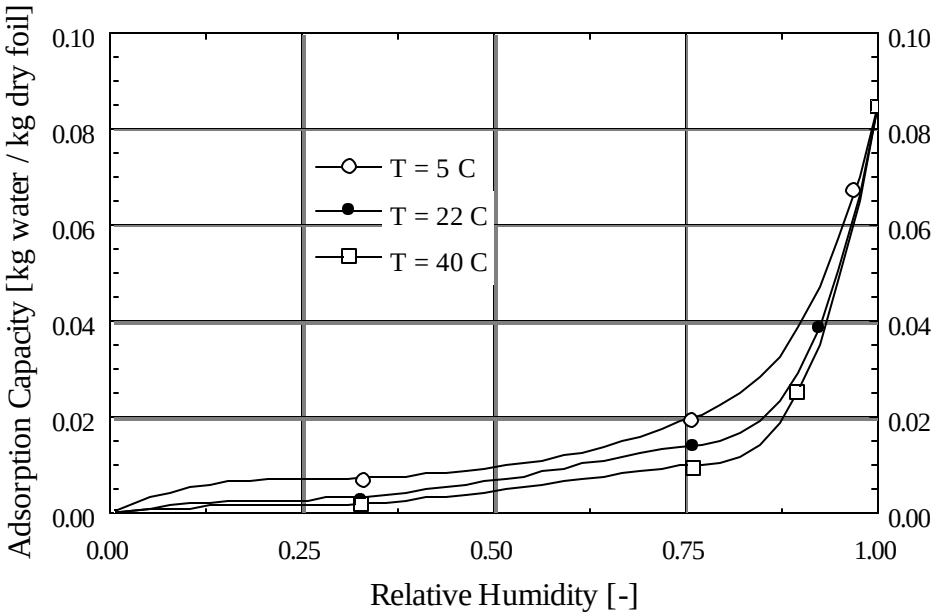

Figure 3.3: Equilibrium Adsorption Isotherms of Water-Based Desiccant

The isotherms show a type III characteristic as it is often found for polymers. Ruthven [29] describes this isotherm type as unfavorable for applications in adsorption columns and regenerative dehumidifiers, but no literature was found by the author that states the advantages or disadvantages of this isotherm type for applications in enthalpy exchangers. A detailed comparison of the performance characteristics for various operating parameters between a typical type I matrix (regular density silica gel) and the water-based polymer desiccant type III matrix will be done in Chapter 5.

The adsorption capacity increases with decreasing temperature for constant relative humidities as seen in Figure 3.3. This behavior is described for many other desiccant materials in the literature as well, and the temperature independence at 100% relative humidity has also been observed for silica gel by many authors (Van den Bulck [36]).

3.2.3 Polanyi-Approximation

The average results for the adsorption capacity as a function of temperature and relative humidity shown in Figure 3.3 were used to apply the Polanyi adsorption theory. The measured adsorption capacities of the water-based desiccant were fit to the Dubinin-Polstyanov equation (Equation. 2.4) as a function of the adsorption potential A using the spreadsheet program Kaleidagraph [34]. The constants $W_{o,1}$, $W_{o,2}$, $E_{o,1}$, $E_{o,2}$, n_1 and n_2 in the equation were optimized with the constraint that the sum of $W_{o,1}$ and $W_{o,2}$ must be equal to the maximum adsorption capacity at 100% relative humidity. The equation that best fits the measured data is:

$$W_m = 0.03878 \cdot \exp\left[-\left(\frac{A}{618.9}\right)^{0.4857}\right] + 0.04668 \cdot \exp\left[-\left(\frac{A}{193.5}\right)^{1.546}\right] \qquad (3.2)$$

where the adsorption capacity W_m is given in kg adsorbed water per kg matrix weight. The resulting curve and the average values of the measured data are shown in Figure 3.4. The original Dubinin-Polstyanov equation suggests small integer numbers for the exponents n_i, but in this case two real numbers were chosen because they result in a better curve fit of the experimentally obtained data.

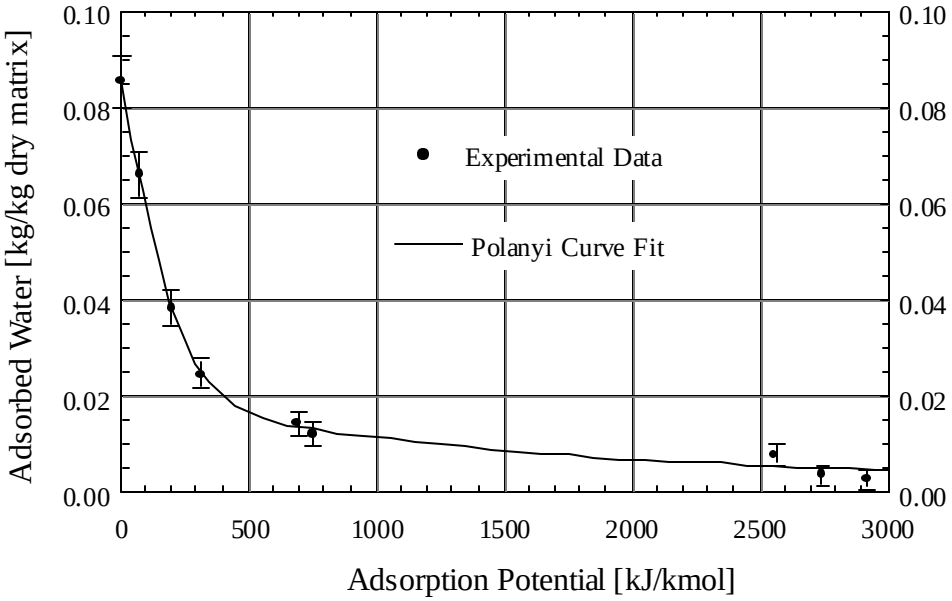

Figure 3.4: Experimental Data and Polanyi Curve Fit

3.2.4 Experimental Uncertainties

Two kinds of uncertainty errors exist:

1. Bias error, represented as U_B
2. Precision error, represented as U_P

Bias and precision errors are defined by Coleman and Steele [10] as follows:
"The bias error (U_B) is the fixed, systematic or constant component of the total error and is sometimes referred to simply as the bias. The precision error (U_P) is the random component of the total error and is sometimes called the repeatability or repeatability error."

The two errors are combined to the total uncertainty in one of the following two ways:

1. $(U_{RSS})^2 = (U_B)^2 + (U_P)^2$ (3.3)

2. $U_{Add} = U_B + U_P$ (3.4)

Coleman and Steele state that the root-sum-square uncertainty (U_{RSS}) yields a confidence interval of approximately 95%, while the additive uncertainty (U_{Add}) yields a confidence interval of approximately 99% if both parts of the error are of the same order of magnitude, and approximately 95% confidence if one is small relative to the other.

If the parameter whose uncertainty is to be determined appears in its defining equation explicitly, the error can be estimated by multiplying its partial derivative with respect to a parameter whose uncertainty is known or can be measured by the uncertainty of that parameter. For example, f is a function of a and b and the uncertainties of a and b are known:

$$f = f(a, b), \quad U_a = \text{known}, \quad U_b = \text{known} \tag{3.5}$$

The uncertainty of U_f can be calculated as it is shown below:

$$U_{fa} = \frac{\partial f_a}{\partial a} \cdot U_a \ , \quad U_{fb} = \frac{\partial f_b}{\partial b} \cdot U_b \tag{3.6}$$

$$U_f = \sqrt{\left(U_{fa}\right)^2 + \left(U_{fb}\right)^2} \tag{3.7}$$

In case the parameter whose uncertainty is to be estimated is given implicitly or the defining equation is not exactly known, the error can still be found by measuring the parameter several times and calculating the Gaussian standard deviation. As noted by Bronstein and Semendjajew [6] an interval of twice the standard deviation to each side of the mean value yields a probability of 95.4%.

In the following section the uncertainties are calculated for each component that contributes to the measured data and thereafter these errors will be combined to estimate the total uncertainty of

the data.

Relative Humidity:

The uncertainty of the relative humidity is a function of the correlation used to calculate it only (Equation 3.1), since the concentration of the salt solution is exactly saturated, as soon as parts of the salt do not dissolve in the water and become visible at the bottom of the jar (Figure 3.1). The total error of this equation is given in the literature to be ± 2%.

$$U_j = 0.02$$

Temperature:

The bias error of the temperature measurement is assumed to be one half of the last significant digit of the used thermometer, 0.5 Kelvin. The lowest temperature occurring in this measurements is T = 278 K and yields the maximum error.

$$U_{B,Temp} = 0.0018$$

The precision error is due to the fact that the jar that contains the sample (Figure 3.1) has to be taken out of the oven/refrigerator and has to be carried to the scale in an insulated box. During this time the temperature of the system may possibly change. The maximum change is assumed to be no greater than 2 K.

$$U_{P,Temp} = 0.0072$$

The total temperature uncertainty calculated by the root-sum-square method becomes

$$U_{Temp} = 0.0074$$

Adsorption Potential:

The error in the adsorption potential A is a combination of the uncertainties for temperature and relative humidity. Combining the two errors with root-sum-square method the total error of the adsorption potential is

$$U_A = 0.0213$$

Adsorption Capacity:

The bias error is caused by the scale that is used and is assumed to be one half of the last significant digit, 0.00005 gram. The smallest amount of adsorbed water that was measured is approximately 0.05 g and therefore the maximum bias error is

$$U_{B,Wm} = 0.001$$

The precision error exists in part because of the extrapolation that is necessary in order to determine the amount of adsorbed water at that time when the sample is taken out of its equilibrium surroundings. This error has a size of approximately 0.005.

However, the most significant part of the error in the adsorption capacity determination is contributed by the different results that are obtained for repeated measurements under the same conditions. The Gaussian standard deviation was calculated and the uncertainty was assumed to be two times as large as the deviation. The precision error was found to be 0.06 for the mass of the humid samples and 0.002 for the dry weight. The combined precision error becomes

$$U_{P,Wm} = 0.0601$$

and the total uncertainty of the measured equilibrium adsorption capacity is

$$U_{Wm} = 0.0601$$

Appropriate error bars for the overall uncertainty of the adsorption capacity are included in Figure 3.4.

5 INSTANTANEOUS REGENERATOR PERFORMANCE IN VARIOUS CONDITIONS

With the experimentally determined matrix property data documented in Chapter 3 and the mathematical models introduced in Chapter 4, all the tools that are necessary to simulate the performance of an enthalpy exchanger of the specified matrix material and design are available.

Investigations comparing enthalpy exchangers and heat exchangers are based on the same constant supply air mass flow rate of 2.28 kg/s. This number is recommended by the American Society of Heating, Refrigerating and Air-Conditioning Engineers (ASHRAE [2]) for the ventilation of a 200 people office building. An equal flow arrangement is chosen based on the idea that the same amount of air supplied to a building has to be exhausted in order to keep the inside pressure constant: $\dot{m}_{sup} = \dot{m}_{exh} = 2.28 \frac{kg}{s}$.

The matrix design chosen for all simulated regenerators is schematically shown in Figure 1.2. The matrix size recommended by a manufacturer (Carnes, [9]) of rotary regenerators for the specified air flow rate is $D = 1.23$ m in diameter and $L = 0.20$ m length in the flow direction. More detailed dimensions of the design are given in Section 5.1.2 in connection with the estimation of the number of transfer units for the matrix.

Section 5.1 concentrates on the effectivenesses and outlet states of a single regenerator and compares the performances of two different desiccant matrix materials in various weather conditions. The contribution that enthalpy and heat exchangers make to complete space-conditioning systems in both cooling and heating modes is documented in Sections 5.3 and 5.4. Performance estimations are done for exchangers with various Lewis numbers and the benefits of each exchanger type are shown for the cooling mode as well as for the heating mode.

5.1 Comparison Between Polymer and Silica Gel Matrices

The performance differences between two equally designed matrices that are made of different desiccant materials can be determined with the experimentally determined property data for the water-based polymer desiccant that is documented in Section 3.2 and equivalent data found in the literature for silica gel (Van den Bulck [36]).

Klein's [21] model for the case of maximum enthalpy exchange was used to compare the two materials, and the minimum rotation speed required to assure a maximum effectiveness was calculated. Note, that the model predicts the same outlet states for both materials, since the number of transfer units is determined by the matrix design, which is the same for both materials. However, the minimum rotation speed will be different for each material, and here a slower speed is clearly preferred because of possible contaminant carry-over and friction losses at high speeds.

Three different supply air inlet states, characterized by temperature and humidity, were investigated for both systems. The exhaust air states were assumed to be the same for each of the three cases, since it is the purpose of space-conditioning systems to maintain constant, comfortable indoor conditions irrespective of the outdoor climate. The basis for the calculation of the two wave speeds l_i, that affect the required minimum rotation speed, are the arithmetic temperature and humidity ratio averages of the supply and the exhaust air streams.

The Polanyi equation determined in Chapter 3 (Equation 3.2) was used for the calculation of the water-based desiccant, while a similar correlation for silica gel is given in the literature (Van den Bulck [36]).

Water-Based Polymer:

$$W_m = 0.03878 \cdot \exp\left[-\left(\frac{A}{618.9}\right)^{0.4857}\right] + 0.04668 \cdot \exp\left[-\left(\frac{A}{193.5}\right)^{1.546}\right] \qquad (3.2)$$

Silica Gel:

$$W_m = 0.106 \cdot \exp\left[-\left(\frac{A}{8590}\right)^2\right] + 0.242 \cdot \exp\left[-\left(\frac{A}{3140}\right)^2\right] \quad (5.1)$$

5.1.1 Minimum Rotation Speed

According to the results of Klein [21] the ratio G/l_1 must be greater than 1.5 in order to operate the enthalpy exchanger at its optimum conditions, where the effectiveness can be calculated as a function of the number of transfer units only. Since the air mass flow rates and the matrix mass are fixed, the wave speed l_1 of the F_1-potential has to be calculated in order to solve for the minimum rotation speed. This can be done using Equation 4.12.

The coefficients a_1 and a_2 are partial derivatives of the desiccant adsorption capacity W_m, which is given by the Dubinin-Polstyanov Equation (Equation 2.4). Because the adsorption potential A is a function of temperature and relative humidity, which involves both humidity ratio and temperature, the temperature is implicit and it is convenient to calculate the derivatives a_1 and a_2 numerically rather than analytically. This numerical calculation was done with an EES program [22] which is shown in Appendix A. The plots of the adsorption capacity W_m versus air temperature and versus air humidity ratio whose slopes represent a_1 and a_2, respectively, are shown in Figure 5.1 to Figure 5.4 for the water-based desiccant and for silica gel.

The plots show a significant difference between the derivatives (slopes) for silica gel and the water-based polymer desiccant that is caused by the different isotherm types of the two materials (type I for silica gel, type III for the water-based polymer). As a result, the operating characteristics of the two materials are different.

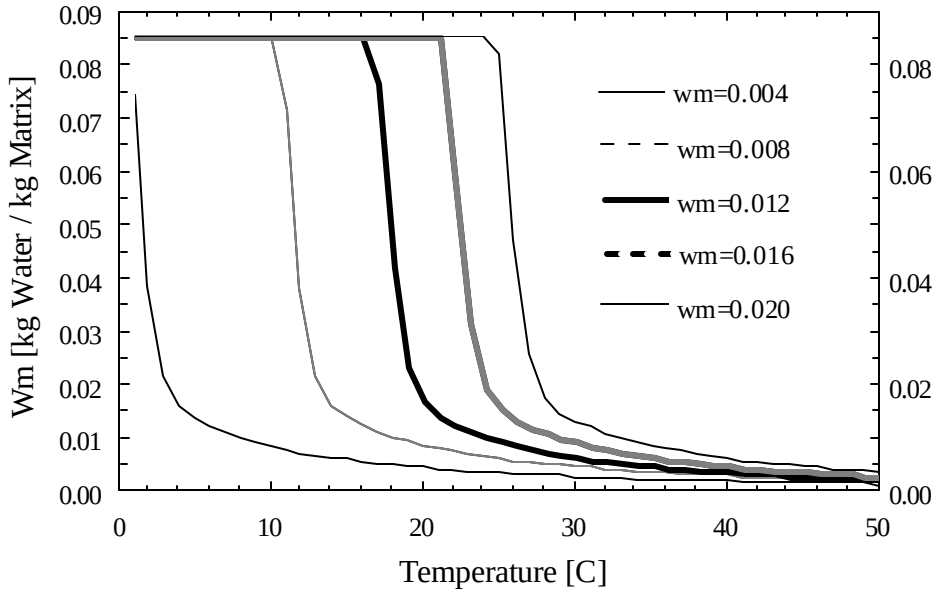

Figure 5.1: Water-Based Polymer: Adsorption Capacity vs. Temperature

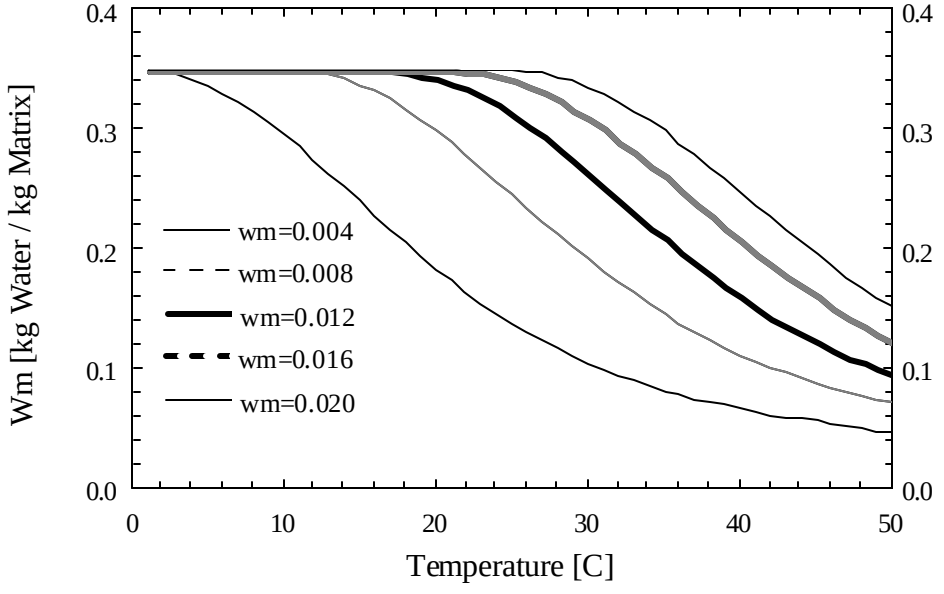

Figure 5.2: Silica Gel: Adsorption Capacity vs. Temperature

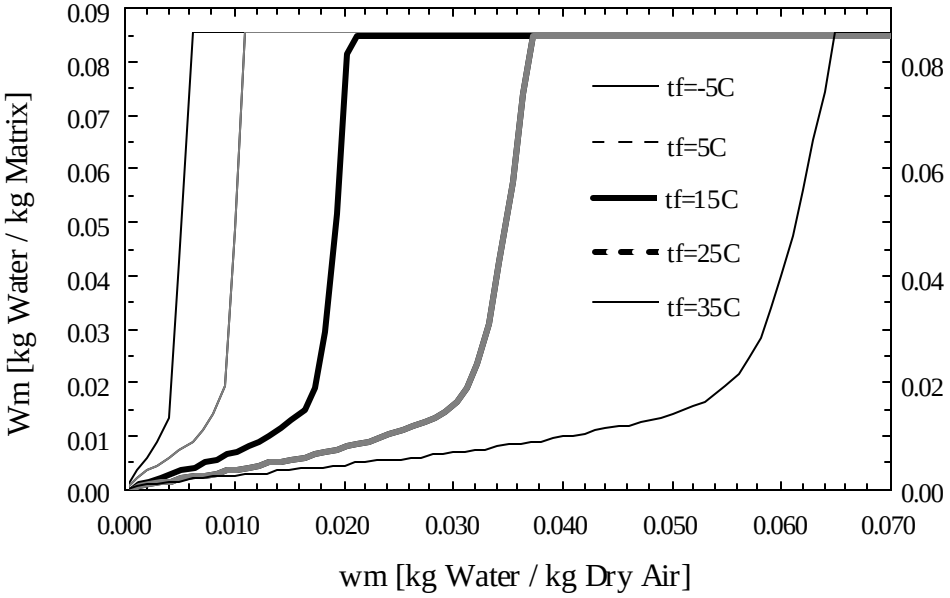

Figure 5.3: Water-Based Polymer: Adsorption Capacity vs. Humidity Ratio

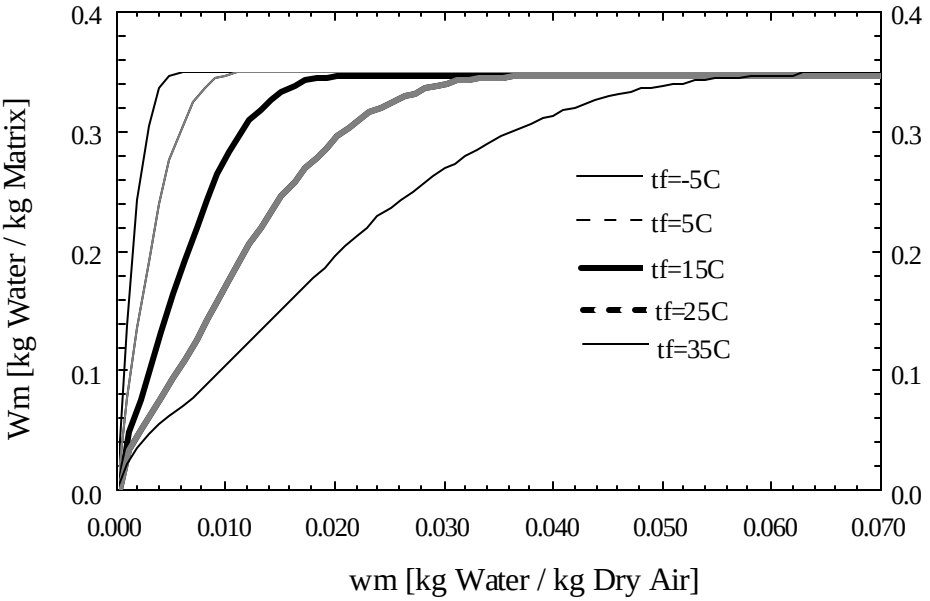

Figure 5.4: Silica Gel: Adsorption Capacity vs. Humidity Ratio

The coefficient a_3 that is defined as:

$$a_3 = \left(\frac{\partial i_f}{\partial T_f} \right)_{w_f} \tag{5.2}$$

is the specific heat of humid air, and it is equal to the sum of the specific heat of dry air, which is assumed to be constant, and the product of humidity ratio and specific heat of water vapor which is also constant:

$$a_3 = c_{p,f} = 1.004 \frac{kJ}{kgK} + w_f \cdot 1.86 \frac{kJ}{kgK} \tag{5.3}$$

The fourth coefficient is defined as:

$$a_4 = \left(\frac{\partial i_f}{\partial w_f} \right)_{T_f} - \left(\frac{\partial I_m}{\partial W_m} \right)_{T_f} \tag{5.4}$$

The first derivative in this equation represents the specific enthalpy of water vapor i_w, while I_m in the second term represents the enthalpy of the matrix and is equal to:

$$I_m = \left(c_{p,m} + W_m \cdot 4.18 \frac{kJ}{kgK} \right) T_f + \int_0^{W_m} \left(i_{fg} - i_s \right) dW_m \tag{5.5}$$

The specific enthalpy of adsorption i_s can be derived from an equation similar to the Clausius-Clapeyron equation for vaporization:

$$\frac{-i_s}{R} = \left(\frac{\partial \ln p_v}{\partial (1/T)} \right)_{W_m} \tag{5.6}$$

Figure 5.5 shows plots of $\ln p_v$ versus $1/T$ (Van't Hoff plots) for a constant amount of adsorbed water. The linearity of these plots indicates that i_s is essentially independent of temperature (Knight [24]).

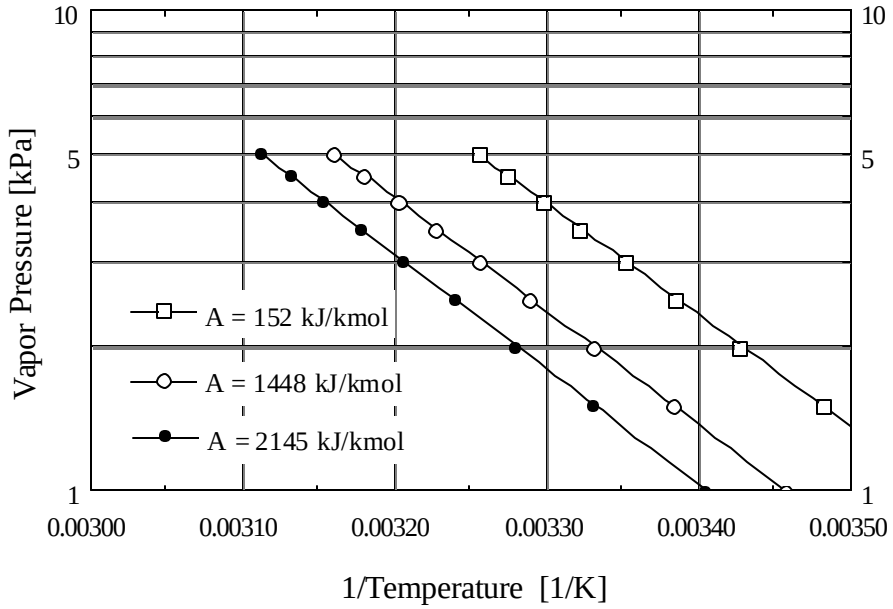

Figure 5.5: Van't Hoff Plots for Constant Adsorption Potentials

Since the lines for different amounts of adsorbed water are parallel, it is assumed that the specific heat of adsorption is constant for the three examined inlet pairs. It is calculated to be:

$$i_s = 2530 \frac{kJ}{kg} \tag{5.7}$$

and the coefficient a_4 becomes:

$$a_4 = i_w - \left(4.18 \frac{kJ}{kg°C} \cdot T[°C] + i_{fg} - i_s \right) \tag{5.8}$$

The values for the specific enthalpies of water can be found in steam tables, i.e. in the appendix of Moran and Shapiro [27].

The last coefficient a_5 represents the specific heat of the matrix and it can be estimated as

the sum of the specific heats of the dry matrix and the adsorbed water

$$a_5 = c_{p,m} + 4.18 \frac{kJ}{kgK} \cdot W_m \tag{5.9}$$

For the water-based desiccant coated aluminum foil the specific heat is assumed to be the specific heat of aluminum (900 J/kg K), since only 5% of the total foil weight is contributed by the desiccant.

The specific heat of silica gel is known as a function of temperature (Van den Bulck [36]).

$$c_{p,m} = 0.917 + \frac{1.578 \cdot T[^\circ C]}{1000} \tag{5.10}$$

Once the dimensionless wave speeds are known, the minimum capacitance rate ratio can be estimated by the constraint:

$$\frac{G_{min}}{l_1} = 1.5 \tag{5.11}$$

and the minimum rotation speed of the matrix is calculated by the definition of G:

$$G_{\min} = \frac{M_m}{T_{j,\max} \cdot \dot{m}_{air}} = \frac{M_m}{\left(\frac{60s}{w_{\min}}\right) \cdot \dot{m}_{air}} \tag{5.12}$$

where the unit of w_{min} is revolutions per minute (rpm). Note, that the density of aluminum foil is approximately 2700 kg/m^3, while the density of silica gel is only 1200 kg/m^3. In order to compare the two materials this fact has to be taken into account by choosing a lower matrix weight for silica gel for the same geometrical design. The calculation of the matrix weight is shown in detail in Section 5.1.2.

As stated above three pairs of inlet conditions were examined. The properties of the inlet states are shown in Table 5.1.

	T_{sup}	T_{exh}	$w_{f,sup}$	$w_{f,exh}$	T_{av}	$w_{f,av}$	φ_{av}
Pair 1	35°C	25°C	0.020	0.010	30°C	0.015	56.2%
Pair 2	15°C	25°C	0.002	0.010	20°C	0.006	41.5%
Pair 3	-15°C	25°C	0.0001	0.010	5°C	0.00505	93.6%

Table 5.1: Properties of Examined Air Inlet States

The inlet pair 1 represents a typical cooling and dehumidifying application in a very warm and humid summer climate as it exists in Miami, FL. The second inlet pair contains an intermediate outdoor state which would be typical for operations during spring and autumn in many moderate climates. In very cold winter conditions as they are found in Chicago, IL, the outdoor air properties are similar to those of inlet pair 3. The enthalpy exchanger has to operate as a heater and humidifier in this case.

All the calculations described above were carried out with the EES program [22] listed in Appendix A, and the results of these calculations are summarized in Table 5.2 to Table 5.4 for the three inlet pairs and for both matrix materials.

Inlet pair 1: T_{av} = 30°C, $w_{f,av}$ = 0.015, φ=56.2%

	Water-Based Desiccant	Silica Gel
a_1	-0.000649	-0.00918
a_2	0.712	10.08
a_3	1.031	1.032
a_4	2530	2530
a_5	0.936	2.214
λ_1	4.637	1.577
λ_2	0.3339	0.0293
ω_{min}	20.7	15.2

Table 5.2: Derivatives and Wave Speeds for Inlet Pair 1

Inlet pair 2: T_{av} = 20°C, $w_{f,av}$ = 0.006, φ = 41.5%

	Water-Based Desiccant	Silica Gel
a_1	-0.000408	-0.01136
a_2	1.037	28.90
a_3	1.015	1.015
a_4	2530	2530
a_5	0.926	1.998
λ_1	2.751	1.041
λ_2	0.3842	0.0172
ω_{min}	12.3	10.0

Table 5.3: Derivatives and Wave Speeds for Inlet Pair 2

Inlet pair 3: T_{av} = 5°C, $w_{f,av}$ = 0.00505, φ = 93.6%

	Water-Based Desiccant	Silica Gel
a_1	-0.0326	-0.00128
a_2	91.62	3.590
a_3	1.013	1.013
a_4	2530	2530
a_5	1.096	2.396
λ_1	1.751	0.954
λ_2	0.0058	0.1234
ω_{min}	7.8	9.2

Table 5.4: Derivatives and Wave Speeds for Inlet Pair 3

A rotation speed that is higher than the calculated minimum speed is not recommended, since a higher rotation speed generally leads to a greater percentage of air that is carried over from one air stream to the other. This carry-over is directly proportional to the rotation speed of the matrix and therefore an enthalpy exchanger ought to be operated at the calculated minimum speed.

A discussion of the calculated minimum rotation speeds and a comparison between the two desiccant materials with respect to their benefits in different operating conditions follow in Section 5.1.3.

5.1.2 Effectiveness and Outlet Properties

According to Section 4.3 the effectivenesses for heat and mass transfer of the enthalpy exchanger can be estimated as a function of only the number of transfer units, if the matrix is operated at a rotation speed equal or greater than the minimum speeds summarized in Tables 5.2 to 5.4.

The number of the transfer units for heat and mass exchange between the air and the matrix are defined as:

$$NTU_t = \frac{h\ A}{\dot{m}_{air}\ c_{p,air}} \tag{5.13}$$

$$NTU_w = \frac{h_w\ A}{\dot{m}_{air}} \tag{5.14}$$

The variables in the denominator are fixed by the inlet conditions, while the variables in the numerator were determined based on a matrix sample that was provided by a local enthalpy exchanger manufacturer (Carnes [9]). The structure of the matrix is the same as the one shown in Figure 1.2, and the dimensions of the cross sectional area are shown in Figure 5.6

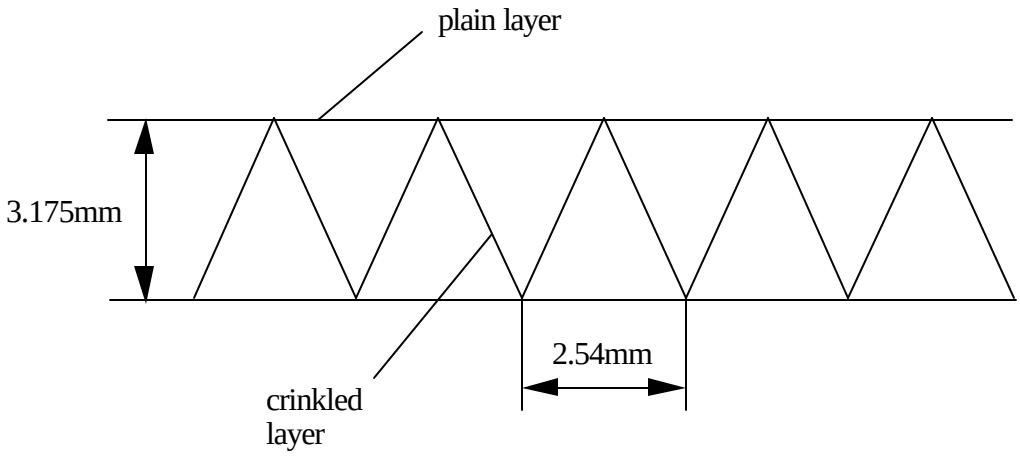

Figure 5.6: Cross Sectional Dimensions of the Investigated Matrix

The part of the cross section shown in Figure 5.6 has a face area of 4.032×10^{-5} m^2 and the

length of foil needed for this area is 4.689×10^{-2} m (only one plain layer has to be taken into account). The energy recovery wheel recommended by the manufacturer for an air flow rate of $\dot{m} = 2.28 \frac{kg}{s}$ has a cross sectional area of 0.539 m^2 and is 0.2032 m deep. Therefore the total area of foil per period becomes 127.5 m^2. Since the air is in contact with the foil on both sides the total surface area per period which is needed to calculate the number of transfer units is $A = 255 m^2$.

The mass of the matrix can now be estimated by multiplying the foil area of the total wheel by the foil thickness and the density of the material. The water-based desiccant matrix weighs approximately 47 kg while a silica gel matrix of the same design weighs only 21 kg due its smaller density.

The heat transfer coefficient is calculated by a correlation for forced convection in internal flows. As stated by Incropera and DeWitt [20], the Nusselt number is approximately equal to 3 for this laminar flow arrangement and the hydraulic diameter of the triangular passes is estimated to be 1.716×10^{-3} m. The heat transfer coefficient becomes:

$$h = \frac{Nu \cdot k_{air}}{D_h} = 46 \frac{W}{m^2 K} \tag{5.15}$$

The number of transfer units for heat transfer between the air and the matrix and vice versa becomes:

$$NTU_T = \frac{255 m^2 \cdot 46 \frac{W}{m^2 K}}{2.28 \frac{kg}{s} \cdot 1020 \frac{J}{kgK}} = 5.04 \tag{5.16}$$

Assuming a Lewis number of unity the number of transfer units for mass transfer is equal to this value:

$$NTU_w = \frac{NTU_T}{Le} = 5.04 \tag{5.17}$$

The overall number of transfer units between the two periods is one half of the NTUs calculated above:

$$NTU_{o,T} = NTU_{o,w} = \frac{NTU_T}{2} = 2.52 \tag{5.18}$$

With these parameters known, the effectivenesses and outlet states of the two air streams can easily be calculated using Equations 4.19 to 4.22. The results for the three inlet pairs are summarized in Table 5.5. The effectivenesses and therefore the properties of the outlet states are the same for both materials since the number of transfer units for heat transfer is a function of the design only and the Lewis number was assumed to be unity. However, as it can be seen from the results of Section 5.1.1, the minimum rotation speed that is required in order to operate the enthalpy exchanger at its optimum conditions where maximum enthalpy exchange is achieved is different for the two materials.

	Inlet Pair 1	**Inlet Pair 2**	**Inlet Pair 3**
NTU_o [-]	2.52	2.52	2.52
e **[%]**	71.6	71.6	71.6
$T_{sup,out}$ [°C]	27.84	22.16	13.64
$w_{f,sup,out}$ [kg/kg]	0.0128	0.00886	0.00859
j **$_{sup,out}$ [%]**	54.9	53.5	87.9

Table 5.5: Effectiveness and Outlet States

5.1.3 Conclusions and Design Guidelines

The results of the calculations for the minimum rotation speeds that are summarized in Tables 5.2 to 5.4 show a tendency that was expected from the knowledge of the equilibrium adsorption isotherms. While the water-based desiccant represents a type III isotherm, silica gel is characterized by a type I isotherm. This means that the rotation speed of a silica gel matrix can be significantly lower in operating conditions represented by the inlet pair 1, because both the gradient and the amount of the adsorption capacity are much greater at low and intermediate humidities. This causes the F_1 potential to proceed slower through the matrix which allows a slower rotation without a breakthrough of the first wave. Therefore a matrix made of silica gel should be preferred compared to a matrix of the water-based polymer desiccant in summer applications.

In heating applications as represented by inlet pair 3 the enthalpy exchanger operates at maximum relative humidities which results in an advantage for the type III isotherm of the water-based desiccant. Here it can be operated at a slightly lower rotation speed than the silica gel matrix and still achieve maximum enthalpy exchange.

A temperature dependence of the performance of the two materials is also observed. A comparison between the inlet pairs 1 and 2 that are both at intermediate humidities but at different temperatures, shows that cold temperatures generally favor the water-based desiccant, while silica gel is the better choice in a hot climate.

5.2 Heat- and Mass Transfer Effectiveness - Catalog Data and Calculated Values

In their design manual (Carnes [9]), the manufacturers of the water-based desiccant matrix specify the effectiveness of their energy recovery wheels as a function of the wheel face velocity v. Apparently assuming a Lewis number of unity, the effectiveness is specified to be equal for both heat and mass (humidity) transfer.

The wheel face velocity is defined as the ratio of the volumetric flowrate of one period $\dot{V}_j$ to the wheel face area A_F of this period: $v = \frac{\dot{V}_j}{A_F}$. For an equal flow arrangement as it is investigated in this study, the wheel face area of one period equals one half of the cross-sectional area of the enthalpy exchanger. Since this area is constant for a particular energy recovery wheel, the effectiveness depends on the air flow rate only.

In Klein's simplified solution for the case of maximum enthalpy exchange [21] the effectiveness for heat transfer is a function of the number of transfer units:

$$NTU_T = \frac{h\,A}{\dot{m}_f\, c_{p,f}} \quad .$$

For a given wheel, the heat transfer coefficient times area product $h\,A$ does not change because of laminar flow through the triangular passes, and the specific heat capacity of air $c_{p,f}$ is also assumed to be constant. Hence, the effectiveness can be expressed in terms of the wheel face velocity inside the enthalpy exchanger, too.

Figure 5.7 shows the heat transfer effectiveness for various wheel face velocity values as published in the manufacturer's catalog data and a comparison with the function calculated by Klein's model. The humidity transfer effectivenesses for Lewis numbers between one and four are also plotted in this graph.

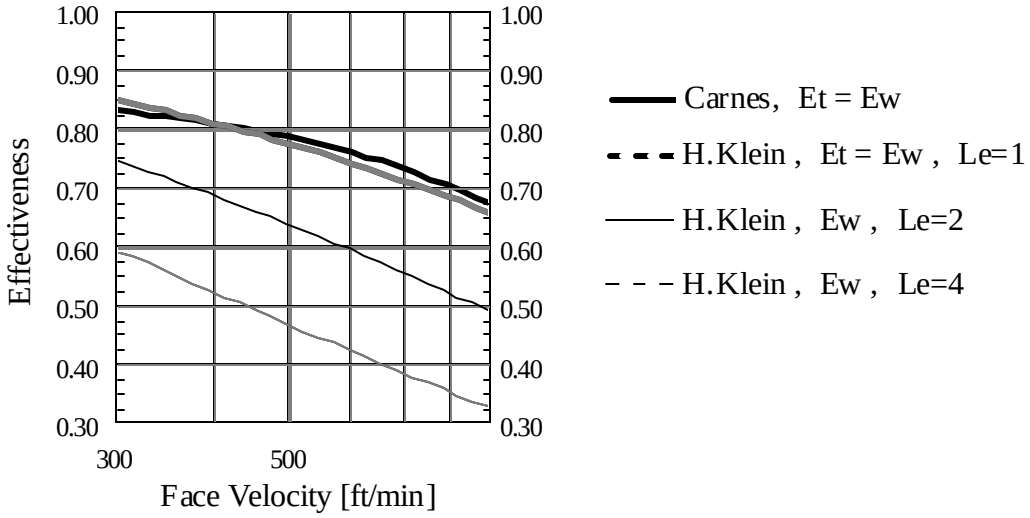

Figure 5.7: Heat- and Mass Transfer Effectivenesses of the Water-Based Polymer Coated Matrix

The two curves that represent the heat transfer effectiveness are almost identical over the entire range of wheel face velocities. This similarity is quite astonishing since only very basic principles were considered for the effectiveness calculation with Klein's model. The foil area was roughly estimated as shown in Chapter 5.1.2 and the Nusselt number and heat transfer coefficient were assumed to be constant for laminar flow within the triangular passes. Nevertheless, it is apparent from Figure 5.7 that Klein's simplified model is a very good approximation to the actual heat transfer effectiveness behavior that is represented by the manufacturer's catalog data. These experimental data were obtained in accordance with ASHRAE-Standard 84-78 under conditions specified in ARI-Standard 1060.

However, the plots of the humidity transfer effectiveness for Lewis numbers greater than one suggest that this parameter has a tremendous effect on the performance of enthalpy exchangers. The effectiveness for humidity transfer for a Lewis number of three or four, as Van den Bulck [36] suggests for rotary regenerators with a silica gel matrix, can be up to two times smaller than the effectiveness calculated for a Lewis number of unity which is claimed by the manufacturer.

The ability to transfer moisture in addition to heat between two air streams is the one

advantage of an enthalpy exchanger compared to a sensible rotary heat exchanger. If this advantage is diminished by a Lewis number that is indeed as large as three or four, it will be questionable whether it is still worthwhile using the more expensive enthalpy exchangers instead of common sensible heat exchangers.

As pointed out previously, there is no easy way of determining the Lewis number of the tested desiccant material, but doing this will be an important task in the future in order to be able to evaluate the actual advantage of enthalpy exchangers in a specified application compared to rotary regenerators that transfer sensible heat only.

5.3 The Enthalpy Exchanger in Cooling Systems

In order to evaluate the benefits of sensible heat exchangers and enthalpy exchangers operating in the cooling mode, the possible cooling load reductions that can be achieved by using these regenerators were calculated for a particular pair of outdoor and indoor conditions. The selected outdoor temperature and humidity represent the summer design conditions for air-conditioning systems in Madison, WI, as published by ASHRAE [1].

Dry bulb temperature : 31°C

Wet bulb temperature : 23°C

Relative humidity : 51.4%

Humidity Ratio : 0.0145

The room conditions were fixed at a comfort level of temperature T = 23°C and relative humidity j = 50%, and the supply and exhaust mass flow rates were again chosen to be 2.28 kg/s each, a value suggested by ASHRAE [2] for the ventilation of a 200 people office building. The cooling system chosen to meet the required cooling and dehumidification loads is a single-zone

system with reheat and an optional rotary regenerator as shown in Figure 1.3.

Due to heat and humidity transfer from the ambient to the cooling zone and heat and humidity generation inside the cooling zone itself, the ventilation air stream has to enter the building (state 4 in Figure 5.8) colder and drier than the conditions to be maintained inside (state 5). The ratio of the latent to sensible heat load, that is the slope of the load-ratio line in Figure 5.8, depends on the heat and humidity transfers to and generations within the cooling zone, but typically the loads are such that the ratio of sensible load to total load (sensible plus latent) is between 70 and 80 percent (Stoecker and Jones [33]).

With this ratio specified, the properties of the fresh supply air entering the building must be on the load-ratio line that passes through the indoor air state (state 5). The exact location of state 4 (supply air, entering the cooling zone) on this line is determined by both the ventilation air flow rate and the absolute size of the loads. For this study a temperature of $T = 15°C$ and a relative humidity of $j = 75\%$ were assumed.

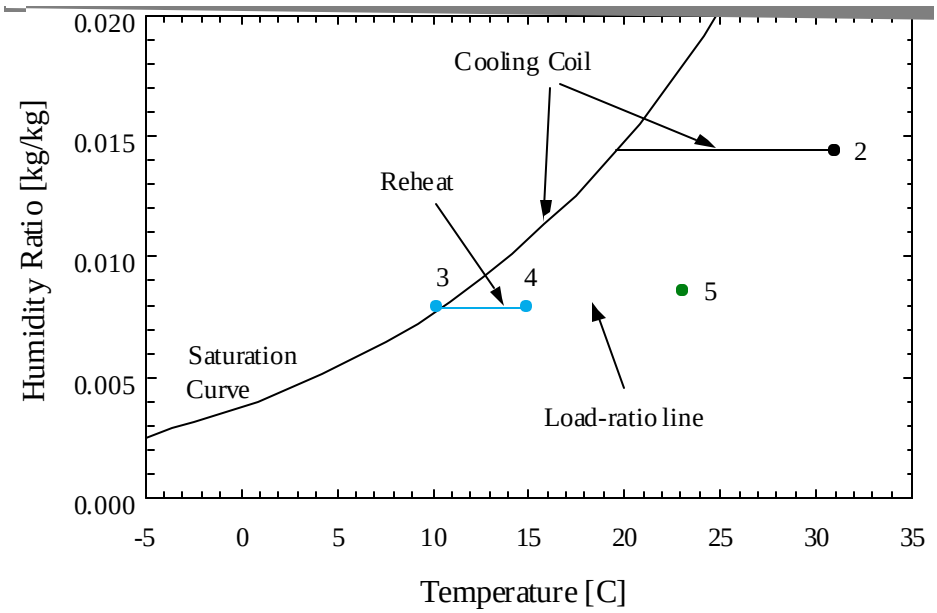

Figure 5.8: Single-Zone Cooling with Reheat. No Regenerator.
Air States Refer to Figure 1.3.

If the cooling system includes a rotary regenerator, the warm and humid supply air is

precooled (sensible heat exchanger) or both precooled and predehumidified (enthalpy exchanger) before it enters the cooling coil as shown in Figures 1.4 and 1.5, respectively. The cooling coil load is thereby decreased by the product of the recovered enthalpy and the supply air flow rate. The load necessary for reheating the supply air stream remains constant.

In most commercial cooling applications, cooler indoor air is mixed with fresh outside air before it enters the cooling coil (between states 2 and 3 in Figure 5.9) in order to decrease the cooling load. In this study a constant fresh outdoor air flow rate of 2.28 kg/s is required to maintain a high indoor air quality in the cooling zone, and therefore a mixing with indoor air must result in an increase in the total circulation rate at states 3, 4, 5 and 6. In this case the regenerator should be installed before the mixing is done since low air flow rates and large temperature differences allow the most efficient regenerator operation. For this reason the regenerator operates in the same conditions as it does without the mixing process (Figure 5.10). The mixing of the air streams does therefore not affect the incremental amount of energy that can be recovered with an enthalpy or heat exchanger and it does not have to be considered when the regenerator benefits are evaluated.

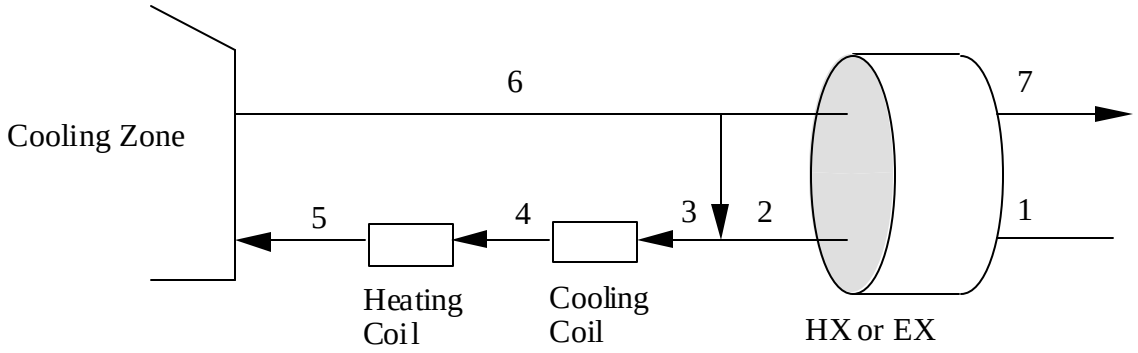

Figure 5.9: Air-Conditioning System with Exhaust Air Mixing

The instantaneous energy savings that can be achieved by enthalpy and heat exchangers for the previously specified operating conditions were calculated with the model developed in Section

4.4 for intermediate and high rotation speeds and are summarized in Figure 5.11. Since the cooling and dehumidification coil has to meet a latent load as well as a sensible load, the amount of total energy (enthalpy) recovered by a rotary regenerator is the appropriate index for evaluating the reductions in the cooling coil load. When there is dehumidification, a significant advantage for the enthalpy exchanger compared to the sensible heat exchanger can be observed. The energy recovery of an enthalpy exchanger is shown for various Lewis numbers of the desiccant matrix material.

As shown in Figure 5.11, an enthalpy exchanger with the ideal Lewis number of one can recover almost 3 times as much total energy as a comparable sensible heat exchanger, and even the enthalpy exchanger with a Lewis number of 4 exceeds the heat exchanger recovery by the factor 2 for the conditions assumed in this analysis.

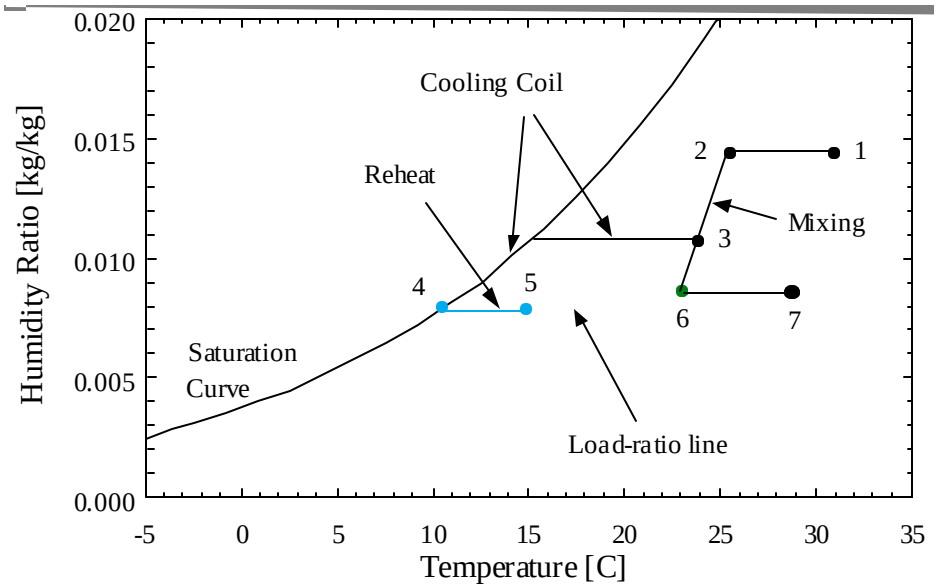

Figure 5.10: Single-Zone Cooling with Reheat, Exhaust Air Mixing and Sensible HX. Air States Refer to Figure 5.9.

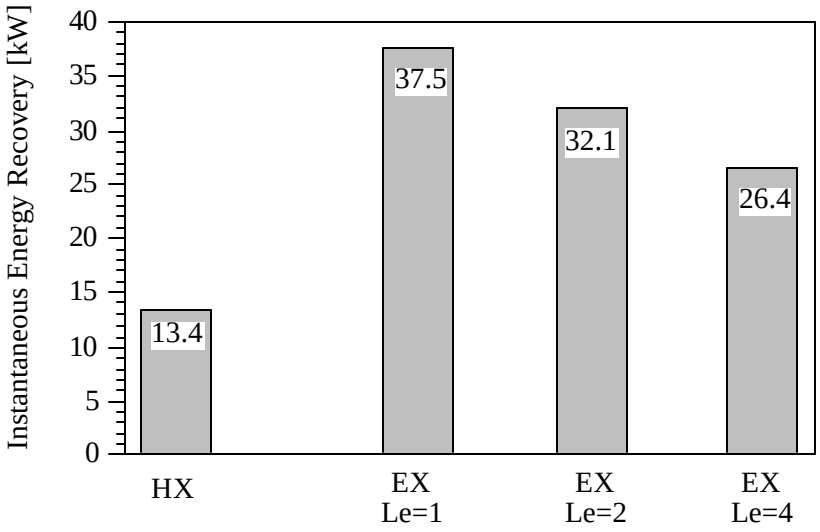

Figure 5.11: Total Energy Recovery of HX and EX in a Cooling System

5.4 The Enthalpy Exchanger in Heating Systems

An air-conditioning system operating in the heating mode has to be capable of both heating and humidifying processes in order to provide comfortable air conditions for the heating zone. Typically a heating coil and an evaporative humidifier are used in series as shown in Figure 5.12 to condition a ventilation supply air stream to a desired temperature and humidity level. Energy from the warmer and more humid exhaust air stream can be recovered by using rotary regenerators to preheat and prehumidify the supply air before it enters the heating coil at state 2. As a result, the load at the heating coil is decreased.

The amount of energy actually needed for the conventional heating and humidification process can be seen on a psychrometric chart (Figure 5.13). The cold and dry supply air is first heated at constant humidity in the heating coil from state 2 to state 3. Then it is passed through the humidifier, where a small amount of water evaporates into the air stream and causes it to become

more humid but also colder (state 3 to 4).

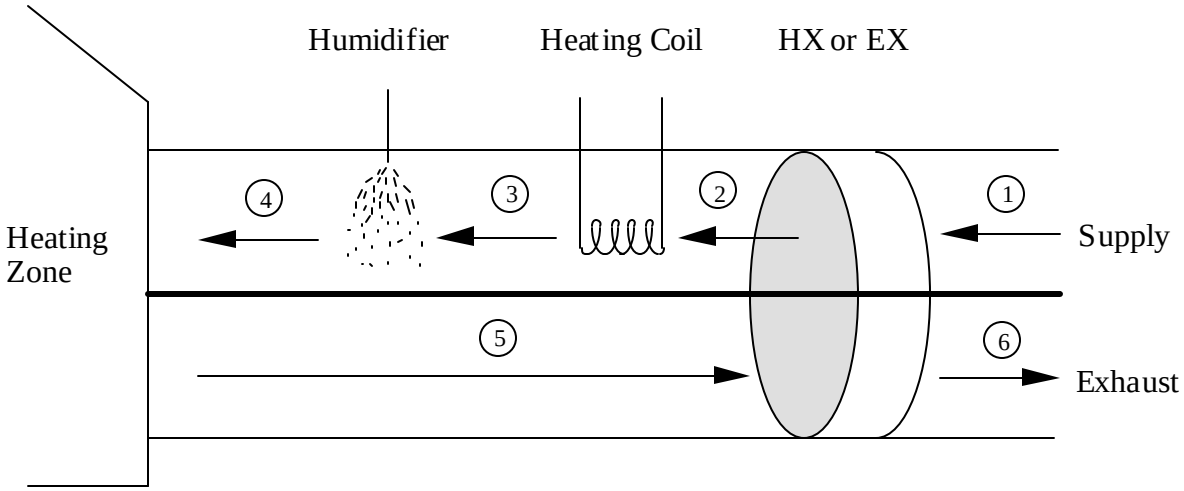

Figure 5.12: Schematic of a Heating System

As stated by Stoecker and Jones [33] this humidification process obeys the "straight-line law" which says that, on a psychrometric chart, the air properties will essentially follow the straight lines of constant wet bulb temperature when a small amount of water evaporates into the air. Since lines of constant wet bulb temperature are almost parallel to lines of constant enthalpy, the specific air enthalpy stays nearly constant throughout humidification. As a result, the heating coil has to heat the supply air at constant humidity beyond its desired dry bulb temperature until it reaches a specific enthalpy that is about the same as the enthalpy of the outlet state that has the desired temperature as well as the desired humidity ratio. Therefore an air stream that is more humid when it enters the heating coil (state 2') reduces the heating load by decreasing the required heating coil outlet temperature (state 3' instead of 3). As a consequence not only the regenerator outlet temperature but also its outlet humidity determine the amount of energy that is needed in addition to the regenerator in order to completely condition a ventilation air stream.

For the reasons stated above, the transfer of enthalpy, that is sensible plus latent heat, between the exhaust and supply air stream is a more important measure than just the supply air temperature rise (sensible heat), when the performances of different regenerator types are

compared. Since enthalpy exchangers are able to transfer both heat and humidity between two air streams they can recover more energy from the exhaust than rotary sensible heat exchangers.

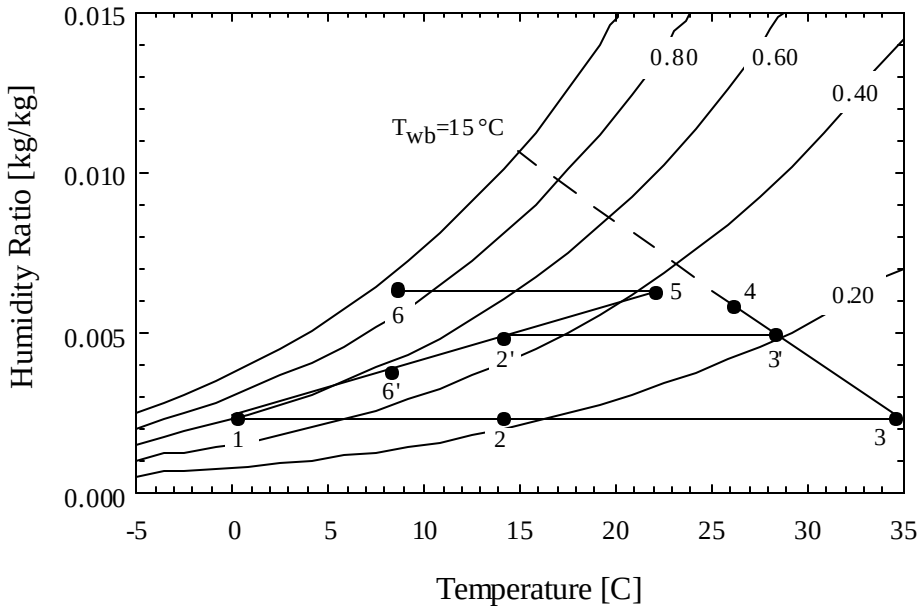

Figure 5.13: Psychrometric Chart for a Heating System

The regenerator performance in the heating system shown in Figure 5.12 was investigated for two different outdoor temperatures and various regenerators, keeping the supply flow rate at 2.28 kg/s and the indoor conditions at T = 23°C and j = 30%. The amount of energy required to operate the humidifier (pumping work for the liquid water) is very small for all systems and can be neglected. Therefore the energy recovery of a rotary regenerator is equal to the reduction in the heating load. The results of the calculations based on the model developed in Section 4.4 are summarized in Figure 5.14.

For an outdoor temperature of T = -15°C, the two enthalpy exchangers with small Lewis numbers of 1 and 2 can still be operated at high effectiveness without condensation occurring in the exhaust stream, while the sensible heat exchanger and the enthalpy exchanger with a large Lewis number of 4 have to be rotated more slowly in order to avoid condensation. For this reason a significant difference in the energy recoveries can be observed for an outdoor temperature of T = -

15°C.

The second outdoor temperature (T = 0°C) was chosen such that all exchangers can safely be operated at their maximum possible effectiveness. Since the difference in humidity ratio between outdoor and indoor air is relatively small in this case, the energy recoveries of the various exchangers differ much less.

Even though the absolute differences between the regenerator recoveries are different for the two temperatures, the ratios between them is approximately equal. In both cases the energy recovery of the enthalpy exchanger with $Le = 4$ is about halfway between the recoveries of the exchanger with $Le = 1$ and the sensible heat exchanger. This proportion was also observed for the operation in the cooling mode (Section 5.3).

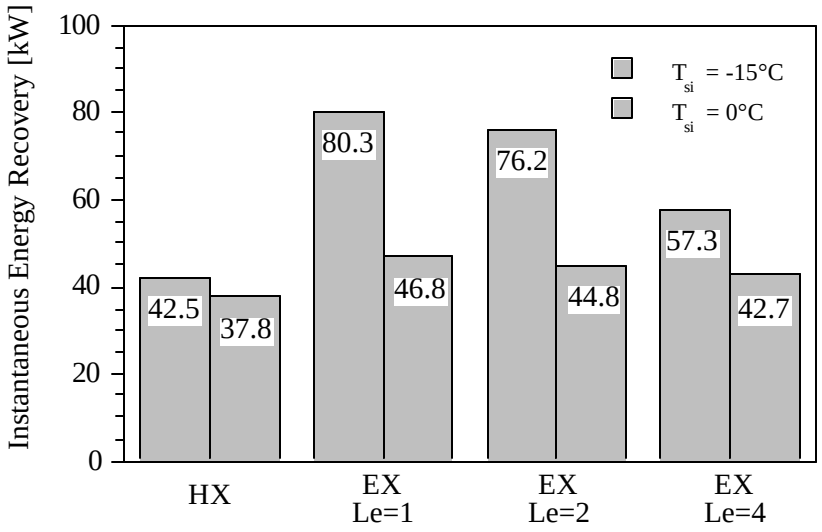

Figure 5.14: Total Energy Recovery of HX and EX in a Heating System

A more detailed investigation of the enthalpy and heat exchanger operation that integrates the possible energy recovery over a whole year for several different locations in the United States will be presented in Chapter 6.

6 ANNUAL PERFORMANCE SIMULATIONS

The regenerator performance calculations for one specific point in time with fixed inlet conditions, as presented in Chapter 5, are useful to compare the basic operating characteristics of various regenerator types or materials, to roughly estimate advantages that result from the use of enthalpy exchangers instead of sensible heat exchangers, and to compare several different system configurations. Moreover, calculations of instantaneous reductions in a building's heating and cooling loads are necessary in order to determine the allowable capacity reductions of the additional heating and cooling equipment

However, when a more detailed economic analysis of the energy savings of a regenerator with respect to its system and installation costs is required, it is necessary to simulate the performance over a longer period of time with varying weather conditions and to integrate the resulting energy recovery. Doing so is especially important for an operation in the heating mode because extraordinarily cold outdoor temperatures could cause condensation and freezing of water vapor on the matrix and could significantly decrease the regenerator effectiveness. In the cooling mode the operating temperatures and humidities are typically within ranges, such that either regenerator type can be operated at its constant, maximum effectiveness. But even in this case it is important to know the integrated energy savings over a period of time, since outdoor conditions are not constant, and the integrated energy savings rather than the power reduction at one point in time, affect the overall reduction in operating costs.

An economic analysis of the regenerator benefits that considers both the capacity reduction and the integrated annual energy recovery is executed in Section 6.3.

6.1 The Simulation Program

Three FORTRAN 77 programs were written based on the simplified model for intermediate and high rotation speeds that was developed in Section 4.4. One program simulates the enthalpy exchanger in the heating mode, one the heat exchanger in the heating mode and the third one is capable of simulating the cooling mode for both regenerator types.

All programs calculate the maximum possible effectiveness that the regenerator can be operated at without excess water or ice accumulating on the matrix. This effectiveness is a function of the matrix design (number of transfer units) and of the air inlet conditions of both supply and exhaust air stream. The ratio of matrix rotation speed to air flow rate that results in this best possible effectiveness is also given as an output.

The FORTRAN programs were designed as subroutines for TRNSYS 14 [23], a transient simulation program that provides weather data for many locations in North America and integrates the energy recovery of the rotary regenerator over a user-defined period of time. TRNSYS 14 consists of many modules that describe and simulate the operation of various components of energy related systems and these can be connected in any way chosen by the user in order to allow the simulation of a complex system. It is also possible to add new modules to the program, as it was done with the three FORTRAN subroutines that are described in the following sections.

6.1.1 Heating Mode (Types 70 and 71)

The Sensible Heat Exchanger (Type 71):

In the rotary sensible heat exchanger, sensible heat is typically transferred between exhaust and supply air stream, resulting in the fact that, on a psychrometric chart, the outlet states are both on horizontal lines that represent the corresponding inlet humidity ratios. However, for some inlet conditions and exchanger effectivenesses the exhaust air can be cooled below its dew point temperature, and condensate or frost, depending on the average matrix temperature, will start to built on the matrix. Due to the matrix rotation, this condensate or frost is carried into the supply air stream, where it evaporates or sublimates (Figure 6.1). In general this condensation/evaporation or sublimation process is desirable since the total amount of energy transferred is increased by the fraction of the latent heat.

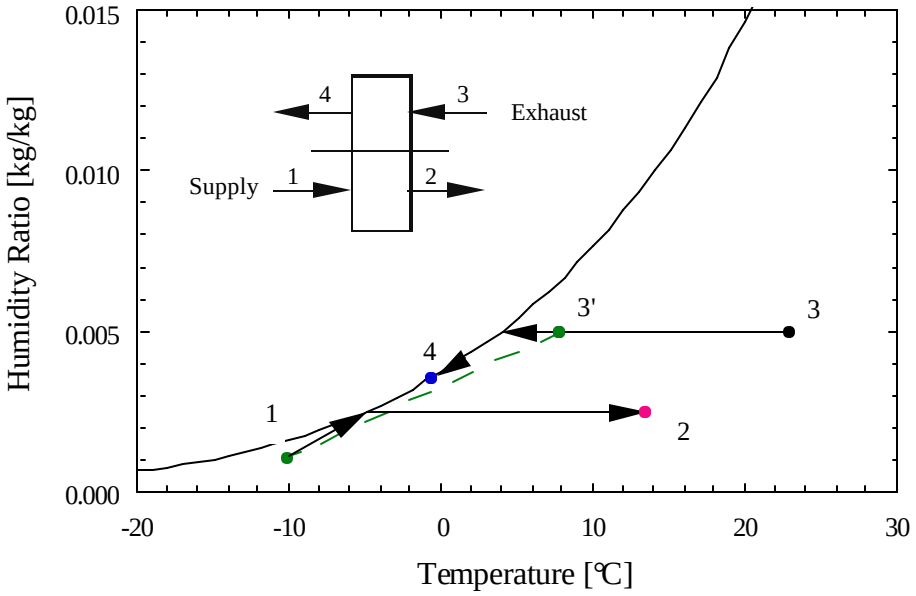

Figure 6.1: Heat Exchanger Operation with Exhaust Condensation and Complete Evaporation into the Supply Stream

At some point however, more water condenses out of the exhaust on the matrix surface

than it can be evaporated into the colder supply air. This condition is referred to as excess water. For temperatures below freezing, the ice layer on the matrix will grow and eventually block the matrix. Even if the condensate does not freeze, the excess water should be avoided, since water in the liquid phase would accumulate at some point in the ventilation system causing leakage and undesirable mold growth.

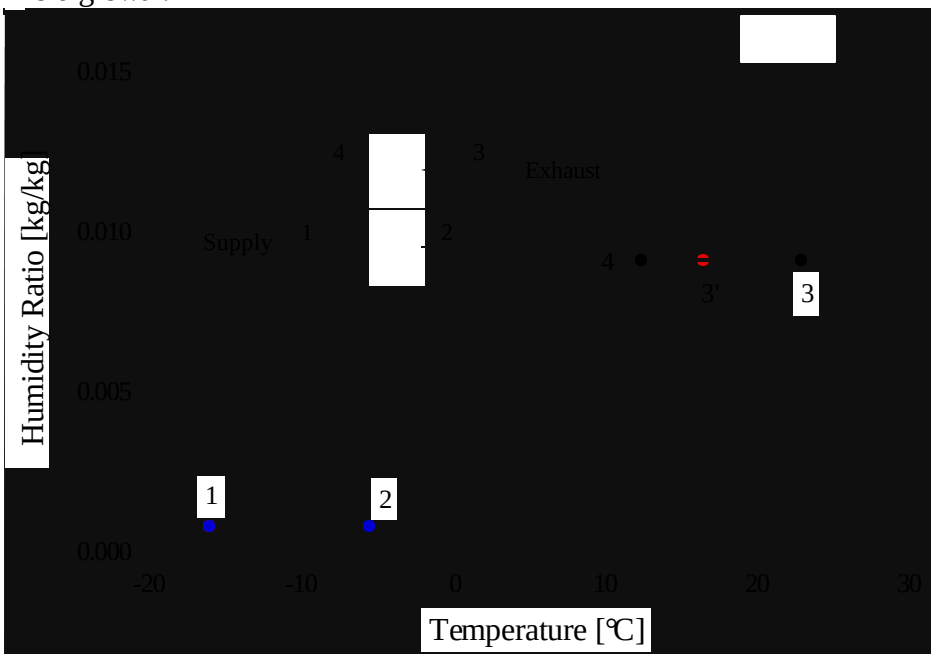

Figure 6.2: Heat Exchanger Operation In Excess Water Conditions

Holmberg [19] investigated the onset conditions of excess water for an enthalpy exchanger and a sensible heat exchanger matrix with a similar structure as shown in Figure 1.2. He found that, if the straight line between state 3' and the supply inlet (state 1) in Figure 6.2 intersects the saturation curve, excess water will form on the matrix. He experimentally determined that state 3' has the same humidity ratio as the exhaust inlet (state 3) and a temperature that exceeds the dew point temperature of state 3 by approximately 4°C. An explanation for this result is that the entering exhaust air is first cooled at constant humidity until it almost reaches its dew point. The actual condensation/evaporation process starts from this point on, and is therefore only affected by the exhaust inlet humidity but not by its initial dry bulb temperature.

<table>
<tr><td colspan="2">Input of all parameters needed for simulation</td></tr>
<tr><td colspan="2">Calculation of supply and exhaust air inlet enthalpies</td></tr>
<tr><td colspan="2">Check for excess water</td></tr>
<tr><td>Then
If excess water</td><td>Else</td></tr>
<tr><td>$T_4 = \text{Max}\ (\ T_{dp,3}\ ,\ T_3-\varepsilon_t(T_3-T_1)$
where $\varepsilon_t = \text{NTU} / (\text{NTU} + 2)$</td><td>Max. temp. effectiveness:
$\varepsilon_t = \text{NTU} / (\text{NTU} + 2)$</td></tr>
<tr><td rowspan="2">$w_4 = w_3$</td><td>$T_4 = T_3-\varepsilon_t(T_3-T_1)$</td></tr>
<tr><td>$w_4 = \text{Min}\ (w_3\ ,\ w_{sat}\ (\ T_4\ )\ )$</td></tr>
<tr><td>$T_2-T_1 = T_3-T_4 \quad , \quad w_2 = w_1$</td><td>$T_2-T_1 = T_3-T_4 \quad , \quad w_2-w_1 = w_3-w_4$</td></tr>
<tr><td colspan="2">Calculation of outlet enthalpies, effectivenesses and the corresponding rotation speed</td></tr>
<tr><td colspan="2">Calculation of recovered sensible and total energies</td></tr>
<tr><td colspan="2">Output of calculated values</td></tr>
</table>

Figure 6.3: Schematic of Subroutine Type 71

The subroutine written for the heat exchanger in the heating mode takes this behavior into account by first calculating the exhaust dew point temperature and state 3', and then by checking whether the connection of state 3' and state 1 intersects with the saturation curve. If there is no intersection, the temperature effectiveness is calculated by Equation 4.22. The humidity stays constant as long as the exhaust outlet temperature, which is fixed by the previously calculated temperature effectiveness, is greater than the dew point temperature of the exhaust inlet. If the exhaust outlet is colder than the inlet dew point temperature, a condensation/evaporation process without excess water as shown in Figure 6.1 occurs and the exhaust outlet is on the saturation curve (state 4). In case of an intersection, an excess water accumulation is avoided by lowering the rotation speed in order to decrease the temperature effectiveness to a point where the exhaust outlet falls on the dew point of its inlet (Figure 6.2). Once the appropriate outlet state is identified, the

temperature effectiveness and both sensible and total heat (enthalpy) recovery of the heat exchanger are determined.

A flow chart of the previously described subroutine (Type 71) is shown in Figure 6.3 and the FORTRAN code is listed in Appendix B.

The Enthalpy Exchanger (Type 70):

The risk of having excess water (or ice) is not quite as crucial for an enthalpy exchanger, since this device transfers not only sensible heat but also humidity (in the adsorbed rather than the condensed phase) between the air streams. Therefore the air property changes will be on a straight line between the two inlet states on a psychrometric chart if a minimum rotation speed is exceeded (Figure 6.4). Holmberg [19] found, that excess water occurs only if the connection between the two air inlets (state 1 and state 3 in Figure 6.3) intersects with the saturation curve (Figure 6.5). Excess water still has to be avoided for the same reasons that apply to the sensible heat exchanger and also because water in the liquid phase could harm the desiccant coating of the matrix.

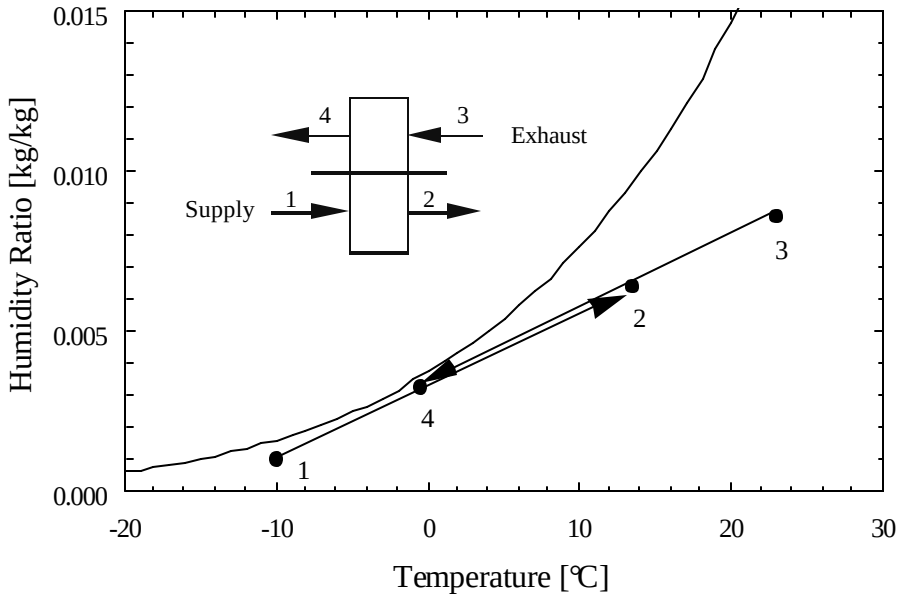

Figure 6.4: Enthalpy Exchanger Operation without Excess Water

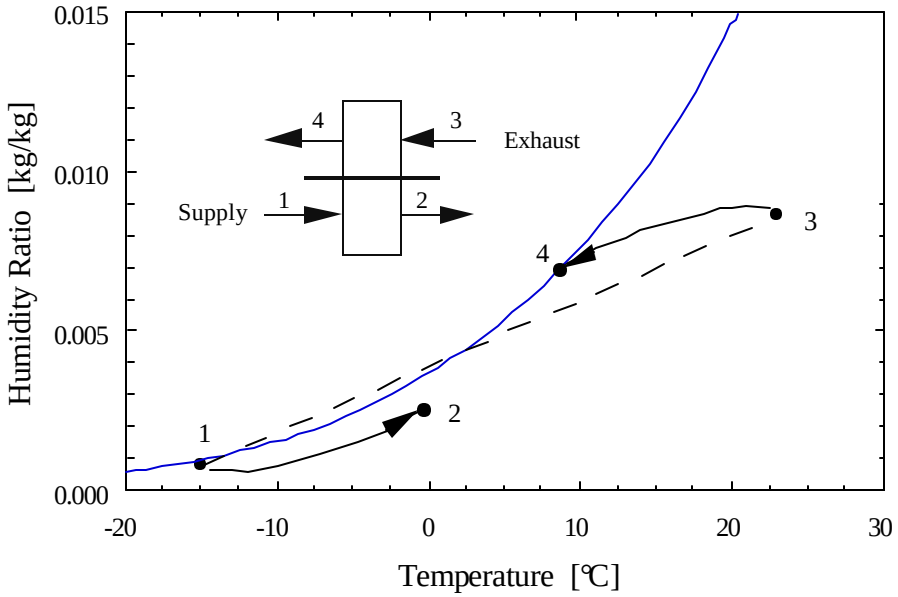

Figure 6.5: Enthalpy Exchanger Operation in Excess Water Conditions

Input of all parameters needed for simulation		
Calculation of supply and exhaust air inlet enthalpies		
Check for excess water		
Then	If excess water	Else
Increase Γ in small increments starting from zero until saturation		Maximum effectiveness: $\varepsilon_T = \varepsilon_w = \varepsilon_i = NTU / (NTU + 2)$
	Determine temp. and enth. effectivenesses as a function of Γ and calculate outlet temp., enth. and hum.	$w_4 = w_3 - \varepsilon_w (w_3 - w_1)$
		$T_4 = T_3 - \varepsilon_T (T_3 - T_1)$
Decrease Γ to leave saturation area and recalculate outlet temperatures and humidities		$w_2 - w_1 = w_3 - w_4$, $T_2 - T_1 = T_3 - T_4$
		Calculation of outlet enthalpies
Calculation of recovered sensible and total energies		
Output of calculated values		

Figure 6.6: Schematic of Subroutine Type 70

The structure of the subroutine for an enthalpy exchanger operating in the heating mode (Type 70, shown in Figure 6.6) is similar to that for the heat exchanger (Type 71). However, in case of a decreased rotation speed, the outlet states (2 and 4) are not on a straight line between the inlets, and their properties have to be estimated by solving the equations for temperature and enthalpy effectiveness that were developed in Section 4.4. In this case the subroutine solves for states 2 and 4 in Figure 6.5, and it again calculates both the sensible and total energy recovery. The program listing is shown in Appendix B.

6.1.2 Cooling Mode (Type 72)

In cooling applications, air temperatures and humidities are usually within ranges that assure no condensation in the warm supply air stream. Therefore both exchanger types can always be operated at a rotation speed which provides maximum effectiveness. For the heat exchanger, the humidity effectiveness is still equal to zero. For the enthalpy exchanger, temperature, humidity and enthalpy effectiveness can be estimated with Equations 4.21 to 4.24. Since the warm and humid supply air has to be further cooled and dehumidified after it exits the regenerator (compare Section 5.3), the amount of total energy (rather than sensible energy) transferred is the appropriate measure for the energy savings. The program listing for subroutine Type 72 is shown in Appendix B.

6.1.3 The TRNSYS Program

All three subroutines described in the previous sections are built into the transient simulation program TRNSYS 14 [23] in a similar manner. So-called "decks" connect the user written subroutines and some of the standard TRNSYS modules that are needed for the simulations. For the transient regenerator performance simulation, a weather data generator (Type 54) and a psychrometric conversion module (Type 33) are needed in order to provide the necessary inputs (supply inlet properties) as a function of time. The supply inlet properties are obtained from the weather generator as a function of time while the exhaust inlet is assumed to remain constant throughout the simulation. The regenerator outputs are integrated (Type 24) and printed to the screen (Type 25) or directly sent to a second printing module in order to display variable changes with respect to time. An information flow diagram for the described modular setup is shown in Figure 6.7 and the deck used to simulate the cooling mode (Type 72) is listed as an example in Appendix C.

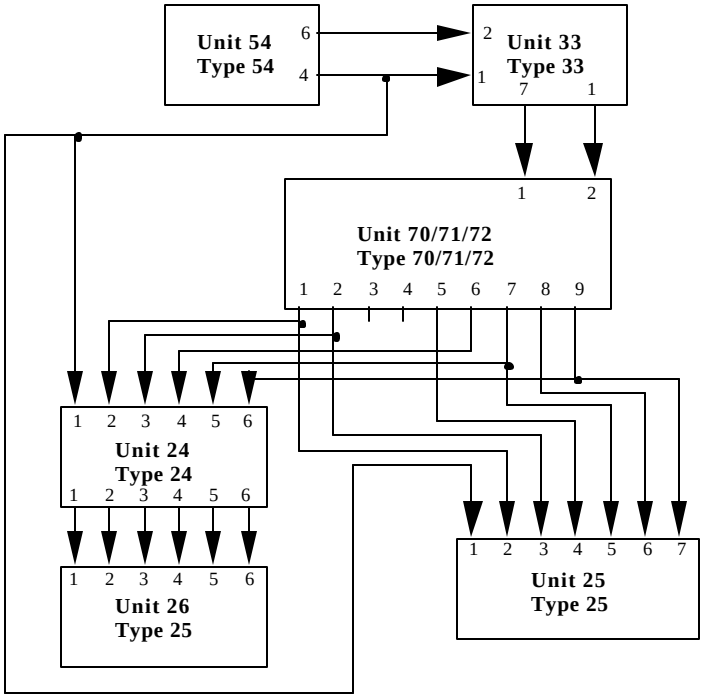

Figure 6.7: TRNSYS Information Flow Diagram

6.1.4 Practical Considerations and Constraints

Because rotary regenerators are used in order to precondition ventilation air streams and to reduce the energy loads of conventional heating and cooling systems, it makes sense only to operate them when ventilation is needed at the same time. Because of their size and high first cost, regenerators are most often used in commercial buildings where the ventilation is commonly shut off during the night. For this reason, the regenerator energy recovery is integrated only for times between 6 AM and 9 PM and it is set to zero for the remaining hours of each day in the following analysis.

Another important task is to choose appropriate on- and off set temperatures for the regenerator wheel. For the heating mode, it is assumed that a heat exchanger as well as an enthalpy exchanger should run as long as the outdoor supply temperature is below 18°C. If the outdoor temperature exceeds this value, the heat generation by electrical equipment and people within the building plus the heat gain by solar radiation would for most situations be such, that no additional heating is required.

Due to the internal heat generations and solar gains, the cooling system must usually operate even if the outdoor temperature is still slightly below the inside room temperature, which was assumed to be constant at 23°C in this study. However, in that case the regenerator cannot contribute to the cooling load, because it would transfer heat from the exhaust to the supply stream which would lead to an increase in the cooling load. Even if the outdoor temperature is slightly above the exhaust temperature, it might not be worthwhile to operate a regenerator since its rotation also draws a small amount of power. In this study, a 24 °C outdoor temperature, thus a 1°C difference between supply and exhaust stream, was chosen to justify an operation of the sensible heat exchanger in the cooling mode.

For an enthalpy exchanger, the optimum on-/ offset temperature can even be greater than 24°C when the outdoor humidity is much smaller than the indoor humidity. In this case the exhaust enthalpy may be greater than the supply enthalpy even though its temperature is lower and a negative energy recovery would again be the consequence. However, the enthalpy of an air stream

is not easy to measure and therefore it is not a suitable constraint for a regenerator operation. The constraint for the start of an operation should still be expressed in terms of temperature, but the on-/ offset temperature might have to be raised up to 28°C in order to achieve the maximum possible energy recovery.

A different optimum control temperature for the enthalpy exchanger is determined for every month of the cooling season, but as it will be documented in Section 6.2, this optimum temperature varies from 24°C only for applications with a very high indoor humidity (i.e., indoor swimming pools) and only for months where the outdoor air is dry (i.e., spring, fall).

6.2 Simulation Results

The annual simulations of the regenerator performance were separately executed for the heating and the cooling mode. The resulting energy recoveries were calculated for three locations in the USA, each representing different weather conditions, in order to display the effect of climate on the regenerator performance. Madison, WI, was chosen as a representative of a relatively cold and not very humid climate, which is typical for the Upper Midwest of the United States. The intermediate conditions of Washington, DC, are characteristic for major parts of the East Coast, and have a special importance due to the high population density in this area. Finally, Houston, TX, was selected to represent the hot and humid climate with only a very short heating season, which is typical for the southern states close to the Gulf of Mexico.

The simulations are based on the same parameters that were chosen for the calculations in Chapter 5. An air flow rates of 2.28 kg/s, representing the ventilation rate of a 200 people office building, and an energy recovery wheel with a number of transfer units between air and the matrix of

5 was investigated. The building indoor temperature was kept constant at 23°C for all cases and three different indoor humidities (30%, 50% and 80% relative humidity) were simulated in order to show the effect of the exhaust humidity on the energy recovery. The constraints specified in Section 6.1.4 apply to all simulations.

6.2.1 Energy Recovery in the Heating Mode

The integrated values for the annual reductions in the heating load are summarized in Tables 6.1 and 6.2 and show that, in general, the amount of recovered energy increases, as the climate becomes colder. This result is expected, since the energy transferred between two air streams is proportional to the enthalpy difference (for enthalpy exchangers) or the temperature difference (for heat exchangers) between the inlet states, assuming the exchanger effectiveness is constant. The actual numbers shown in the table are not exactly proportional because very low outdoor temperatures and high indoor humidities cause a decreased effectiveness due to the risk of excess water, but the general effect can still be observed. Heat recoveries in Madison are on average 30% greater than in Washington, and recoveries in Houston are only about one third of the corresponding numbers in Washington.

The influence of indoor humidity j_{ei} on the total energy recovery of the enthalpy exchanger Q_{tot} is governed by the same relations. The higher the water content in the exhaust, the greater the enthalpy difference between exhaust and supply, and the more enthalpy can be recovered. However, as it can be best seen in the results of the coldest climate (Madison), higher indoor humidities result in a greater risk of excess water and force a slower matrix rotation speed. The effectiveness decreases, and even though the enthalpy difference between exhaust and supply in

Madison is greater for the 80% indoor humidity case than for the 50% and 30% cases, the total energy transfer decreases.

Location	j_{ei} [%]	Q_{tot} [kW hr]	Q_{sens} [kW hr]	Hrs. of Operation
Madison, WI	30	126,500	123,200	3,975
	50	123,700	103,600	
	80	112,600	61,400	
Washington, DC	30	91,300	90,200	3,395
	50	101,500	85,200	
	80	129,300	64,200	
Houston, TX	30	30,500	30,400	1,842
	50	31,400	30,300	
	80	54,200	28,300	

Table 6.1: Sensible Heat Exchanger Recovery During the Heating Season

Location	j_{ei} [%]	Q_{tot} [kW hr]	Q_{sens} [kW hr]	Hrs. of Operation
Madison, WI	30	148,700	130,900	3,975
	50	185,300	119,000	
	80	147,300	63,800	
Washington, DC	30	99,900	90,900	3,395
	50	147,100	89,800	
	80	164,600	65,100	
Houston, TX	30	11,200	30,400	1,842
	50	37,900	30,400	
	80	74,200	28,500	

Table 6.2: Enthalpy Exchanger Recovery During the Heating Season

The amount of sensible heat recovered Q_{sens} which is also displayed in Tables 6.1 and 6.2 is a good measure of how long a regenerator can be operated at high effectiveness. Both supply and exhaust temperatures are the same for all three exhaust humidities, and therefore the differences

in the recovery of sensible heat, that are equivalent to the air stream temperature change, are a function of the matrix rotation speed only. It can be seen that the sensible heat recovery decreases with increasing indoor humidity, and the rate of this decrease is a function of the climate. For the cold Madison conditions, the sensible heat recovery is very sensitive to the exhaust humidity, whereas it remains almost constant for all three humidities in the much warmer Houston climate. This behavior is expected and can be explained by Holmberg's [19] definition of the excess water onset that was briefly summarized in Section 6.1.1. Excess water will occur if the connection between exhaust and supply inlet crosses the saturation curve on a psychrometric chart. The chance of this happening is much greater at low temperatures, where the saturation curve is almost horizontal and the saturation humidities are very low, than it is at warmer temperatures as they occur in Houston.

The results also show the advantages that enthalpy exchangers have compared to sensible heat exchangers. The total heat recovery is generally greater for an enthalpy exchanger than for a heat exchanger due to the amount of latent heat that can be transferred in addition to the sensible heat. The quantity of this advantage depends on the humidities of supply and exhaust, but, in general, it is between 20 and 30 percent. For cold climates the advantage of an enthalpy exchanger becomes even greater than this number because of the longer time that it can be operated at high effectiveness without excess water. Under some conditions, the enthalpy exchanger is capable of recovering 50% more total energy than a sensible heat exchanger.

One case can be seen in Tables 6.1 and 6.2, where the total energy recovery of a sensible heat exchanger is actually greater than the enthalpy exchanger recovery (Houston, 30% indoor humidity). This result is due to the fact that the outdoor (supply) humidity is greater than the chosen indoor (exhaust) humidity. Therefore the sensible heat transferred by a heat exchanger is greater than the sum of sensible and latent heat transferred by an enthalpy exchanger and the heat exchanger yields a better enthalpy effectiveness. However, in heating applications the indoor humidity ratio is, due to humidity generation within the building, never less than the supply air humidity ratio, and

therefore this particular case represents a rather theoretical occasion that has no practical importance. For a heating operation in Houston a relative indoor humidity of 50% is a more reasonable value, and for this value the enthalpy exchanger works again better than the heat exchanger.

6.2.2 Energy Recovery in the Cooling Mode

The cooling simulations are executed for the same locations and operating conditions as the heating simulations, and energy recoveries are also integrated between 6 o'clock in the morning at 9 o'clock in the evening. The results for the annual simulations shown in Tables 6.3 and 6.4 display again a general trend for the energy recovery as a function of the location. A warm and humid climate yields greater reductions in the cooling load, and since both regenerators can be operated at their maximum effectiveness at all times, this trend holds for all indoor humidities.

The results also show that, different than in the heating mode, the energy recovery by a sensible heat exchanger is not a function of the exhaust humidity. The reason for this behavior is that the heat exchanger matrix has neither to be slowed down in order to avoid excess water, nor does a condensation/evaporation process without excess water take place on the matrix. Therefore the temperature effectiveness during operation is always constant at its maximum value, and the humidity effectiveness is at all times equal to zero. The enthalpy exchanger recovery is still a function of the exhaust humidity. The lower the exhaust humidity, the greater becomes the enthalpy difference between supply and exhaust inlets, and since temperature-, humidity- and enthalpy effectiveness are all constant, the enthalpy recovery increases.

Location	j_{ei} [%]	Q_{tot} [kW hr]	Hrs. of Operation
Madison, WI	30 50 80	4,093	575
Washington, DC	30 50 80	7,751	1,008
Houston, TX	30 50 80	25,070	2,361

Table 6.3: Sensible Heat Exchanger Recovery During the Cooling Season

Location	j_{ei} [%]	Q_{tot} [kW hr]	Hrs. of Operation
Madison, WI	30	21,690	575
	50	13,430	575
	80	4,238	389
Washington, DC	30	41,970	1,008
	50	27,350	1,008
	80	9,968	801
Houston, TX	30	143,000	2,361
	50	108,800	2,361
	80	60,207	2,335

Table 6.4: Enthalpy Exchanger Recovery During the Cooling Season

Care must be taken for cases of high indoor air humidity. Here it is possible that the indoor exhaust air enthalpy is greater than the outdoor supply air enthalpy even though its temperature is lower. In that case, there would be a negative energy recovery which would result in an increase in the cooling load, and the enthalpy exchanger must be turned off. A solution to this problem is to increase the on-/ offset temperature, and for the simulations done in this study a separate optimum control temperature was determined for each location and for each month of the cooling season.

The best temperature was found by simulating the regenerator performance for varying control temperatures and by comparing the resulting energy recoveries.

This problem occurred only for the highest indoor humidity of 80% and only for outdoor conditions that are fairly dry. For example, the warm and humid Houston climate does not show this problem at all, and in Washington and Madison, it is most serious during the spring and fall months when the outdoor air is typically drier than in the middle of the summer. As explained in Section 6.1.4, this problem applies only to enthalpy exchangers, since sensible heat exchangers transfer sensible heat only which is proportional to temperature, regardless of the humidity levels. The optimum control temperatures for the 80% exhaust humidity cases in Washington and Madison are shown for each month of the cooling season in Table 6.5.

For the reasons mentioned above, the advantage of an enthalpy exchanger over a heat exchanger depends on the indoor humidity, but for a likely value of 50% the enthalpy exchanger energy recovery was found to be three to four times greater than the recovery yielded by a comparable heat exchanger. The size of this factor is a function of the location's climate, and it increases with increasing humidity.

	Washington, DC	Madison, WI
May	28 °C	29 °C
June	25 °C	26 °C
July	24 °C	25 °C
August	24 °C	24 °C
September	25 °C	25 °C

October	28 °C	26 °C

Table 6.5: Optimum Control Temperatures for Enthalpy Exchanger Operation with Very High Indoor Humidity (80%)

6.3 Economic Analysis

The following economic analysis is divided into three sections. First the effect that rotary regenerators have on the initial cost of a complete space-conditioning system is investigated and thereafter annual savings that can result from a regenerator operation are calculated. Finally, an investigation of possible life cycle savings over a period of 15 years is made. Based on the previously described case of a 200 people office building, the three parts of the analysis are executed for all of the three locations, that were investigated in Section 6.2.

6.3.1 Installation Cost

The difference in the initial cost between systems with and without rotary regenerators is determined by the cost of the regenerator itself, and also by the maximum reduction in the heating and cooling loads that can be achieved by using regenerators. These reductions, that are due to the fact that energy from the exhaust air stream, which would otherwise be dumped, is directly used to precondition the supply air, result in the possibility of installing significantly smaller and cheaper additional heating and cooling equipment.

Information about the system costs of both enthalpy and sensible heat exchanger were provided by a local manufacturer of rotary regenerators. Wheels equipped with a constant speed drive cost $ 3,700 without and $ 4,500 with a water adsorbing polymer coating. In order to operate the exchangers in near optimal conditions as they are described in the previous sections, a variable speed motor and sophisticated control equipment, adding up to approximately $ 3,500 for either regenerator type, have to be purchased. Therefore the total enthalpy exchanger cost becomes $ 8,000, while the sensible heat exchanger is available for $ 7,200.

Approximate values for the price of conventional heating and cooling systems are published in the Means Facilities Cost Data Catalog [26] in terms of cost per capacity. The heating equipment cost for an incremental capacity change of a system that is appropriate for a 200 people office building, is round about $ 30 per kW, whereas $ 150 in installation costs can be saved for every kilowatt reduction in the maximum cooling capacity.

The simulation program described in Section 6.1 was used to calculate the allowable capacity reductions for the three different locations, and ASHRAE [1] design conditions were used to specify the weather conditions at which the maximum loads occur. For the two colder climates (Madison and Washington) an indoor humidity of 30% during the heating season and 50% during the cooling season was chosen, and for the humid Houston climate a year round constant value of 50% was assumed.

The results for the changes in the initial system cost, that are caused by the use of rotary regenerators are displayed in Tables 6.6 and 6.7.

Location	Madison, WI	Washington, DC	Houston, TX
Regenerator Cost	$ 7,200	$ 7,200	$ 7,200
Cool. Cap. Reduction	17 kW	18 kW	22 kW
Savings Cool. System	- $ 2,550	- $ 2,700	- $ 3,300
Heat. Cap. Reduction	42 kW	42 kW	26 kW
Savings Heat. System	- $ 1,260	- $ 1,260	- $ 780
Total Additional Cost	$ 3,390	$ 3,240	$ 3,120

Table 6.6: The Effect of a Heat Exchanger on the Initial System Cost

It can be seen in the tables that the reductions in the maximum cooling loads increase with increasing outdoor supply temperatures. Furthermore, due to its potential of transferring latent heat between two air streams, the enthalpy exchanger is capable of reducing the maximum cooling system capacity by a number that is nearly 2.5 times greater than the reduction allowed by a sensible heat exchanger. This result is in accordance with numbers predicted by Bowlen [5].

Location	Madison, WI	Washington, DC	Houston, TX
Regenerator Cost	$ 8,000	$ 8,000	$ 8,000
Cool. Cap. Reduction	37 kW	43 kW	50 kW
Savings Cool. System	- $ 5,550	- $ 6,450	- $ 7,500
Heat. Cap. Reduction	70 kW	69 kW	64 kW
Savings Heat. System	- $ 2,100	- $ 2,070	- $ 1,920
Total Additional Cost	$ 350	- $ 520	- $ 1,420

Table 6.7: The Effect of an Enthalpy Exchanger on the Initial System Cost

As described earlier, the values for the allowable decrease in heating capacities are not

directly proportional to the design weather conditions, since very cold temperatures cause an operation with decreased effectiveness. Therefore the reduction allowed by the enthalpy exchanger is almost constant for the three locations although the winter design temperatures differ significantly. In Houston the exchanger can still be operated at its maximum effectiveness, and the energy recovery is almost equal to the recoveries that are achieved in Washington and Madison at colder temperatures but necessarily slower rotation speeds. For the sensible heat exchanger the rotation speed has to be slowed down in Houston, too, and its heating capacity reduction is about 1.5 times smaller than in the other two locations.

As shown in Table 6.6, the additional cost of a complete space-conditioning system that includes a sensible heat exchanger compared to one without a regenerator is almost constant for the three investigated locations. The slight advantage of the warmer climates can be explained by the fact that cooling equipment is more expensive than heating equipment in terms of cost per capacity.

For systems including an enthalpy exchanger, the additional first cost is for all cases significantly less than for the heat exchanger systems. The dependence on the climate is much stronger for the enthalpy exchanger, since the reductions in heating capacity are nearly constant and the reductions in the cooling capacity increase significantly, the warmer and more humid the climate is. In Washington and Houston, the total cost of a system with an enthalpy exchanger is shown to be even less than the cost of a system without a regenerator.

It should be noted, that the energy that can be saved by a sensible heat or an enthalpy exchanger has to be recovered from the exhaust. For this reason the exhaust air must be collected and conveyed to the location of the rotary regenerator. Depending on the building design, doing this might require a significant constructional effort, and the cost of the extra exhaust air ducting or piping has to be added to the results in Tables 6.6 and 6.7 and weighed against the operating savings that will be determined in the following section.

6.3.2 Annual Operating Savings

The annual operating savings that can be achieved by using regenerators are governed by the integrated values of the annual energy recoveries for heating and cooling (determined in Section 6.2), and by the energy cost that would have to be paid, if the same conditioning process was executed with conventional heating and cooling equipment.

The operating cost of a common gas furnace is approximately $ 0.021 per kWhr of heat. An average price for electricity is $ 0.08 per kWhr and assuming a cooling system with a coefficient of performance (COP) of 3, the operating cost for cooling becomes $ 0.026 per kWhr.

Even though the amount of energy required by the regenerator drive is assumed to be negligible, the regenerator still incurs some operating costs. Since the small channels through which the two air streams are passed lead to a pressure drop of the air, a greater amount of energy is required to operate the fans of the ventilation system. A pressure drop of approximately 250 Pa is given in the manufacturer's catalog (Carnes [9]) for the operating parameters chosen in this study, resulting in an increase in the fan power by 950 W for two air streams of 2.28 kg/s each. The ventilation system is run 15 hours a day for 365 days a year, and therefore the use of a rotary regenerator requires an additional energy of 5,200 kWhr per year to overcome this pressure drop.

The results for the annual operating savings made possible by the use of a rotary regenerator are summarized for the three investigated locations in Tables 6.8 and 6.9. The indoor humidities of the cooling zones are assumed to be 50% for all locations and the humidities of the heating zones are 30% for Madison and Washington and 50% for Houston.

Location	Madison, WI	Washington, DC	Houston, TX
Heating Recovery	126,500 kW hr	91,300 kW hr	31,400 kW hr
Heating Savings	$ 2,657	$ 1,917	$ 659
Cooling Recovery	4,093 kW hr	7,751 kW hr	25,070 kW hr

Cooling Savings	$ 106	$ 202	$ 652
Increase Fan Power	- 5,200 kW hr	- 5,200 kW hr	- 5,200 kW hr
Cost of Fan Power	- $ 400	- $ 400	- $ 400
Total Oper. Savings	$ 2,363	$ 1,719	$ 911

Table 6.8: Annual Operating Savings - Heat Exchanger

The annual operating savings show that a sensible heat exchanger provides greater savings in cold climates than in warm and humid climates, since it operates fairly poorly in the cooling mode. The enthalpy exchanger works well in cold as well as in warm and humid climates, and therefore its operating savings are greater for both extremes (Madison and Houston) than they are for the intermediate Washington climate. In general, enthalpy exchangers allow significantly higher annual savings than sensible heat exchangers.

Location	Madison, WI	Washington, DC	Houston, TX
Heating Recovery	148,700 kW hr	99,900 kW hr	37,900 kW hr
Heating Savings	$ 3,123	$ 2,098	$ 796
Cooling Recovery	13,430 kW hr	27,350 kW hr	108,800 kW hr
Cooling Savings	$ 349	$ 711	$ 2,829
Increase Fan Power	- 5,200 kW hr	- 5,200 kW hr	- 5,200 kW hr
Cost of Fan Power	- $ 400	- $ 400	- $ 400
Total Oper. Savings	$ 3,072	$ 2,409	$ 3,225

Table 6.9: Annual Operating Savings - Enthalpy Exchanger

6.3.3 Life Cycle Savings

A life time of 15 years is assumed in order to calculate the accumulated life cycle savings (LCS) of the two regenerator types. A five percent inflation rate for natural gas and electricity is chosen, and

the resulting cash flows are discounted to a present worth with an interest or discount rate of eight percent. The installation cost (again without any additional ducting or piping expenses that might be required) has to be paid immediately, whereas the cash flows that result from the annual operating savings are assumed to occur at the end of each year.

The present worth P of a serious of annual cash flows A_n can be determined as a function of the system life time N, the geometric gradient g of the cash flow serious (inflation) and the discount rate i (see Bussey and Eschenbach [8]). For an inflation rate less than the discount rate as it is assumed in this study, the present worth becomes:

$$P = \frac{A_1}{1+g} \cdot \frac{(1+x)^N - 1}{x(1+x)^N} \tag{6.1}$$

where $x = \frac{1+i}{1+g} - 1 = \frac{1.08}{1.05} - 1 = 0.02857$

and A_1 : Cash flow at end of first year

Table 6.10 summarizes the obtained values for the present worth of the accumulated life cycle savings in US Dollars for both exchanger types in three different climates.

Location	Regenerator	Installation Cost	Present Worth Oper. Savings	Present Worth LCS
Madison, WI	HX	- 3,390	27,146	23,756
	EX	- 350	35,291	34,941
Washington, DC	HX	- 3,240	19,748	16,508
	EX	520	27,674	28,194
Houston, TX	HX	- 3,120	10,465	7,345
	EX	1,420	37,048	38,468

Table 6.10: Life Cycle Savings

All investigated systems have life cycle savings whose present worth is greater than zero for the assumptions on that the foregoing calculations are based. However, the sensible heat exchanger in a very warm and humid climate results in savings that are significantly smaller than all other values, indicating that this would be a relatively bad investment. In general, it can be seen that the heat exchanger payoff increases with colder weather conditions.

The enthalpy exchanger allows higher life cycle savings for the two extreme climates than for the intermediate conditions in Washington. The advantage of an enthalpy exchanger over a sensible heat exchanger is significant at all locations, but it becomes most important in the warm and humid climate where the sensible heat exchanger performs fairly poor. However, the calculation of the life cycle savings for both exchanger types are based on the same system lifetime of 15 years. No information concerning the durability of the desiccant used in the enthalpy exchanger is available, but if the investigated polymer coating has a shorter life time than the aluminum wheel itself, the enthalpy exchanger performance will become similar to the sensible heat exchanger performance towards the end of the assumed 15 year life time, and the economic benefits of the enthalpy exchanger will decrease.

7 ADSORPTION MEASUREMENT - VOLATILE ORGANIC COMPOUNDS

Volatile organic compounds (VOCs) are often the cause for bad indoor air quality. They are typically hydrocarbons with 6 to 17 carbon atoms and their concentration in indoor air is usually much larger than in outdoor air. These pollutants are emitted from sources within buildings, such as people, building materials, carpets, copy machines, etc., and their concentration is tried to be kept down by ventilation systems.

The reason for measuring the matrix adsorption capacity for VOCs is the potential of any rotary enthalpy or heat exchanger to exchange VOCs in addition to water vapor between the two air streams that are passed through it in counterflow arrangement. If the desiccant material is able to adsorb these hazardous contaminants, they could be transferred from the exhaust air, where there is a high concentration of VOCs, to the supply air , in the same way as humidity is exchanged.

Of course, this process is undesirable since much higher air flow rates would be required to keep the conditioned indoor air at a low contaminant level, if the concentration of the supply air stream were raised inside the enthalpy exchanger. As a result the fan power would increase and bigger and more expensive regenerators would have to be installed.

For this reason a well-designed enthalpy exchanger has to consist of a matrix that is able to adsorb large amounts of water vapor but as little VOCs as possible.

7.1 Gas Chromatography and Frontal Analysis Technique

Gas chromatography is a separation procedure in which a mixture of gases is passed through a column that contains an adsorbent. This adsorbent can be of solid or liquid nature. The various gases and vapors in the solution have different affinities to the adsorbent and are separated on their way through the column. The components with higher affinity to the adsorbent are adsorbed in greater amounts and therefore need a longer time to exit the column than the components with lower attraction to the adsorbent. A detector at the column outlet receives a signal which is characteristic for a particular combination of adsorbent and gas composition. If the adsorption column is calibrated, the gas composition can be determined.

The frontal analysis technique used in this study is based on the same adsorption principles but it works the other way round. In this case a constant, known inlet concentration of one solute in a carrier gas is passed through a column that contains an unknown adsorbent and the outlet signal is used to determine the adsorption capacity of the adsorbent for the specific solute.

The frontal analysis technique with the system shown schematically in Figure 7.1, is essentially a mass balance of the solute stream running through the gas chromatograph.

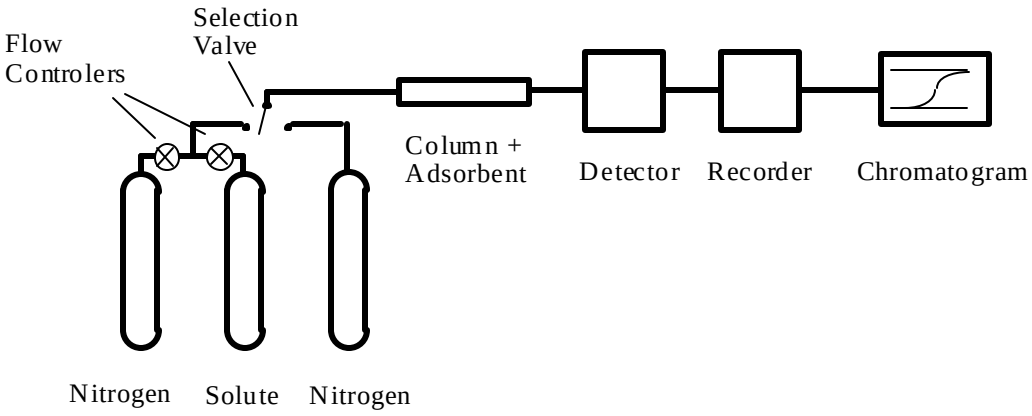

Figure 7.1 Schematic of Gas Chromatograph System

Initially, a carrier gas which does not affect the detector signal is passed through the column. At time t_o the two stream selection valve is switched and a mixture of the same carrier gas and a

solute of known concentration is passed through the chromatograph and contacts the adsorbent sample. The sample filters the solute out of the gas mixture until saturated conditions are reached. During this first period the detector signal remains constant since only the carrier gas exits the column outlet. Once the adsorbent is saturated with the gas mixture entering the column (time t_{end}), the mixture exits the column in the same concentration as it entered. The detector signal displays this outlet concentration and the measurement is terminated.

In an ideal case, the detector signal, which is directly proportional to the outlet concentration, stays constant until the adsorbent is completely saturated and it steps up with an infinite slope at t_{end}. This ideal behavior is shown in Figure 7.2.

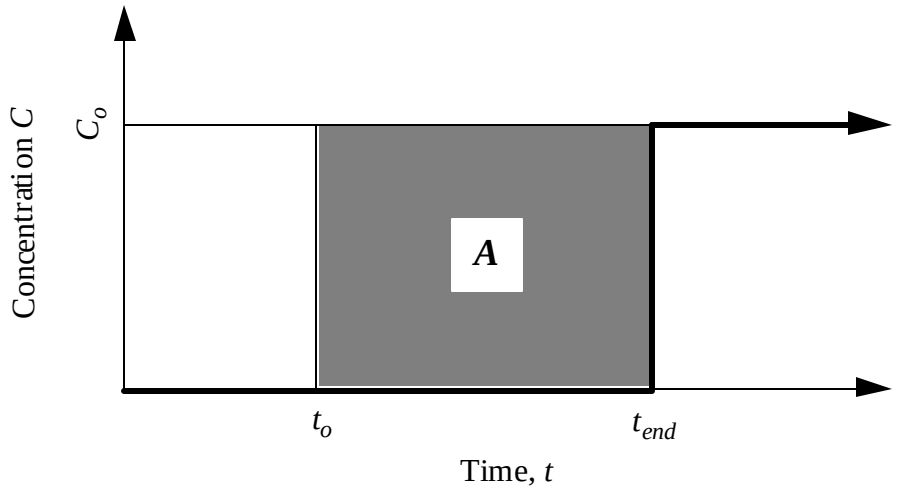

Figure 7.2 Idealized Frontal Chromatogram

Knowing the gas flowrate of the mixture $\dot{m}_{mix}$ and the concentration C_o, of the solute, the amount adsorbed $m_{ads} = m_{in} - m_{out}$ can be evaluated multiplying the flowrate by the shaded area *A* in Figure 7.2:

$$m_{ads} = \dot{m}_{mix} A = \dot{m}_{mix} C_o (t_{end} - t_o) \tag{7.1}$$

A nondimensionalized value q of the amount adsorbed can be obtained by dividing this number by the mass of the adsorbent sample m_{sam}:

$$q = \frac{m_{ads}}{m_{sam}} = \frac{\dot{m}_{mix} A}{m_{sam}} \tag{7.2}$$

However, in a real system there are resistances to mass transfer between the gas and the sample (adsorption) which result in a dispersion of the detector signal. As shown in Figure 7.3 the shaded area A that has to be determined in order to calculate the amount adsorbed, is no longer rectangular, thus has to be obtained by integration:

$$A = \int_{t_o}^{t_{end}} (C_o - C)\, dt = C_o (t_{end} - t_o) - \int_{t_o}^{t_{end}} C\, dt \tag{7.3}$$

The definition of the time t_{end} used in this study is described in Section 7.3.3.

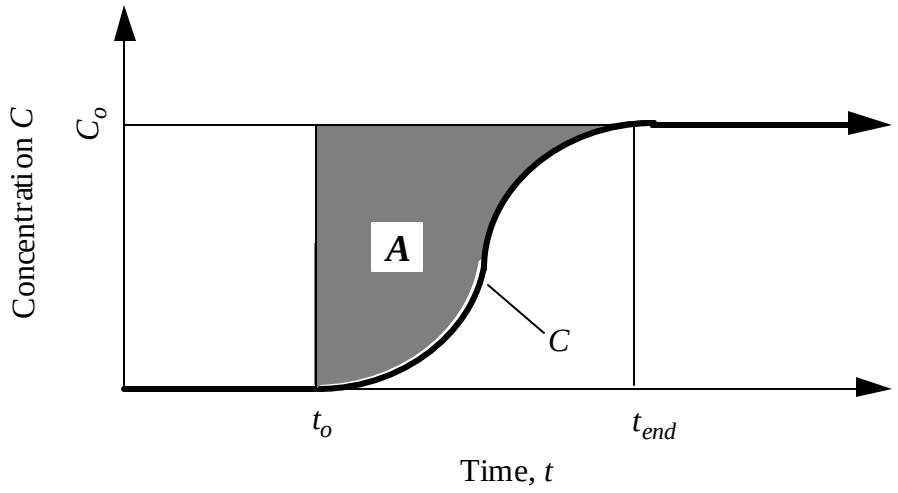

Figure 7.3 Diffuse Frontal Chromatogram

7.2 System Components

In this section, the system used to measure the adsorption capacity of the water-based polymer desiccant for several volatile organic compounds is discussed. The total system is shown in Figure 7.4, and a brief description of the components follows.

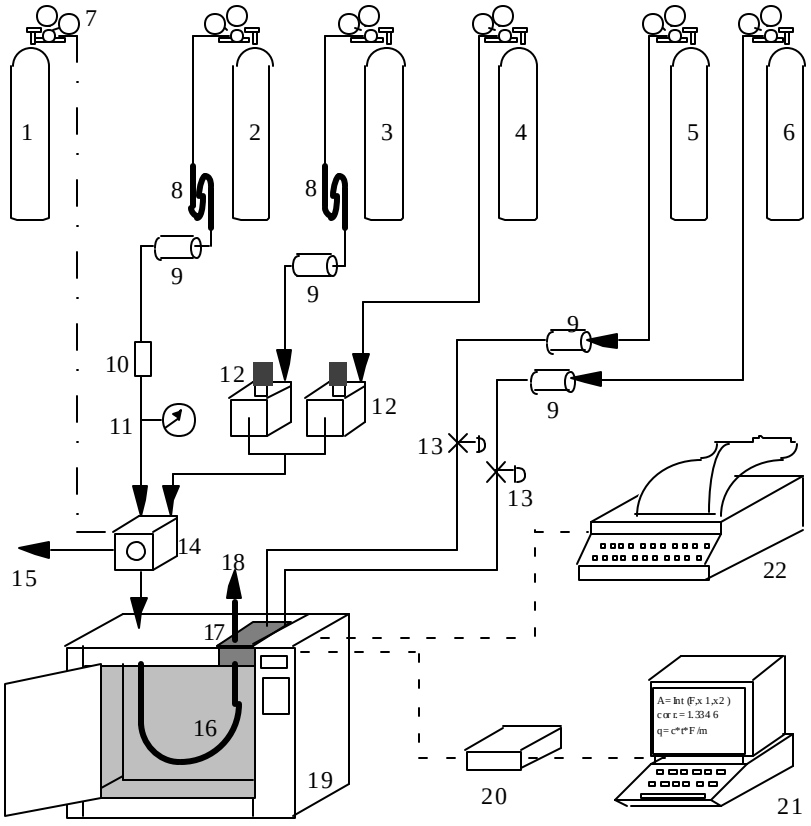

1. Compressed Air
2. Carrier Gas
3. Nitrogen Diluent
4. Contaminant-N_2 Mix
5. Compressed Air
6. Hydrogen
7. Pressure Regulator
8. Hydrocarbon Trap
9. Moisture Trap
10. Chemical Trap
11. Pressure Gauge
12. Flow Controller
13. On/Off Valves
14. Two-Stream Selection Valve
15. Vent to Atmosphere
16. Glass Column and Filter
17. Flame Ionization Detector
18. Detector Exhaust
19. Gas Chromatograph
20. A/D Converter
21. Personal Computer
22. Electronic Integrator

Figure 7.4 Experimental System. Adapted from Schaefer [30]

7.2.1 Gas Chromatograph

The Hewlett-Packard gas chromatograph, type 5890 Series II, is the centerpiece of the experimental system. In its oven compartment, it contains the glass column with the adsorbent sample. The oven temperature can be set in 1°C steps from slightly above room temperature up to 450°C. However, a maximum temperature of 175°C should not be exceeded, because a valve located inside the oven could otherwise be damaged. An operation at or below room temperature is also not possible, since the used chromatograph is not equipped with an optional cooling equipment.

The two-stream-selection valve shown in Figure 7.5 controls whether the carrier gas or the solute mixture is passed through the adsorption column and it is operated by compressed air. The valve can be switched by the keypad on the front side of the gas chromatograph. Other important functions of the keypad are the adjustment of the Range-command (described in Section 7.2.2) and the oven temperature, the signal display and a timer, which is used together with the flowmeter in order to determine the gas flowrates (Section 7.2.4).

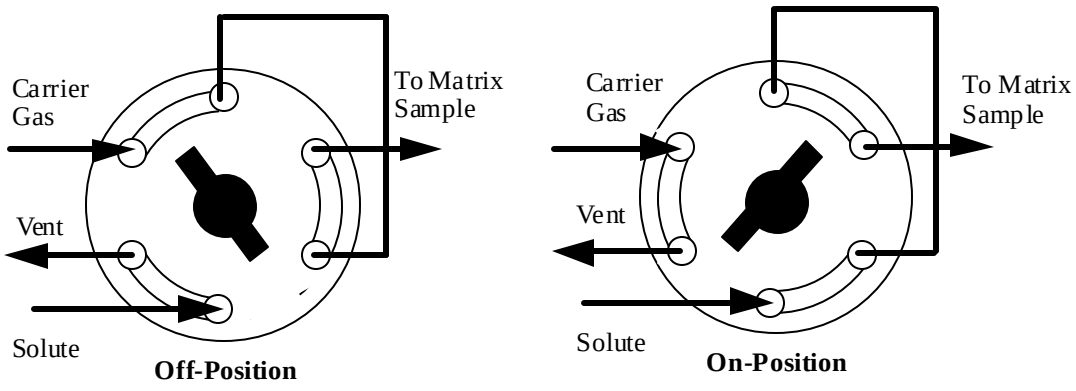

Figure 7.5 Pneumatic Gas Stream Selection Valve. Adapted from Schaefer [30]

7.2.2 Flame Ionization Detector

The flame ionization detector (FID) is a device to measure the contaminant concentration in the gas mixture exiting the adsorption column. Most organic substances and all the VOCs tested in this study are detectable with the FID. A schematic of the detector is shown in Figure 7.6. The operating principle of the FID is that a steady flame is maintained with constant hydrogen and air streams. The gas mixture that exits the column is passed through the flame where the organic compounds are burned and form ions. These ions are received in the collector where a polarizing voltage is present. They are attracted by this voltage and produce a current proportional to the amount of organic contaminant burned in the flame. The current runs through a resistor and results in a voltage that is also proportional to the concentration and can be measured. The output signal must be calibrated with a gas mixture of known composition and then every measured voltage can be transformed into a contaminant concentration.

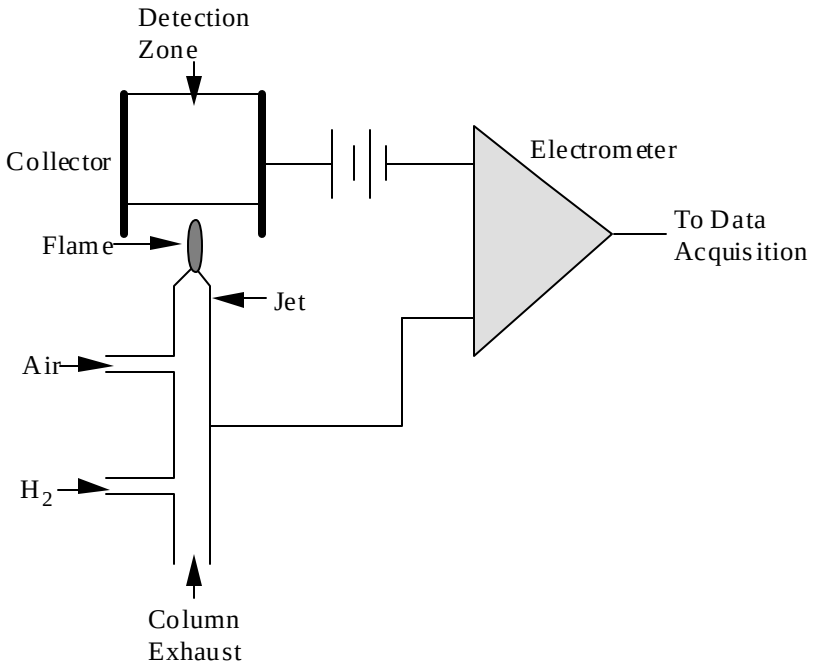

Figure 7.6 Flame Ionization Detector. Adapted from Buffington and Wilson [7]

The reason why a flame ionization detector was used in this study is its linear output signal which is directly proportional over a wide range. This proportionality can typically by observed

from the smallest detectable concentration up to a concentration 10^6 to 10^7 times greater than this value. The sensitivity for organic contaminants is dependent on the molecular structure of the contaminant and ranges between 10 and 100 picograms per ml of carrier gas.

The sensitivity of the FID is, for a given jet diameter, a function of the flame size and shape, and these parameters are governed by the air and hydrogen flowrates. The hydrogen flowrate has a much greater impact on the sensitivity than the air flowrate which is kept constant at approximately 300 ml/min. Figure 7.7 shows the effect of the hydrogen flowrate on the output signal for constant air and solute flowrates. As seen in the plot, the hydrogen flowrate should be adjusted between 55 and 62 ml/min in order to receive the maximum signal.

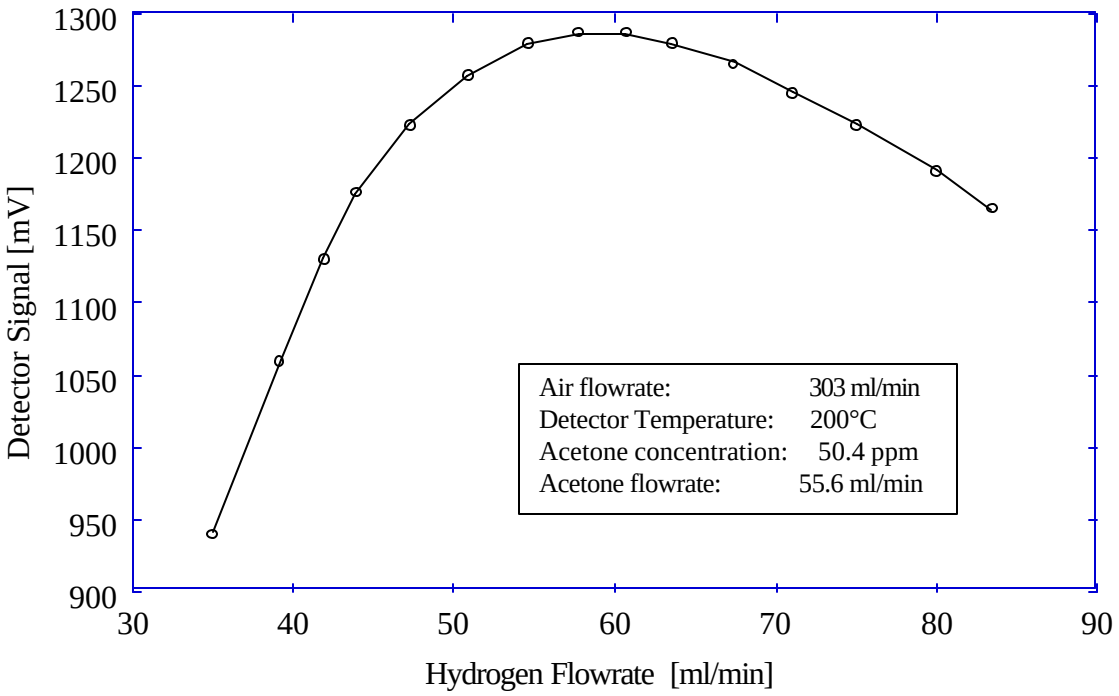

Figure 7.7 FID Sensitivity Optimization. Adapted from Schaefer [30]

The output is always a signal between zero and one volt and every voltage exceeding this interval is getting truncated. Therefore it is important to make sure that the highest signal occurring at maximum concentration is smaller than 1 V. This can be achieved by setting the Range 2 command with the chromatograph keypad. The effect of the setting is to enter the value of Range in Equation 7.4, where each increase of the Range parameter by one lowers the signal transmitted to the PC by one half.

$$\text{Voltage to PC} = \frac{\text{Detector Signal}}{2^{\text{Range}}} \tag{7.4}$$

7.2.3 Data Acquisition

The detector signal is transmitted to a personal computer and saved on a disc. The time steps in which the saving is done can be chosen by the operator but have to be greater than 10 seconds. The best choice depends on the duration of the measurement which is a function of the contaminant flowrate and the adsorption capacity of the sample. For samples that adsorb only a very small amount of contaminants the time steps between two recordings ought to be as short as possible.

The FID signal is also transmitted to an electronic integrator that is used as an x-y plotter only. It creates a visual copy of the recorded outlet concentration-time function and helps finding the time when a measurement can be terminated.

7.2.4 Gas Supply and Flowmeter

The gas supply for the chromatograph consists of six gas cylinders, six pressure regulators, four moisture, one chemical and two hydrocarbon traps and two flow controllers in the arrangement shown in Figure 7.4.

All of the six gas cylinders are fitted with pressure regulators that throttle the high pressure inside the cylinders to a much lower operating pressure. They are designed in a way that the operating pressure remains constant regardless of pressure changes inside the cylinder. Thus, the gas flow rates are constant for the entire measurement and do not have to be adjusted during the run.

Two cylinders contain compressed air. One of them is used to operate the two-stream selection valve that selects the gas stream passing through the column. The other cylinder provides air for the flame ionization detector.

There are also two cylinders filled with nitrogen and one of them is used as carrier gas which is passed through the column in order to desorb the desiccant sample. The second nitrogen cylinder can be used to dilute the contaminant-nitrogen mixture kept in a separate cylinder. This mixing is done with the flow controllers and allows to vary the contaminant concentration. Both nitrogen cylinders have a grade of ultra high purity which implies a purity of 99.999% and the concentration of the contaminant gas cylinder is certified to a ±5% error. The hydrogen is needed to supply fuel for the flame in the FID.

Moisture traps are located between all cylinders and their end uses. In addition both of the nitrogen cylinders are equipped with hydrocarbon traps and the carrier gas used to desorb the matrix sample is also passed through a chemical trap before it enters the column.

All the gas flow rates in this system are determined with a Hewlett-Packard soap film flowmeter. The flowmeter can be connected to the exhaust of the FID with a special adapter that seals itself with an O-ring. It has marks at volumes of 1 ml, 10 ml and 100 ml in flow direction, and

depending on the particular gas flowrate the time elapsed between initializing one soap bubble and the passing of one of these marks is measured and the flowrate can be calculated:

$$\dot{V} = \frac{V}{t} \tag{7.5}$$

In order to avoid a bursting of the bubbles inside the flowmeter, its inner surface should be wetted by running several bubbles through the meter before the actual time measurement is started.

7.2.5 Matrix Sample

The sample of the water-based polymer desiccant matrix was the same coated aluminum foil as described in Chapter 3.1. However the foil was cut into many small pieces in order to fit into the narrow adsorption column and the pieces were put loosely in the column in order to expose the largest possible surface area to the surrounding gas stream.

Before the sample can be cut into pieces it has to be dried and weighed in the way described in Section 3.1.2 in order to be able to evaluate the nondimensionalized adsorption capacity (Equation 7.2). The dry weight of the tested sample was in the range of 2 grams.

7.3 Test Procedure

This section describes the procedure necessary to measure the adsorption capacity of the matrix sample for several organic contaminants using the experimental system discussed above. It starts with the preparations that have to be made before the actual measurement is started and ends with a description of the analysis of the test data obtained.

7.3.1 Preparations

After the adsorption column containing the matrix sample is installed inside the oven compartment of the gas chromatograph, several preparations have to be made before an actual adsorption capacity measurement can be started.

First, the oven temperature has to be set to the desired value. In this study a temperature of 35°C was chosen because it is high enough above the surrounding room temperature to assure that it can be kept constant during the entire measurement. This is important since the oven temperature can be controlled by a heating element and a fan only. On the other hand side 35°C is still low enough to assume that the measured data will be characteristic for a real application in an air conditioning system. The oven temperature has to be constant until the volumetric flowrates of all gas streams are measured since the specific volume of gases is a quite strong function of temperature.

The next step is to adjust the desired concentration of the contaminant-nitrogen mixture with the two flow controllers. This can be done by setting the solute flowrate to a constant value and adding a certain flowrate of pure nitrogen to dilute the contaminant until the right concentration is

achieved. The total flowrate of the solute-diluent mixture should be between approximately 55 and 60 ml/min. Usually, this adjustment is executed right after a previous run since the procedure requires to pass a contaminant stream through the column and the matrix sample has to be desorbed again before a new measurement can be started.

The desorption of the matrix sample is done by switching the two-stream selection valve via the keypad to the Off-position and passing pure carrier gas through the column. During this desorption the oven temperature is also kept at 35°C. Although a higher temperature can speed up the process of desorption, this one should be chosen to prevent the sample from losing its adsorption capacity because of a high temperature treatment. Such a behavior was observed by Boor [4] in the investigations of activated carbon. Due to the small adsorption capacity of the water-based polymer material, the desorption times are short and two or three hours are well in excess of the time needed to completely desorb the sample. During the desorption the On/Off valves of the contaminant and diluent gas cylinders are switched to the Off-position until just a few minutes prior to the next run.

After the desorption is finished, the Range parameter has to be chosen depending on the kind and the concentration of the contaminant. Usually a value of either one or zero is appropriate.

The last things that need to be prepared are the setting of the clock and the time steps between recordings with the personal computer and the ignition of the FID flame. Several minutes prior to the test all the gas cylinders are switched to the On-position in order to assure steady flowrates once the measurement is started, and the contaminant stream is directed to the fume hood while the two-stream selection valve is still in the Off-position.

7.3.2 Run Execution

The steps that are necessary to execute the adsorption capacity measurement are the start of the data acquisition program, the switching of the pneumatic two-stream-selection valve and the entering of the plot command with the integrator keypad. The sequence and timing in that these steps have to be executed are determined by the time that the contaminant stream takes to travel from the selection valve to the FID and the logging time interval of the data acquisition software.

The gas travel time can be determined by passing a contaminant stream through an empty glass column and measuring the time between switching the selection valve and the first signal received by the FID. For a volumetric flowrate of 55 ml/min and an oven temperature of 35°C it was determined to equal approximately 7 seconds.

The data acquisition software takes about 25 seconds to initialize and then pauses for the time step between two recordings until the first FID-signal is logged. For example, if the program is set to record the signal every 10 seconds, then there will be a delay of approximately 35 seconds from the moment the command is entered to the recording of the first data point.

In order to achieve an accordance between the data recorded by the personal computer and the visual chromatogram plotted by the electronic integrator, the integrator must be started at the same time the first data point is recorded, thus 35 seconds after entering the command to start the data acquisition program. There is no delay between the command is entered to the keypad and the integrator starts plotting.

Moreover, the recording of the first data point ought to occur at the precise moment the contaminant stream first reaches the FID. Therefore the two-stream-selection valve has to be switched to its On-position 7 seconds prior to the first recording and the start of the electronic integrator.

Hence, for the given example, the data acquisition program is started at time zero, the pneumatic selection valve is switched at $(35 - 7) = 28$ seconds and the electronic integrator is

started 35 seconds after the command to start recording was entered to the PC.

After the outlet concentration measured by the FID reaches 99% of the inlet concentration approximately 200 more data points have to be recorded before the measurement can be terminated. Boor [4] determined that this is the number of data points after that the arithmetic average of the outlet concentration does not change anymore.

7.3.3 Data Analysis

The raw data obtained from a measurement is in form of a table containing one column for time and another column for the signal. Neither column starts with a value of zero and therefore the two columns have to be manipulated to the form shown in Table 7.1. Since the FID signal is proportional to the contaminant concentration in [ppm] and the inlet concentration is known, the voltage signal can easily be converted to a concentration.

In order to determine the area A in Figure 7.8 that represents the amount adsorbed the time t_{end} has to be defined. This is done by selecting the first data point for which the manipulated signal is approximately 99% of the maximum manipulated signal V_{max} that occurs during the whole run, as it was suggested by Boor [4]. At this time t_{end} the adsorbent is assumed to be saturated and the mean voltage of all the following data points $\overline{V}_{\max}$ is calculated and then considered to be the maximum voltage of the test run. By doing this the influence of the noise in the output signal is eliminated.

Data Point #	Raw Time [s]	Raw Signal [V]	Manipulated Time [s]	Manipulated Signal [V]	Manipulated Signal [ppm]
1	37448	0.01126	0	0	0
2	37506	0.01126	58	0	0
3	37570	0.01126	122	0	0
.	.	.	.	.	.
.	.	.	.	.	.
11	38045	0.45883	597	0.44757	21.8
12	38104	0.52515	656	0.51389	25.0
13	38169	0.59106	721	0.57980	28.3
.	.	.	.	.	.
.	.	.	.	.	.
26	38947	0.89514	1499	0.88388	43.4
27	39005	0.90098	1557	0.88972	43.7
28	39071	0.90390	1623	0.89264	43.8
.	.	.	.	.	.
.	.	.	.	.	.
230	51189	0.91214	13741	0.90088	44.1
231	51245	0.91214	13797	0.90088	44.1
232	51304	0.91214	13856	0.90088	44.1

Table 7.1 Raw and Manipulated Data

Now the unshaded area below the concentration curve in Figure 7.8 can be integrated numerically from time t_o to t_{end} and the shaded area A that is proportional to the amount adsorbed is the difference between the rectangle C_o (t_{end} - t_o) and this integral. The nondimensionalized adsorption capacity q is then calculated by Equations 7.2 and 7.3.

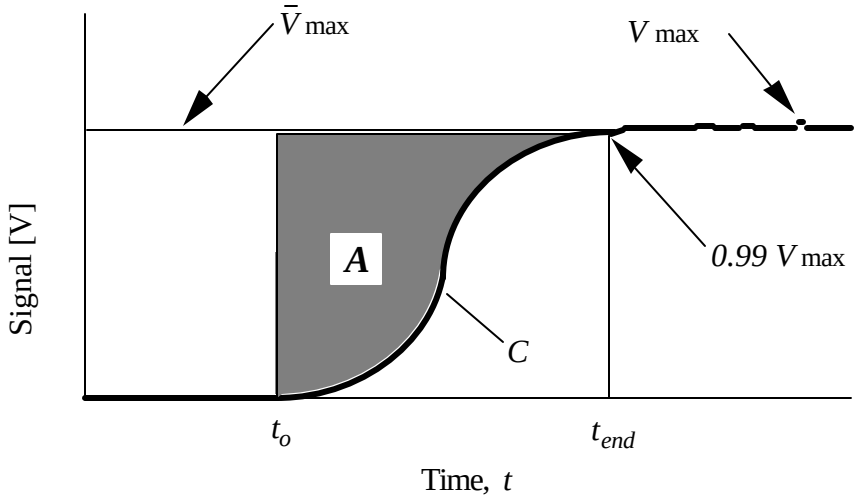

Figure 7.8 Method for Area Analysis

7.4 Results

The adsorption capacity of the matrix material was determined for two organic contaminants, propane (C_3H_8) and toluene (C_7H_8). These two substances have different molecular weights and they were chosen in order to investigate if the adsorption capacity might be a function of the molecular weight of the contaminant. This effect was observed for activated carbon samples examined by Boor [4].

The adsorption capacity of activated carbon, a typical filter material, was also determined for propane in order to assess how the adsorption capacity of the water-based polymer desiccant compares to such a filter material. The dry weight of the matrix sample was determined to be 1.8368 g and the activated carbon mass was in the range of 0.03 g.

The propane tests were executed at an oven temperature of 35°C and the maximum possible propane concentration of 43.9 ppm. Thus, there was no diluent nitrogen stream mixed with the solute. The adsorption chromatograms for an empty column, the water-based polymer

sample and an activated carbon sample are shown in Figures 7.9, 7.10 and 7.11, respectively. As seen by the rectangular shape of the outlet concentration that reaches its maximum immediately at time t_0 (Figure 7.10), the adsorption capacity of the matrix for propane is negligible. The curve is identical to the one measured without any samples.

A measurement with a lower propane concentration is not necessary because the use of a diluent would only have a decreasing effect on the adsorption capacity that is already negligible with this highest possible concentration.

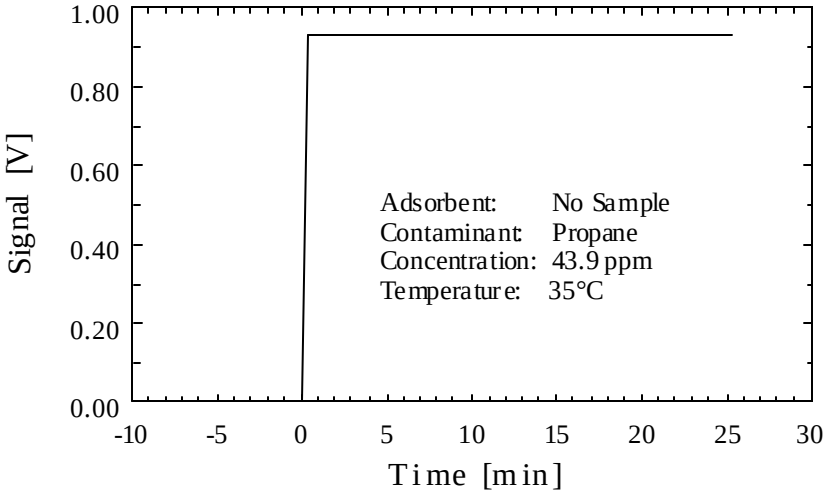

Figure 7.9 Propane Chromatogram. No Sample

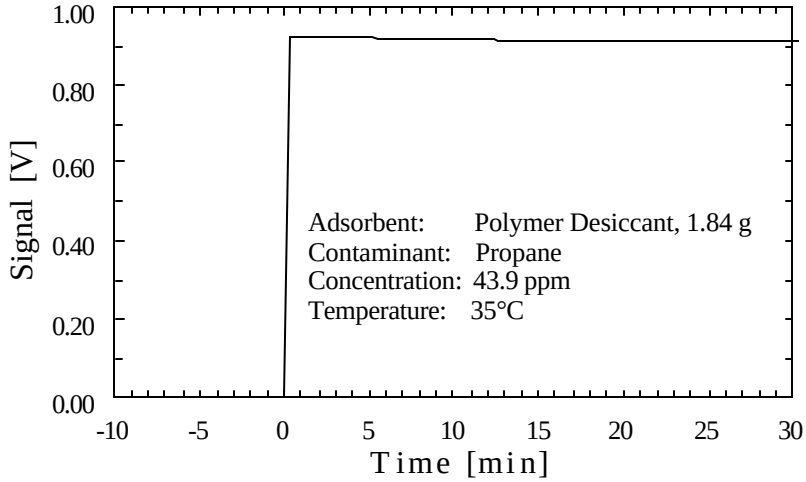

Figure 7.10 Propane Chromatogram. Matrix Sample

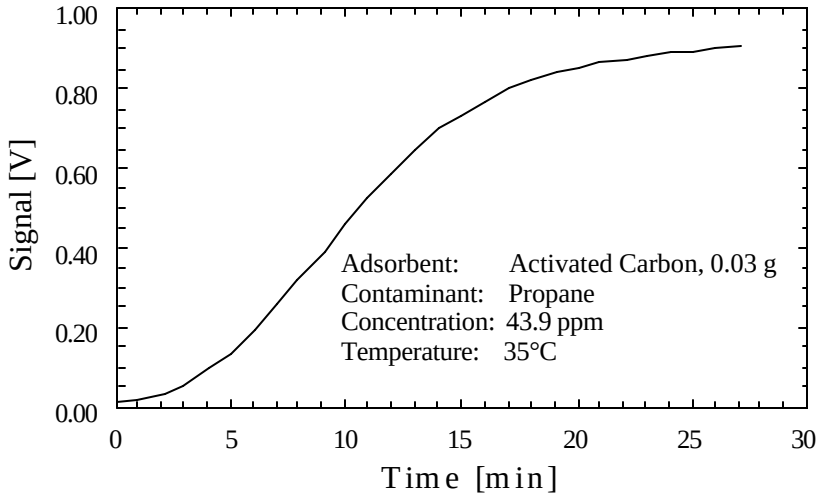

Figure 7.11 Propane Chromatogram. Activated Carbon

The toluene tests were also done at 35°C and a maximum possible concentration of 10.31 ppm and the results are similar to the ones of the propane tests. Again, the outlet concentration has a rectangular shape reaching the maximum value immediately after the two-stream-selection valve is switched to its On-position (Figure 7.12).

Therefore the water-based polymer desiccant neither adsorbs propane nor the heavier toluene in an amount that has an impact on the enthalpy exchanger performance or the indoor air quality. Since water is adsorbed by the material as it was shown in Chapter 3, the adsorption seems to be governed by the molecules' dipole character rather than by the molecular weight. The fact that the tested contaminants are not adsorbed by the desiccant material is desirable for use in rotary regenerators since contaminants will not be transferred from the exhaust to the supply air stream by an adsorption-desorption mechanism.

However, contaminants could still be transferred by the mechanical mechanism of carry-over, but this is a function of the regenerator design rather than the matrix material which is investigated here.

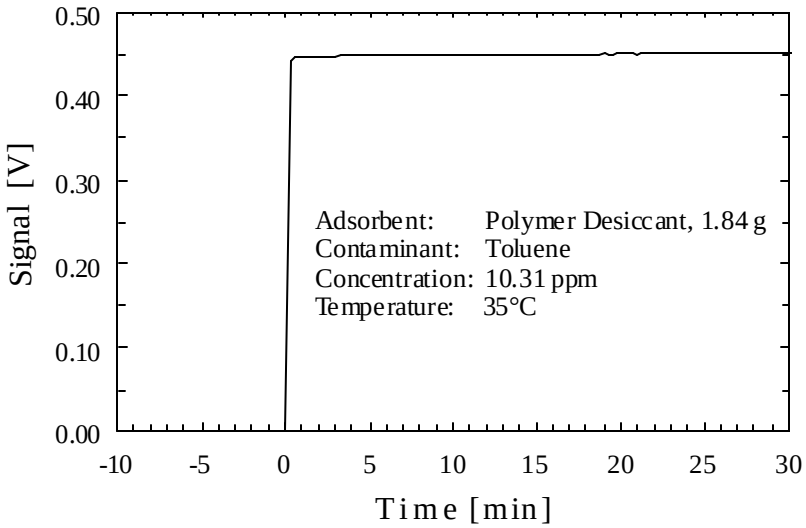

Figure 7.12 Toluene Chromatogram. Matrix Sample

7.5 Experimental Uncertainties

A very rigorous uncertainty analysis of the same experimental system that is used here was conducted by Boor [4]. He found a total error for the amount adsorbed *q* that ranged from 6-8% for measurements without a diluent to 7-15% for measurements that included the use of a diluent to lower the contaminant concentration.

Since the adsorption capacities measured in this study are negligible anyway, a more detailed analysis of the experimental error is abandoned.

8 CONCLUSIONS AND RECOMMENDATIONS

8.1 Conclusions

In the foregoing study, a desiccant material used as a matrix in a commercially available rotary heat and mass exchanger was experimentally examined in order to obtain its specific heat and adsorption isotherms that are characteristic for the exchanger performance. It was found that a fraction of approximately 95 weight percent of the material is contributed by an aluminum foil, while only 5 percent are due to the desiccant polymer coating. Thus, the heat capacity is approximately equal to that of pure aluminum, and - when operated at the same rotation speed - the enthalpy exchanger will meet the same sensible load as a rotary heat exchanger that consists of an uncoated aluminum matrix of the same design.

The desiccant adsorption capacity for water vapor was measured for various temperature-humidity combinations and a type III isotherm behavior, as it is typical for many macro-porous adsorbents, was observed. The maximum water uptake of the desiccant was determined to be approximately 160% of the coating weight (8% of the total foil weight), and it was shown that the uncertainty involved in the measurements for the adsorption capacity is about 6% of the measured value.

The effect of the isotherm shape on the enthalpy exchanger performance was analyzed by comparing the water-based polymer desiccant (type III) with a silica gel (type I) matrix. If a Lewis number of one is assumed, the maximum effectiveness that can be achieved by the enthalpy exchanger is independent of the isotherm type and also independent of the amount of desiccant on the matrix, as long as the line between the two air inlet states does not intersect the saturation curve on a psychrometric chart. Only the minimum rotation speed that is required in order to obtain this optimum operation is affected by these two parameters. A lower rotation speed is preferred because of a smaller potential for carry-over between the two air streams and also because of

reduced friction losses. It was shown that the type I isotherm material has advantages with respect to this criterion in intermediate and in warm conditions, whereas the type III material is slightly better in cold conditions. The optimum effectiveness is the same for both materials, and the difference in the rotation speed required to achieve this optimum is within a few revolutions per minute for all investigated cases. Thus, it cannot be concluded that materials with either isotherm type are generally favorable for use in enthalpy exchangers.

The effect of matrix Lewis numbers other than one was investigated for regenerator operation in heating as well as in cooling systems. In both cases it was shown that a material with a Lewis number of four allows an instantaneous enthalpy recovery (sensible plus latent heat) that is about halfway between the corresponding recoveries of an ideal enthalpy exchanger with a Lewis number of one and a sensible heat exchanger with an effective Lewis number of infinity. The absolute differences between the regenerator types are very different for various operating conditions.

Based on numerical solutions for the problem of combined heat and mass transfer in enthalpy exchangers obtained with the computer program MOSHMX, a new computational model was developed that allows transient performance simulations of sensible heat and enthalpy exchangers (Le=1) over any user-defined period of time with varying weather conditions. The integrated annual energy savings obtained with this model were compared for three locations with differing climates in the United States, and an economic analysis based on the initial installation costs and the possible operating savings of rotary regenerators was undertaken for the case of a ventilation system of a 200 people office building. Even though rotary regenerators are fairly expensive, the total first cost of a complete space-conditioning system does not increase significantly when rotary heat or enthalpy exchangers are included in the system, because their installation allows a capacity reduction in the additional heating and cooling equipment. For the case of an enthalpy exchanger in an intermediate or warm and humid climate, the savings due to these capacity reductions are even greater than the initial regenerator cost, resulting in a decreasing first cost for the

complete system. Operating savings can be achieved by both regenerator types in any location, such that positive life cycle savings result. However, it was found that, compared to all other regenerator-climate combinations, the sensible heat exchanger performs poorly in a warm and humid climate. The life cycle savings over a 15 year period range from $ 7,000 to $ 24,000 present worth for the sensible heat exchanger and from $ 28,000 to $ 38,000 present worth for the enthalpy exchanger with a Lewis number of one.

Finally, the adsorption capacities of the water-based polymer desiccant for two volatile organic compounds that may be responsible for poor indoor air quality were measured using the method of gas chromatography. It was shown that the matrix material does not adsorb propane or toluene in measurable amounts. Therefore there will probably not be a contaminant transfer of theses type of compounds from the exhaust to the clean supply stream by an adsorption-desorption mechanism.

8.2 Unresolved Issues

The effect of mechanical carry-over between the two air streams due to matrix rotation has been neglected in all calculations. For cases of high rotation speed this effect might influence the overall regenerator performance. Moreover, the actual Lewis number of the investigated desiccant matrix material was not measured. Suggestions in the literature for this parameter vary from 1 to 4 and in this study an ideal Lewis number of unity was assumed in most calculations. For this reason the life cycle savings evaluated in Section 6.3.3 might over predict the actual benefits of the particular enthalpy exchanger that was analyzed in this study.

The adsorption capacity of the desiccant was not measured for all contaminants that are typically the reason for poor air quality inside commercial and public buildings. It would be of special interest to investigate whether cigarette smoke, which is often the major problem in space-

conditioning of public buildings like casinos and restaurants, can be transferred from the exhaust to the supply stream by an adsorption-desorption mechanism. The influence that such contaminants have on the adsorption capacity for water vapor and on the durability of the desiccant material is also an issue that can significantly affect the benefits of rotary enthalpy exchangers compared to rotary sensible heat exchangers. The investigation concerning the material durability could best be performed on an enthalpy exchanger operating as part of an actual space-conditioning application.

APPENDIX A

EES Worksheet

```
"Numerical Calculation of Wave Speeds lambda1 and lambda2 "
"for Carnes' Water Based Polymer Matrix"
""
"Inputs:"
T_air_1=258.15      "K"
T_air_2=296.15      "K"
w_air_1=0.0008      "kg/kg"
w_air_2=0.0087      "kg/kg"
p=101.3             "kPa"
c_P_mat=0.9         "kJ/kg K"
"     Adjust Guess Value for lambda !!!     "
"************************************************************************"
"Average Inlet States:"
T_air_av=(T_air_1+T_air_2)/2
w_air_av=(w_air_1+w_air_2)/2
"Constants:"
R=8.314
"Calculation of a1:"
T_p=T_air_av+0.01
T_m=T_air_av-0.01
w_air_av=0.622*p_v/(p-p_v)
phi_p_a1=p_v/p_sat_p
phi_m_a1=p_v/p_sat_m
p_sat_p=Pressure(Steam,T=T_p,X=1)
p_sat_m=Pressure(Steam,T=T_m,X=1)
A_p_a1=-R*T_p*ln(phi_p_a1)
A_m_a1=-R*T_m*ln(phi_m_a1)
W_m_p_a1=(0.03878*exp(-(A_p_a1/618.89)^0.48566)+0.04668*exp(-
(A_p_a1/193.49)^1.5464))
W_m_m_a1=(0.03878*exp(-(A_m_a1/618.89)^0.48566)+0.04668*exp(-
```

(A_m_a1/193.49)^1.5464))
a1=(W_m_p_a1-W_m_m_a1)/(T_p-T_m)
"Calculation of a2:"
w_air_p=w_air_av+0.00001
w_air_m=w_air_av-0.00001
w_air_p=0.622*p_v_p/(p-p_v_p)
w_air_m=0.622*p_v_m/(p-p_v_m)
phi_p_a2=p_v_p/p_sat
phi_m_a2=p_v_m/p_sat
p_sat=Pressure(Steam,T=T_air_av,X=1)
A_p_a2=-R*T_air_av*ln(phi_p_a2)
A_m_a2=-R*T_air_av*ln(phi_m_a2)
W_m_p_a2=(0.03878*exp(-(A_p_a2/618.89)^0.48566)+0.04668*exp(-
(A_p_a2/193.49)^1.5464))
W_m_m_a2=(0.03878*exp(-(A_m_a2/618.89)^0.48566)+0.04668*exp(-
(A_m_a2/193.49)^1.5464))
a2=(W_m_p_a2-W_m_m_a2)/(w_air_p-w_air_m)
"Calculation of a3:"
a3=SpecHeat(AirH2O,T=T_air_av,p=p,w=w_air_av)
"Calculation of a4:"
a4=Enthalpy(Steam,T=T_air_av,x=1)-(SpecHeat(Water,T=T_air_av,p=p)*(T_air_av-
273.15)+(Enthalpy(Steam,T=T_air_av,x=1)-Enthalpy(Water,T=T_air_av,x=0))-2530)
"Calculation of a5:"
W_m_av=(W_m_p_a1+W_m_m_a1+W_m_p_a2+W_m_m_a2)/4
a5=c_P_mat+SpecHeat(Water,T=T_air_av,p=p)*W_m_av
*"**********"*
"Calculation of Wave Speeds lambda1,2 and Average Combined Capacitance Ratio gamma:"
a2*a5*lambda^2+(a1*a4-a2*a3-a5)*lambda+a3=0
gamma=1/lambda
*"**********"*
"Mimimum Rotation Speed for Maximum Enthalpy Exchange"
gamma*Capgamma=1.5
Capgamma=46/((60/omega_min)*2.28)

APPENDIX B

Type 70, Enthalpy Exchanger in Heating Mode, FORTRAN Listing

```
      SUBROUTINE TYPE 70 (time,xin,out,t,dtdt,par,info,icntrl,*)

*-----------------------------------------------------------------------
* This subroutine calculates the max.effectiveness of an EX and the
* according outlet states with the constraint that no excess water
* accumulates on the matrix.
*-----------------------------------------------------------------------
      implicit none
* TRNSYS VARIABLES

      integer*4 info(15)
      integer icount,ni,nd,np,icntrl(2)
      character*3 ycheck(2),ocheck(12)
      real*8 xin(2),out(12)
      real*4 t,dtdt,par(4),time

* TYPE 70 VARIABLES

      real*8 NTU                    ! NTU between air and matrix
      real*8 Tsi,Tso,Tei,Teo              ! supply/exhaust, inlet/outlet temp.
      real*8 Tprime                 ! saturation temp. at w=wei
      real*8 wsi,wso,wei,weo              ! supply/exhaust, inlet/outlet humrat.
      real*8 wsat,wprime                  ! humrat.to check intersec.with sat.
      real*8 deltaTpr,deltawpr            ! temp.and humrat.diff.betw. 1 and 3'
      real*8 isi,iso,iei,ieo        ! supply/exhaust, inlet/outlet enth.
      real*8 di,disens              ! enth.diff.betw.supply in-and outlet
      real*8 Et,Ei,Ew                     ! temp.,enth.and hum.effectiveness
      real*8 Qrec,Qrecsens                ! power reduction in heating load
      real*8 mfsup                  ! mass flow rate of supply air stream
      real*8 at,at1,at2,at3               ! parameters for effect. curve fit
      real*8 bt,bt1,bt2,bt3               ! parameters for effect. curve fit
      real*8 ai,ai1,ai2,ai3,ai4,ai5       ! parameters for effect. curve fit
      real*8 bi,bi1,bi2,bi3               ! parameters for effect. curve fit
      real*8 ci,ci1,ci2             ! parameters for effect. curve fit
      real*8 p,psat                       ! total and sat.pressure
      real*8 C1,C2,C3,C4,C5,C6,C7         ! constants for sat.pressure
      real*8 C8,C9,C10,C11,C12,C13        ! constants for sat.pressure
      real*8 Tkel                         ! temperature in Kelvin
```

```
      real*8 R                                  ! gas constant
      real*8 A0,A1,A2,A3,A4,A5                  ! constants for enth.calc.
      real*8 dB,dC                              ! function of temp.in enth.equ.
      real*8 term1,term2                        ! terms in enth.equ.
      real*8 ivsi,ivso,ivei,iveo,idair          ! enthalpies of vapor and dry air
      real*8 cpair                              ! specific heat of air
      real*8 Gamma                              ! combined capacitance rate ratio
      real*8 phiso                        ! rel.hum.of supply outlet
      real*8 daytime                      ! time of day (0-24)
      real*8 control                      ! control variables for on/off switch
      real*8 hr                                 ! integrates hours of operation

*-----------------------------------------
* First Call, Info Array....
*-----------------------------------------
      if (info(7).ge.0) goto1

      np=4                        ! # of parameter
      info(6)=12            ! # of outputs
      info(9)=1                   ! call type every timestep
      ni=2                        ! # of inputs
      nd=0                        ! # of derivatives

      call typeck(1,info,ni,np,nd)

*-------------------------------------------------
* set variable types
*-------------------------------------------------
      data ycheck/'TE1','DM1'/
      data ocheck/'TE1','DM1','TE1','DM1','SE1','PW3','DM1',
     @           'DM1','DM1','DM1','PW3','DM1'/
      call rcheck(info,ycheck,ocheck)
      return 1

*-------------------------------------------------------
* Input of the Two Inlet States
*-------------------------------------------------------
1     Tsi=xin(1)            ! [C]
      Tei=par(1)            ! [C]
      wsi=xin(2)            ! [kg/kg]
      wei=par(2)            ! [kg/kg]
      mfsup=par(3)          ! [kg/s]
      NTU=par(4)            ! between air and matrix (not NTUo !!)
      p=101.3               ! [kPa]
```

```
    cpair=1.004         ! [kJ/kg K]
    R=0.461520          ! [kJ/kg K]
    hr=1                ! [hr]

*-------------------------------------------------------
* Control Vars. Operation Between 6 AM and 9 PM, Tamb < 18 C
* -------------------------------------------------------
    daytime=dmod(time,24)
    if (6.lt.daytime.and.daytime.le.21.and.Tsi.lt.18) then
        control=1
    else
        control=0
    endif
```

```
      if (control.eq.0) then
        di=0
           disens=0
           Tso=Tsi
           wso=wsi
           Gamma=0
           Teo=Tei
           weo=wei
           Et=0
           Ew=0
           Ei=0
           hr=0
           goto 50
      endif

*-------------------------------------------------------
* Constants
*-------------------------------------------------------
      C1=-5.6745359e3
      C2=-5.1523057e-1
      C3=-9.677843e-3
      C4=6.2215701e-7
      C5=2.0747825e-9
      C6=-9.4842024e-13
      C7=4.1635019
      C8=-5.8002206e3
      C9=-5.5162560
      C10=-4.8640239e-2
      C11=4.1764768e-5
      C12=-1.4452093e-8
      C13=6.5459673
      A0=0.199798e4
      A1=0.18035706e1
      A2=0.36400463e-3
      A3=-0.14677622e-5
      A4=0.28726608e-8
      A5=-0.17508262e-11

*-------------------------------------------------
* Calculate Parameters Needed for Evaluation of Et,Ei
*-------------------------------------------------
10    at1=0.02259-1.376e-3*Tsi-6.91e-6*Tsi**2
      at2=0.09084-3.263e-4*tsi+7.4e-6*Tsi**2
      at3=0.7388-0.01994*Tsi+3.829e-4*Tsi**2
```

```
      at=at1+at2/NTU**at3
       bt1=-1.007+0.0093*Tsi+2.778e-4*Tsi**2
       bt2=-1.533+0.02287*Tsi-2.356e-4*Tsi**2
       bt3=1.111-2.667e-3*Tsi+1.378e-4*Tsi**2
      bt=bt1+bt2/NTU**bt3

       ai4=3.381e-3-9.679e-4*Tsi
       ai5=3.381e-3-4.127e-5*Tsi
       if (Tsi.le.0) then
          ai1=ai4
       else
          ai1=ai5
       endif
       ai2=5.088e-4+4.89e-6*Tsi
       ai3=-5.298e-6-7.652e-7*Tsi
      ai=ai1+ai2*NTU+ai3*NTU**2
       bi1=6.237e-3+8.827e-3*Tsi-6.042e-4*Tsi**2
       bi2=-0.02123+1.323e-4*Tsi
       bi3=4.908e-4+6.46e-6*Tsi
      bi=bi1+bi2*NTU+bi3*NTU**2
       ci1=-0.4087+0.00253*Tsi+3.34e-4*Tsi**2
       ci2=-1.449+0.02337*Tsi-5.578e-4*Tsi**2
      ci=ci1+ci2/NTU**0.8

*-------------------------------------------------
* Calculation of Enthalpies for Both Inlets
*-------------------------------------------------
*              ****Enthalpy of Supply Inlet****
20  Tkel=Tsi+273.15
      if (Tkel.ge.273.15) then
         psat=exp(C8/Tkel+C9+C10*Tkel+C11*Tkel**2+C12*Tkel**3
     @        +C13*dlog(Tkel))
      else
         psat=exp(C1/Tkel+C2+C3*Tkel+C4*Tkel**2+C5*Tkel**3+C6*Tkel**4
     @        +C7*dlog(Tkel))
      endif
      dB=255.2597394e-8*exp(1734.29/Tkel)/Tkel**2
      dC=0.104e-14-0.335297e-17*exp(3645.09/Tkel)
      term1=A0+A1*Tkel+A2*Tkel**2+A3*Tkel**3+A4*Tkel**4+A5*Tkel**5
      term2=-R*Tkel**2*dB*1000*psat+0.5*dC*(1000*psat)**2
      ivsi=term1+term2
      isi=cpair*Tsi+wsi*ivsi

*                ****Enthalpy of Exhaust Inlet****
```

```
      Tkel=Tei+273.15
      if (Tkel.ge.273.15) then
        psat=exp(C8/Tkel+C9+C10*Tkel+C11*Tkel**2+C12*Tkel**3
     @       +C13*dlog(Tkel))
      else
        psat=exp(C1/Tkel+C2+C3*Tkel+C4*Tkel**2+C5*Tkel**3+C6*Tkel**4
     @       +C7*dlog(Tkel))
      endif
      dB=255.2597394e-8*exp(1734.29/Tkel)/Tkel**2
      dC=0.104e-14-0.335297e-17*exp(3645.09/Tkel)
      term1=A0+A1*Tkel+A2*Tkel**2+A3*Tkel**3+A4*Tkel**4+A5*Tkel**5
      term2=-R*Tkel**2*dB*1000*psat+0.5*dC*(1000*psat)**2
      ivei=term1+term2
      iei=cpair*Tei+wei*ivei


*-------------------------------------------------------------
* Check for Excess Water
*-------------------------------------------------------------
      wsat=0.622*psat/(p-psat)
      Tprime=Tei
      wprime=wei

30    do while (Tprime.gt.Tsi.and.wsat.gt.wprime)
        Tprime=Tprime-0.1
        wprime=wprime-0.1*(wei-wsi)/(Tei-Tsi)
        Tkel=Tprime+273.15
        if (Tkel.ge.273.15) then
          psat=exp(C8/Tkel+C9+C10*Tkel+C11*Tkel**2+C12*Tkel**3
     @         +C13*dlog(Tkel))
        else
          psat=exp(C1/Tkel+C2+C3*Tkel+C4*Tkel**2+C5*Tkel**3+C6*Tkel**4
     @         +C7*dlog(Tkel))
        endif
        wsat=0.622*psat/(p-psat)

        goto 30
      enddo

*-------------------------------------------------------------
* Check Intersection and Calc. Et,Ei accordingly
*-------------------------------------------------------------
40    if (Tprime.le.Tsi) then
*             **** no intersec.,thus,max.effect.****
```

```
      Et=NTU/(NTU+2)
      Ei=Et
      Ew=Et
      Tso=Tsi+Et*(Tei-Tsi)
      Teo=Tei+Et*(Tsi-Tei)
      iso=isi+Ei*(iei-isi)
      ieo=iei+Ei*(isi-iei)
      wso=wsi+Ew*(wei-wsi)
      weo=wei+Ew*(wsi-wei)
      di=iso-isi
         disens=1.01*(Tso-Tsi)
      Gamma=5
    else
*           **** inters.,thus,calc.effect.with curvefit****
      Gamma=0                ! set Gamma=0 and outlet=inlet
      Et=0
      Ei=0
      Ew=0
      Tso=Tsi
      Teo=Tei
      wso=wsi
      weo=wei
      iso=isi
      ieo=iei
*             ****Calc. wsat for T=Tei=Teo****
      Tkel=Teo+273.15
      if (Tkel.ge.273.15) then
        psat=exp(C8/Tkel+C9+C10*Tkel+C11*Tkel**2+C12*Tkel**3
   @         +C13*dlog(Tkel))
      else
        psat=exp(C1/Tkel+C2+C3*Tkel+C4*Tkel**2+C5*Tkel**3+C6*Tkel**4
   @         +C7*dlog(Tkel))
      endif
      wsat=0.622*psat/(p-psat)

*               ****Increase Gamma until Sat.****
45    do while (weo.lt.wsat.and.Gamma.lt.5)
        Gamma=Gamma+0.01
        Et=NTU/(NTU+2)*(1-exp(at*Gamma**2+bt*Gamma))
        Ei=NTU/(NTU+2)*(1-exp(ai*Gamma**3+bi*Gamma**2+ci*Gamma))
        Tso=Tsi+Et*(Tei-Tsi)          ! Calc.new Outlets
        Teo=Tei+Et*(Tsi-Tei)
        iso=isi+Ei*(iei-isi)
        ieo=iei+Ei*(isi-iei)
```

```
*                ****Calc.new wso****
      Tkel=Tso+273.15
      if (Tkel.ge.273.15) then
        psat=exp(C8/Tkel+C9+C10*Tkel+C11*Tkel**2+C12*Tkel**3
     @          +C13*dlog(Tkel))
      else
        psat=exp(C1/Tkel+C2+C3*Tkel+C4*Tkel**2+C5*Tkel**3+C6*Tkel**4
     @          +C7*dlog(Tkel))
      endif
         dB=255.2597394e-8*exp(1734.29/Tkel)/Tkel**2
      dC=0.104e-14-0.335297e-17*exp(3645.09/Tkel)
      term1=A0+A1*Tkel+A2*Tkel**2+A3*Tkel**3+A4*Tkel**4+A5*Tkel**5
      term2=-R*Tkel**2*dB*1000*psat+0.5*dC*(1000*psat)**2
      ivso=term1+term2
      idair=cpair*Tso
      wso=(iso-idair)/ivso

*                ****Calc.new weo****
      Tkel=Teo+273.15
      if (Tkel.ge.273.15) then
        psat=exp(C8/Tkel+C9+C10*Tkel+C11*Tkel**2+C12*Tkel**3
     @          +C13*dlog(Tkel))
      else
        psat=exp(C1/Tkel+C2+C3*Tkel+C4*Tkel**2+C5*Tkel**3+C6*Tkel**4
     @          +C7*dlog(Tkel))
      endif
      wsat=0.622*psat/(p-psat)
```

```
          dB=255.2597394e-8*exp(1734.29/Tkel)/Tkel**2
          dC=0.104e-14-0.335297e-17*exp(3645.09/Tkel)
          term1=A0+A1*Tkel+A2*Tkel**2+A3*Tkel**3+A4*Tkel**4+A5*Tkel**5
          term2=-R*Tkel**2*dB*1000*psat+0.5*dC*(1000*psat)**2
          iveo=term1+term2
          idair=cpair*Teo
          weo=(ieo-idair)/iveo

          di=iso-isi
             disens=1.01*(Tso-Tsi)

          goto 45
        enddo

*               ****Decrease Gamma to Get out of Saturation****
        if (Gamma.lt.5) then
          Gamma=Gamma-0.01
          Et=NTU/(NTU+2)*(1-exp(at*Gamma**2+bt*Gamma))
          Ei=NTU/(NTU+2)*(1-exp(ai*Gamma**3+bi*Gamma**2+ci*Gamma))
          Tso=Tsi+Et*(Tei-Tsi)
          Teo=Tei+Et*(Tsi-Tei)
          iso=isi+Ei*(iei-isi)
          ieo=iei+Ei*(isi-iei)

*               ****Calc. new wso****
          Tkel=Tso+273.15
          if (Tkel.ge.273.15) then
            psat=exp(C8/Tkel+C9+C10*Tkel+C11*Tkel**2+C12*Tkel**3
     @           +C13*dlog(Tkel))
          else
            psat=exp(C1/Tkel+C2+C3*Tkel+C4*Tkel**2+C5*Tkel**3+C6*Tkel**4
     @           +C7*dlog(Tkel))
          endif
             wsat=0.622*psat/(p-psat)
          dB=255.2597394e-8*exp(1734.29/Tkel)/Tkel**2
          dC=0.104e-14-0.335297e-17*exp(3645.09/Tkel)
          term1=A0+A1*Tkel+A2*Tkel**2+A3*Tkel**3+A4*Tkel**4+A5*Tkel**5
          term2=-R*Tkel**2*dB*1000*psat+0.5*dC*(1000*psat)**2
          ivso=term1+term2
          idair=cpair*Tso
          wso=(iso-idair)/ivso
          if (wso.gt.wsat) then
               wso=wsat
```

```
      endif

*           ****Calc. new weo****
      Tkel=Teo+273.15
```

```
          if (Tkel.ge.273.15) then
            psat=exp(C8/Tkel+C9+C10*Tkel+C11*Tkel**2+C12*Tkel**3
     @           +C13*dlog(Tkel))
          else
            psat=exp(C1/Tkel+C2+C3*Tkel+C4*Tkel**2+C5*Tkel**3+C6*Tkel**4
     @           +C7*dlog(Tkel))
          endif
          dB=255.2597394e-8*exp(1734.29/Tkel)/Tkel**2
          dC=0.104e-14-0.335297e-17*exp(3645.09/Tkel)
          term1=A0+A1*Tkel+A2*Tkel**2+A3*Tkel**3+A4*Tkel**4+A5*Tkel**5
          term2=-R*Tkel**2*dB*1000*psat+0.5*dC*(1000*psat)**2
          iveo=term1+term2
          idair=cpair*Teo
          weo=(ieo-idair)/iveo

          di=iso-isi
             disens=1.01*(Tso-Tsi)
        endif

*               ****Hunidity Effectiveness****
        Ew=(wso-wsi)/(wei-wsi)

      endif

*----------------------------------------
* Power Reduction In Heating Load
*----------------------------------------
50    Qrec=di*mfsup
      Qrecsens=disens*mfsup

*-----------------------------------------------
* Outputs
*-----------------------------------------------
60    out(1)=Tso
      out(2)=wso
      out(3)=Teo
      out(4)=weo
      out(5)=di
      out(6)=Qrec
      out(7)=Et
      out(8)=Ew
      out(9)=Ei
      out(10)=Gamma
      out(11)=Qrecsens
```

```
out(12)=hr

return 1
End
```

Type 71, Sensible Heat Exchanger in Heating Mode, FORTRAN Listing

```
      SUBROUTINE TYPE 71 (time,xin,out,t,dtdt,par,info,icntrl,*)
*-----------------------------------------------------------------
* This subroutine calculates the maximum effectiveness of a HX with
* the constraint that no excess water accumulates on the matrix
*-----------------------------------------------------------------
      implicit none
*     TRNSYS VARIABLES
      integer*4 info(15)
      integer icount,ni,nd,np,icntrl(2)
      character*3 ycheck(2),ocheck(12)
      real*8 xin(2),out(12)
      real*4 t,dtdt,par(4),time

*     TYPE 71 VARIABLES
      real*8 NTU                        ! NTU between air and matrix
      real*8 Tsi,Tso,Tei,Teo                  ! supply/exhaust, inlet/outlet temp.
      real*8 Tprime,Teisat                    ! sat.temp. and sat.temp.+3 at wei
      real*8 wsi,wso,wei,weo                  ! supply/exhaust, inlet/outlet humrat.
      real*8 wsat,wprime                      ! humrat. to check intersec. with sat.
      real*8 deltaTpr,deltawpr                ! temp.and humrat.diff.betw. 1 and 3'
      real*8 isi,iso,iei,ieo            ! supply/exhaust, inlet/outlet enth.
      real*8 Et,Ew,Ei                   ! temp.,hum.and enth. effectiveness
      real*8 Qrec,Qrecsens                    ! reduction in heating power
      real*8 mfsup                      ! mass flow rate of supply air stream
      real*8 at,at1,at2,at3             ! parameters in temp. effect. equation
      real*8 bt,bt1,bt2,bt3                   ! parameters in temp. effect. equation
      real*8 p,psat                           ! absolut and sat. pressure
      real*8 C1,C2,C3,C4,C5,C6,C7             ! constants for sat. pressure
      real*8 C8,C9,C10,C11,C12,C13            ! constants for sat. pressure
      real*8 Tkel                             ! temperature in Kelvin
      real*8 R                                ! gas constant
      real*8 A0,A1,A2,A3,A4,A5                ! constants for enth. equation
      real*8 dB,dC                      ! functions of temp. in enth. equ.
      real*8 term1,term2                      ! terms in enth. equ.
      real*8 ivsi,ivso,ivei,iveo,idair        ! enthlpies of vapor and dry air
      real*8 di,disens                  ! enth. difference between in and outlet
      real*8 cpair                            ! specific heat of dry air
      real*8 Gamma,f1gamma,f2gamma      ! rotation speed and var.to calc.it
      real*8 phiso                            ! rel.hum.os supply outlet
      real*8 daytime
      real*8 control,hr                 ! on/off switch
```

```
*-------------------------------------------
* First Call, Info Array....
*-------------------------------------------
      if (info(7).ge.0) goto 1

      np=4                  ! # of parameters
      info(6)=12             ! # of outputs
      info(9)=1              ! call type71 every timestep
      ni=2                  ! # of inputs
      nd=0                  ! # of derivatives

      call typeck(1,info,ni,np,nd)

*-------------------------------------------
* Set Variable Types
*-------------------------------------------
      data ycheck/'TE1','DM1'/
      data ocheck/'TE1','DM1','TE1','DM1','SE1','PW3','DM1',
     @           'DM1','DM1','DM1','PW3','DM1'/
      call rcheck(info,ycheck,ocheck)
      return 1

*-----------------------------------------------------------
* Input of the Two Inlet States
*-----------------------------------------------------------
1     Tsi=xin(1)                  !  in [C]
      Tei=par(1)                  !  in [C]
      wsi=xin(2)                  !  in [kg/kg]
      wei=par(2)                  !  in [kg/kg]
      mfsup=par(3)                !  in [kg/s]
      NTU=par(4)                  !  air to matrix (not overall!)
      p=101.3                     !  in [kPa]
      R=0.461520                  !  in [kJ/kgK]
      cpair=1.004                 !  in [kJ/kgK]
      hr=1

*-----------------------------------------------------------
* Control Vars. Operation Between 6 AM and 9 PM, Tamb < 18 C
* -----------------------------------------------------------
      daytime=dmod(time,24)
      if (6.lt.daytime.and.daytime.le.21.and.Tsi.lt.18) then
            control=1
      else
```

```
          control=0
      endif
      if (control.eq.0) then
        di=0
          disens=0
          Tso=Tsi
          wso=wsi
          Gamma=0
          Teo=Tei
          weo=wei
          Et=0
          Ew=0
          Ei=0
          hr=0
          goto 70
      endif
*-------------------------------------------------------------
* Constants
*-------------------------------------------------------------
      C1=-5.6745359e3
      C2=-5.1523057e-1
      C3=-9.677843e-3
      C4=6.2215701e-7
      C5=2.0747825e-9
      C6=-9.4842024e-13
      C7=4.1635019
      C8=-5.8002206e3
      C9=-5.5162560
      C10=-4.8640239e-2
      C11=4.1764768e-5
      C12=-1.4452093e-8
      C13=6.5459673
      A0=0.199798e4
      A1=0.18035706e1
      A2=0.36400463e-3
      A3=-0.14677622e-5
      A4=0.28726608e-8
      A5=-0.17508262e-11
*-------------------------------------------------
* Calculate Parameters Needed for Evaluation of Et
*-------------------------------------------------
10    at1=0.02259-1.376e-3*Tsi-6.91e-6*Tsi**2
      at2=0.09084-3.263e-4*tsi+7.4e-6*Tsi**2
```

```
      at3=0.7388-0.01994*Tsi+3.829e-4*Tsi**2
     at=at1+at2/NTU**at3
      bt1=-1.007+0.0093*Tsi+2.778e-4*Tsi**2
      bt2=-1.533+0.02287*Tsi-2.356e-4*Tsi**2
      bt3=1.111-2.667e-3*Tsi+1.378e-4*Tsi**2
     bt=bt1+bt2/NTU**bt3
*-------------------------------------------------
* Calculation of Enthalpies for Both Inlets
*-------------------------------------------------
*              ****Enthalpy of Supply Inlet****
20  Tkel=Tsi+273.15
     if (Tkel.ge.273.15) then
       psat=exp(C8/Tkel+C9+C10*Tkel+C11*Tkel**2+C12*Tkel**3
    @        +C13*dlog(Tkel))
     else
       psat=exp(C1/Tkel+C2+C3*Tkel+C4*Tkel**2+C5*Tkel**3+C6*Tkel**4
    @        +C7*dlog(Tkel))
     endif
     dB=255.2597394e-8*exp(1734.29/Tkel)/Tkel**2
     dC=0.104e-14-0.335297e-17*exp(3645.09/Tkel)
     term1=A0+A1*Tkel+A2*Tkel**2+A3*Tkel**3+A4*Tkel**4+A5*Tkel**5
     term2=-R*Tkel**2*dB*1000*psat+0.5*dC*(1000*psat)**2
     ivsi=term1+term2
     isi=cpair*Tsi+wsi*ivsi
*               ****Enthalpy of Exhaust Inlet****
     Tkel=Tei+273.15
     if (Tkel.ge.273.15) then
       psat=exp(C8/Tkel+C9+C10*Tkel+C11*Tkel**2+C12*Tkel**3
    @        +C13*dlog(Tkel))
     else
       psat=exp(C1/Tkel+C2+C3*Tkel+C4*Tkel**2+C5*Tkel**3+C6*Tkel**4
    @        +C7*dlog(Tkel))
     endif
     dB=255.2597394e-8*exp(1734.29/Tkel)/Tkel**2
     dC=0.104e-14-0.335297e-17*exp(3645.09/Tkel)
     term1=A0+A1*Tkel+A2*Tkel**2+A3*Tkel**3+A4*Tkel**4+A5*Tkel**5
     term2=-R*Tkel**2*dB*1000*psat+0.5*dC*(1000*psat)**2
     ivei=term1+term2
     iei=cpair*Tei+wei*ivei

*-------------------------------------------------------
* Calc.Sat.Temp. and Tprime at w=wei, calc.deltaTpr,deltawpr
*-------------------------------------------------------
```

```
30  wprime=wei
    psat=p/(0.622/wei+1)
    Teisat=4064.75/(19.016-dlog(10*psat))-236.25
    Tprime=Teisat+4        ! definition by Holmberg
    deltaTpr=Tprime-Tsi
    deltawpr=wprime-wsi

*           ****Calculate wsat for initial Tprime****
    Tkel=Tprime+273.15
    if (Tkel.ge.273.15) then
      psat=exp(C8/Tkel+C9+C10*Tkel+C11*Tkel**2+C12*Tkel**3
   @       +C13*dlog(Tkel))
    else
      psat=exp(C1/Tkel+C2+C3*Tkel+C4*Tkel**2+C5*Tkel**3+C6*Tkel**4
   @       +C7*dlog(Tkel))
    endif
    wsat=0.622*psat/(p-psat)

*---------------------------------------------------------------
* Check for Excess Water
*---------------------------------------------------------------
 40   do while (Tprime.gt.Tsi.and.wsat.gt.wprime)
       Tprime=Tprime-0.1
       wprime=wprime-0.1*deltawpr/deltaTpr

*           ****Calc. New wsat****
       Tkel=Tprime+273.15
       if (Tkel.ge.273.15) then
         psat=exp(C8/Tkel+C9+C10*Tkel+C11*Tkel**2+C12*Tkel**3
   @          +C13*dlog(Tkel))
```

```
        else
          psat=exp(C1/Tkel+C2+C3*Tkel+C4*Tkel**2+C5*Tkel**3+C6*Tkel**4
     @         +C7*dlog(Tkel))
        endif
        wsat=0.622*psat/(p-psat)

        goto 40
      enddo
*-----------------------------------------------------------------
* Calculate Max. Effectiveness Without Freezing
*-----------------------------------------------------------------
50  if (Tprime.le.Tsi) then
*             ****No Excess Water, thus, Max. Speed****
        Et=NTU/(NTU+2)
        Teo=Tei+Et*(Tsi-Tei)
        weo=wei
*            ****Calc. wsat=wsat(Teo)****
        Tkel=Teo+273.15
        if (Tkel.ge.273.15) then
          psat=exp(C8/Tkel+C9+C10*Tkel+C11*Tkel**2+C12*Tkel**3
     @         +C13*dlog(Tkel))
        else
          psat=exp(C1/Tkel+C2+C3*Tkel+C4*Tkel**2+C5*Tkel**3+C6*Tkel**4
     @         +C7*dlog(Tkel))
        endif
        wsat=0.622*psat/(p-psat)
*             ****outlet state follows Saturation line****
        if (wsat.lt.weo) then
          weo=wsat
        endif

      else
*             ****Risk of Excess Water => stop at Saturation****
        Et=NTU/(NTU+2)
        Teo=Tei+Et*(Tsi-Tei)
        weo=wei
*              ****Calc. wsat for Max. Effect.****
        Tkel=Teo+273.15
        if (Tkel.ge.273.15) then
          psat=exp(C8/Tkel+C9+C10*Tkel+C11*Tkel**2+C12*Tkel**3
     @         +C13*dlog(Tkel))
        else
          psat=exp(C1/Tkel+C2+C3*Tkel+C4*Tkel**2+C5*Tkel**3+C6*Tkel**4
```

```
     @          +C7*dlog(Tkel))
        endif
        wsat=0.622*psat/(p-psat)
*               ****outlet state must stop at saturation line****
        if (weo.gt.wsat) then
          Teo=Teisat
          weo=wei
        endif
      endif
*-------------------------------------------------------------
* Calculation of the Remaining Outlet Properties
*-------------------------------------------------------------
*               ****Exhaust Outlet Enthalpy****
60  Tkel=Teo+273.15
      if (Tkel.ge.273.15) then
        psat=exp(C8/Tkel+C9+C10*Tkel+C11*Tkel**2+C12*Tkel**3
     @       +C13*dlog(Tkel))
      else
        psat=exp(C1/Tkel+C2+C3*Tkel+C4*Tkel**2+C5*Tkel**3+C6*Tkel**4
     @       +C7*dlog(Tkel))
      endif
      dB=255.2597394e-8*exp(1734.29/Tkel)/Tkel**2
      dC=0.104e-14-0.335297e-17*exp(3645.09/Tkel)
      term1=A0+A1*Tkel+A2*Tkel**2+A3*Tkel**3+A4*Tkel**4+A5*Tkel**5
      term2=-R*Tkel**2*dB*1000*psat+0.5*dC*(1000*psat)**2
      iveo=term1+term2
      ieo=cpair*Teo+weo*iveo

*               ****Supply Outlet Properties****
      Tso=Tsi+Tei-Teo
      wso=wsi+wei-weo
      iso=isi+iei-ieo

*             ****Enthalpy Transfer****
      di=iso-isi
      disens=1.01*(Tso-Tsi)

*--------------------------------
* Effectivenesses
*--------------------------------
      Et=(Tso-Tsi)/(Tei-Tsi)
      Ew=(wso-wsi)/(wei-wsi)
      Ei=(iso-isi)/(iei-isi)
```

```
*-------------------------------------------
* Calculation of Rotation Speed
*-------------------------------------------
65  if (Et.lt.NTU/(NTU+2)) then
        f1gamma=dlog(1-Et*(NTU+2)/NTU)
           f2gamma=bt**2/(4*at**2)+f1gamma/at
           if (f2gamma.le.0) then
              f2gamma=0
           endif
        Gamma=-bt/(2*at)-(f2gamma)**0.5
        if (Gamma.gt.5) then
          Gamma=5
        endif
      else
        Gamma=5
      endif

*-------------------------------------------------------------
* Recovered Power
*-------------------------------------------------------------
70   Qrec=di*mfsup
      Qrecsens=disens*mfsup

*-----------------------------------------------------
* Outputs
*-----------------------------------------------------
      out(1)=Tso
      out(2)=wso
      out(3)=Teo
      out(4)=weo
      out(5)=di
      out(6)=Qrec
      out(7)=Et
      out(8)=Ew
      out(9)=Ei
      out(10)=Gamma
      out(11)=Qrecsens
      out(12)=hr

      Return 1
      End
```

Type 72, Cooling Mode for Both EX and HX, FORTRAN Listing

```
      SUBROUTINE TYPE 72 (time,xin,out,t,dtdt,par,info,icntrl,*)

*-----------------------------------------------------------------------
* This subroutine calculates the max.effectiveness of an EX or HX and the
* according outlet states in the cooling mode
*-----------------------------------------------------------------------
      implicit none
*   TRNSYS VARIABLES

      integer*4 info(15)
      integer icount,ni,nd,np,icntrl(2)
      character*3 ycheck(2),ocheck(10)
      real*8 xin(2),out(10)
      real*4 t,dtdt,par(6),time

*   TYPE 70 VARIABLES

      real*8 mode                         ! HX=1 or EX=2
      real*8 NTU                    ! NTU between air and matrix
      real*8 Tsi,Tso,Tei,Teo              ! supply/exhaust, inlet/outlet temp.
      real*8 wsi,wso,wei,weo              ! supply/exhaust, inlet/outlet humrat.
      real*8 wsat                         ! humrat.at saturation
      real*8 isi,iso,iei,ieo        ! supply/exhaust, inlet/outlet enth.
      real*8 di                           ! enth.diff.betw.supply in-and outlet
      real*8 Et,Ei,Ew                     ! temp.,enth.and hum.effectiveness
      real*8 Qrec                   ! power reduction in heating load
      real*8 mfsup                  ! mass flow rate of supply air stream
      real*8 p,psat                       ! total and sat.pressure
      real*8 C1,C2,C3,C4,C5,C6,C7         ! constants for sat.pressure
      real*8 C8,C9,C10,C11,C12,C13        ! constants for sat.pressure
      real*8 Tkel                         ! temperature in Kelvin
      real*8 R                            ! gas constant
      real*8 A0,A1,A2,A3,A4,A5      ! constants for enth.calc.
      real*8 dB,dC                        ! function of temp.in enth.equ.
      real*8 term1,term2                  ! terms in enth.equ.
      real*8 ivsi,ivso,ivei,iveo,idair    ! enthalpies of vapor and dry air
      real*8 cpair                        ! specific heat of air
      real*8 hr                           ! integrate hours of operation
      real*8 control,Tcon                 ! on/off switch at T=Tcon
      real*8 daytime
```

```
*-----------------------------------------
* First Call, Info Array....
*-----------------------------------------
      if (info(7).ge.0) goto1

      np=6                        ! # parameters
      info(6)=10          ! # outputs
      info(9)=1                   ! call subroutine every timestep
      ni=2                        ! # inputs
      nd=0                        ! # derivatives

      call typeck(1,info,ni,np,nd)

*-------------------------------------------------
* set variable types
*-------------------------------------------------
      data ycheck/'TE1','DM1'/
      data ocheck/'TE1','DM1','TE1','DM1','SE1','PW3','DM1',
     @           'DM1','DM1','TD1'/
      call rcheck(info,ycheck,ocheck)
      return 1

*-------------------------------------------------------
* Input of the Two Inlet States and Regenerator Type
*-------------------------------------------------------
1     mode=par(5)                 ! HX=1, EX=2
      Tcon=par(6)                 ! control temp.for on/off switch
      Tsi=xin(1)          ! [C]
      Tei=par(1)          ! [C]
      wsi=xin(2)          ! [kg/kg]
      wei=par(2)          ! [kg/kg]
      mfsup=par(3)                ! [kg/s]
      NTU=par(4)                  ! between air and matrix (not NTUo !!)
      p=101.3                     ! [kPa]
      cpair=1.004                 ! [kJ/kg K]
      R=0.461520                  ! [kJ/kg K]

*-------------------------------------------------
* Calculation of Effectivenesses for Temp. and Hum.
*-------------------------------------------------
10    daytime=dmod(time,24)
      if (6.lt.daytime.and.daytime.le.21.and.Tsi.gt.Tcon) then
            control=1
      else
```

```
      control=0
endif
if (control.eq.0) then
  Et=0
  Ew=0
      Ei=0
      Tso=Tsi
      Teo=Tei
      wso=wsi
      weo=wei
      di=0
      hr=0
      goto 45
```

```
      else
        Et=NTU/(NTU+2)
           hr=1
        if (mode.eq.1) then
              Ew=0
        else
              Ew=Et
        endif
      endif

*-----------------------------------------------------------
* Constants
*-----------------------------------------------------------
      C1=-5.6745359e3
      C2=-5.1523057e-1
      C3=-9.677843e-3
      C4=6.2215701e-7
      C5=2.0747825e-9
      C6=-9.4842024e-13
      C7=4.1635019
      C8=-5.8002206e3
      C9=-5.5162560
      C10=-4.8640239e-2
      C11=4.1764768e-5
      C12=-1.4452093e-8
      C13=6.5459673
      A0=0.199798e4
      A1=0.18035706e1
      A2=0.36400463e-3
      A3=-0.14677622e-5
      A4=0.28726608e-8
      A5=-0.17508262e-11

*-------------------------------------------------
* Calculation of Enthalpies for Both Inlets
*-------------------------------------------------
*              ****Enthalpy of Supply Inlet****
20  Tkel=Tsi+273.15
      if (Tkel.ge.273.15) then
        psat=exp(C8/Tkel+C9+C10*Tkel+C11*Tkel**2+C12*Tkel**3
     @       +C13*dlog(Tkel))
      else
        psat=exp(C1/Tkel+C2+C3*Tkel+C4*Tkel**2+C5*Tkel**3+C6*Tkel**4
     @       +C7*dlog(Tkel))
```

```
      endif
      dB=255.2597394e-8*exp(1734.29/Tkel)/Tkel**2
      dC=0.104e-14-0.335297e-17*exp(3645.09/Tkel)
      term1=A0+A1*Tkel+A2*Tkel**2+A3*Tkel**3+A4*Tkel**4+A5*Tkel**5
      term2=-R*Tkel**2*dB*1000*psat+0.5*dC*(1000*psat)**2
      ivsi=term1+term2
      isi=cpair*Tsi+wsi*ivsi

*               ****Enthalpy of Exhaust Inlet****
      Tkel=Tei+273.15
      if (Tkel.ge.273.15) then
        psat=exp(C8/Tkel+C9+C10*Tkel+C11*Tkel**2+C12*Tkel**3
     @       +C13*dlog(Tkel))
      else
        psat=exp(C1/Tkel+C2+C3*Tkel+C4*Tkel**2+C5*Tkel**3+C6*Tkel**4
     @       +C7*dlog(Tkel))
      endif
      dB=255.2597394e-8*exp(1734.29/Tkel)/Tkel**2
      dC=0.104e-14-0.335297e-17*exp(3645.09/Tkel)
      term1=A0+A1*Tkel+A2*Tkel**2+A3*Tkel**3+A4*Tkel**4+A5*Tkel**5
      term2=-R*Tkel**2*dB*1000*psat+0.5*dC*(1000*psat)**2
      ivei=term1+term2
      iei=cpair*Tei+wei*ivei

*-------------------------------------------------
* Calculation of outlet States
*-------------------------------------------------
30  Tso=Tsi+Et*(Tei-Tsi)
      wso=wsi+Ew*(wei-wsi)
      Teo=Tei+Et*(Tsi-Tei)
      weo=wei+Ew*(wsi-wei)

*               ****Enth.of Supply Outlet****
      Tkel=Tso+273.15
      if (Tkel.ge.273.15) then
        psat=exp(C8/Tkel+C9+C10*Tkel+C11*Tkel**2+C12*Tkel**3
     @       +C13*dlog(Tkel))
      else
        psat=exp(C1/Tkel+C2+C3*Tkel+C4*Tkel**2+C5*Tkel**3+C6*Tkel**4
     @       +C7*dlog(Tkel))
      endif
      dB=255.2597394e-8*exp(1734.29/Tkel)/Tkel**2
      dC=0.104e-14-0.335297e-17*exp(3645.09/Tkel)
      term1=A0+A1*Tkel+A2*Tkel**2+A3*Tkel**3+A4*Tkel**4+A5*Tkel**5
```

```
      term2=-R*Tkel**2*dB*1000*psat+0.5*dC*(1000*psat)**2
      ivso=term1+term2
      iso=cpair*Tso+wso*ivso

*               ****Enth.of Exhaust Outlet****
      Tkel=Teo+273.15
      if (Tkel.ge.273.15) then
        psat=exp(C8/Tkel+C9+C10*Tkel+C11*Tkel**2+C12*Tkel**3
     @       +C13*dlog(Tkel))
      else
        psat=exp(C1/Tkel+C2+C3*Tkel+C4*Tkel**2+C5*Tkel**3+C6*Tkel**4
     @       +C7*dlog(Tkel))
      endif
      dB=255.2597394e-8*exp(1734.29/Tkel)/Tkel**2
      dC=0.104e-14-0.335297e-17*exp(3645.09/Tkel)
      term1=A0+A1*Tkel+A2*Tkel**2+A3*Tkel**3+A4*Tkel**4+A5*Tkel**5
      term2=-R*Tkel**2*dB*1000*psat+0.5*dC*(1000*psat)**2
      iveo=term1+term2
      ieo=cpair*Teo+weo*iveo

*---------------------------------------------
* Enthalpy Transfer and Effectiveness
*---------------------------------------------
40  di=isi-iso
      Ei=di/(isi-iei)

*-----------------------------------------
* Recovered Heat Flow
*-----------------------------------------
45  Qrec=di*mfsup

*--------------------------------
* Outputs
*--------------------------------
50    out(1)=Tso
      out(2)=wso
      out(3)=Teo
      out(4)=weo
      out(5)=di
      out(6)=Qrec
      out(7)=Et
      out(8)=Ew
      out(9)=Ei
      out(10)=hr
```

```
Return 1
End
```

APPENDIX C

TRNSYS Deck for Cooling Mode, Both EX and HX

```
ASSIGN \TRNSYS14\gunnar\Cooling.LST    6
ASSIGN \TRNSYS14\WDATA.DAT 10
ASSIGN \TRNSYS14\gunnar\Cooling.PLT 11
ASSIGN \TRNSYS14\gunnar\Cooling.Out 12

* * * * * * * * * * * * * * * * * * * * * * * * * * * * * * * * * * * * * * *
*                                                                             *
*              HX or EX Simulation in Cooling Mode                            *
*          Sensible + Latent Heat Recovery Are Considered                     *
*                              Annual Simulation                              *
*                                                                             *
* * * * * * * * * * * * * * * * * * * * * * * * * * * * * * * * * * * * * * *

EQUATIONS 3
START=1
STOP=8760
PERIOD=8760

SIMULATION START STOP  1.0
WIDTH 72

UNIT 54 TYPE 54 WEATHER DATA GENERATOR
PARAMETERS 6
1 10 220 1 2 1

UNIT 33 TYPE 33 PSYCHROMETRICS
PARAMETERS 4
2 1 0 1
INPUTS 2
54,4 54,6
```

```
-10 0.8

UNIT 72 TYPE 72 HX/EX Cooling Mode
PARAMETERS 6
  23  0.0141  2.28   5     2     24
* Tei  wei   mfsup  NTU  HX/EX  Tcon
INPUTS 2
33,7 33,1
10 0.005

UNIT 24 TYPE 24 INTEGRATOR
PARAMETERS 1
PERIOD
INPUTS 5
54,4  72,1  72,2  72,6  72,10
0 10 0.005 50 1

UNIT 25 TYPE 25 PRINTER
PARAMETERS 5
1 START STOP 11 2
INPUTS 7
54,4  72,1  72,2  72,5  72,7  72,8  72,9
Tsi  Tso   wso deltaIsup Et   Ew   Ei

UNIT 26 TYPE 25 PRINTER 2
PARAMETERS 5
PERIOD START STOP 12 1
INPUTS 5
24,1  24,2  24,3  24,4  24,5
TambInt TsoInt wsoInt Qrec Op.hrs
C*hr C*hr hr kW*hr hr

End
```

REFERENCES

1. ASHRAE, *Handbook of Fundamentals,* American Society of Heating, Refrigerating and Air-Conditiong Engineers, Atlanta, GA, 1993

2. ASHRAE, Standard 62-1989, American Society of Heating, Refrigerating and Air-Conditioning Engineers, Atlanta, GA, 1989

3. Barrer, R. M., *Zeolites and Clay Minerals as Sorbents and Molecular Sieves*, Academic Press, New York, NY, 1978

4. Boor, R. L., *Adsorption and Activated Carbon,* M.S. Thesis in Mechanical Engineering, University of Wisconsin-Madison, 1992

5. Bowlen, K. L., *Energy Recovery from Exhaust Air for Year Round Environmental Control*

6. Bronstein, I. N. and Semendjajew, K. A., *Taschenbuch der Mathematik*, 24. Auflage, Verlag Harri Deutsch, Frankfurt/Main, 1989

7. Buffington, R. and Wilson, M. K., *Detectors for Gas Chromatography - A Practical Primer*, Hewlett Packard part number 5958-9433, Printed in USA, 1987

8. Bussey, L. E. and Eschenbach, T. G., The Economic Analysis of Industrial Projects, Second Edition, Prentice Hall, Englewood Cliffs, NJ, 1992

9. Carnes, Energy Recovery Wheel Design Manual, Carnes Company, 448 S. Main St., Verona, WI 53593, 1989

10. Coleman, H. W., and Steele, W. G., *Experimentation and Uncertainty Analysis for*

Engineers, Wiley-Interscience, 1989

11. Corradini, M. L. and Mitchell, J. W., Class Notes, NEEP 373 Energy and the Environment, University of Wisconsin-Madison, Fall Semester 1994

12. CRC Handbook of Chemistry and Physics, 73rd Edition, CRC Press, Boca Raton, Fl., 1992-1993

13. CRC Handbook of Tables for Applied Engineering Science, Second Edition, CRC Press, Boca Raton, Fl., 1972

14. Dubinin, M. M., *Physical Adsorption of Gases and Vapors in Micropores*, Prog. Surf. Membrane Sci., Vol. 9, pp. 1-70, 1975

15. Duffie, J. A. and Beckman, W.A., *Solar Engineering of Thermal Processes*, Second Edition, Wiley-Interscience, New York, NY, 1991

16. Fisk, W. J., *Onset of Freezing in Residential Air-to-Air Heat Exchangers*, ASHRAE Transactions, Vol. 93, Pt. 1B, 1985

17. Gregg, S. J., and Sing, K. S. W., *Adsorption, Surface Area and Porosity*, Academic Press, New York, NY, 1982

18. Hausen, H., *Wärmeübergang im Gegenstrom*, Gleichstrom und Kreuzstrom, Springer Verlag, 1. Auflage, Berlin, 1950

19. Holmberg, R. B., *Prediction of Condensation and Frosting Limits in Rotary Wheels for Heat Recoveries in Buildings*, ASHRAE Transactions 1989, V. 95, Pt. 1

20. Incropera, F. P. and DeWitt, D. P., *Introduction to Heat Transfer*, Second Edition, John Wiley & Sons, New York, NY., 1990

21. Klein, H., *Heat and Mass Transfer in Regenerative Enthalpy Exchangers*, M.S. Thesis in Chemical Engineering, University of Wisconsin-Madison, 1988

22. Klein, S. A. and Alvarado, F. L., EES, Engineering Equation Solver, F-Chart Software, 4406 Fox Bluff Rd., Middleton, WI 53562

23. Klein, S. A., et al., TRNSYS - A Transient Simulation Program, Solar Energy Laboratory, University of Wisconsin-Madison, Version 14.1, 1994

24. Knight, K. M., *Analysis and Design of Adsorptive Processes for Air Quality Control*, Ph.D. Thesis in Mechanical Engineering, University of Wisconsin-Madison, 1992

25. Maclaine-cross, I. L., MOSHMX, A Method of Solving Heat and Mass Transfer, Monash University, Australia, 1974

26. Means Facilities Cost Data, 7th Edition, R.S. Means Company, Inc., Kingston, MA, 1992

27. Moran, M. J., and Shapiro, H. N., *Fundamentals of Engineering Thermodynamics*, Second Edition, John Wiley & Sons, New York, NY., 1992

28. Polanyi, M., Section III. - *Theory of the Adsorption of Gases. A General Survey and some Additional Remarks.*, Trans. Far. Soc., Vol. 28, pp. 316-333, 1932

29. Ruthven, D. M., *Principles of Adsorption and Adsorption Processes*, pp. 124-166, John Wiley & Sons, New York, NY., 1984

30. Schaefer, M., *Measurement of Adsorption Isotherms by Means of Gas Chromatography*, M.S. Thesis in Chemical Engineering, University of Wisconsin-Madison, 1991

31. Schultz, K. J., *Experimental Analysis of a Rotary Silica Gel Dehumidifier*, ASME,

Winter Annual Meeting of Combined Heat and Mass Transfer in Porous Media, 1987

32. Sing, K. S. W., *Reporting Physisorption Data for Gas/Solid Systems*, Pure and Applied Chemistry, Vol. 54, No. 11, pp. 2201-2218, 1982

33. Stoecker, W. F. and Jones, J. W., *Refrigeration and Air Conditioning*, Second Edition, McGraw-Hill, New York, NY, 1982

34. Synergy Software, Kaleidagraph, Synergy Software, 2457 Perkiomen Ave., Reading, PA 19606

35. Van den Bulck, E., *Analysis of Solid Desiccant Rotary Dehumidifiers*, M.S. Thesis in Mechanical Engineering, University of Wisconsin-Madison, 1983

36. Van den Bulck, E., *Convective Heat and Mass Transfer in Compact Regenerative Dehumidifiers*, Ph.D. Thesis in Mechanical Engineering, University of Wisconsin-Madison, 1987